

DESIGN AND TUNING OF FUZZY PID CONTROLLERS
FOR MULTIVARIABLE PROCESS SYSTEMS

ERANDA HARINATH

**DESIGN AND TUNING OF FUZZY PID CONTROLLERS FOR
MULTIVARIABLE PROCESS SYSTEMS**

by

©Eranda Harinath, B.Sc (Eng).

A thesis Submitted to the
School of Graduate Studies
in partial fulfillment of the
requirements for the degree of

Master of Engineering

Faculty of Engineering and Applied Science
Memorial University of Newfoundland
January, 2007
St. John's, Newfoundland, Canada



Library and
Archives Canada

Bibliothèque et
Archives Canada

Published Heritage
Branch

Direction du
Patrimoine de l'édition

395 Wellington Street
Ottawa ON K1A 0N4
Canada

395, rue Wellington
Ottawa ON K1A 0N4
Canada

Your file *Votre référence*
ISBN: 978-0-494-31251-3
Our file *Notre référence*
ISBN: 978-0-494-31251-3

NOTICE:

The author has granted a non-exclusive license allowing Library and Archives Canada to reproduce, publish, archive, preserve, conserve, communicate to the public by telecommunication or on the Internet, loan, distribute and sell theses worldwide, for commercial or non-commercial purposes, in microform, paper, electronic and/or any other formats.

The author retains copyright ownership and moral rights in this thesis. Neither the thesis nor substantial extracts from it may be printed or otherwise reproduced without the author's permission.

AVIS:

L'auteur a accordé une licence non exclusive permettant à la Bibliothèque et Archives Canada de reproduire, publier, archiver, sauvegarder, conserver, transmettre au public par télécommunication ou par l'Internet, prêter, distribuer et vendre des thèses partout dans le monde, à des fins commerciales ou autres, sur support microforme, papier, électronique et/ou autres formats.

L'auteur conserve la propriété du droit d'auteur et des droits moraux qui protègent cette thèse. Ni la thèse ni des extraits substantiels de celle-ci ne doivent être imprimés ou autrement reproduits sans son autorisation.

In compliance with the Canadian Privacy Act some supporting forms may have been removed from this thesis.

Conformément à la loi canadienne sur la protection de la vie privée, quelques formulaires secondaires ont été enlevés de cette thèse.

While these forms may be included in the document page count, their removal does not represent any loss of content from the thesis.

Bien que ces formulaires aient inclus dans la pagination, il n'y aura aucun contenu manquant.


Canada

Abstract

Multivariable processes are often found in many industries such as chemical, refinery, and aerospace. The complex and nonlinear nature of multi-input and multi-output (MIMO) systems makes multivariable control a challenging task. Multivariable control become difficult in the presence of loop interactions where different control loops in the multivariable system exhibits coupled behavior in the control variables. When the multivariable system is broken into several single-input-single-output (SISO) control systems, the individual control loops can be characterized by equal number of SISO control problems. However, when interactions exists, an individual control loop will be affected by more than one control variable in the multivariable system. Therefore design of MIMO control systems is often a challenging research area in the area of multivariable control.

There are many multivariable control techniques which have been developed to address the above issues, including advanced multivariable control techniques such as model predictive control. Among them, proportional integral derivative (PID) control has been the most common in industries. Application of fuzzy logic for control problems have been shown to improve overall performance significantly. Although there are many applications related to SISO based fuzzy PID systems, the application and design of fuzzy PID systems for multivariable systems are less common. The adaptive and nonlinear nature of fuzzy control allows fuzzy PID systems to handle nonlinear systems more efficiently than using linear PID controllers.

The objective of this thesis is to develop a technique to design and tune PID type fuzzy controllers for multivariable process systems. In this work, the standard additive model (SAM) based fuzzy system is selected to design the rule base. The SAM

inference system follows a special volume and centroid of membership based technique for defuzzification. A nonlinearity study has been performed to show the advantages of using a SAM based inference system against traditional min-max-gravity based inference systems. The SAM system is implemented on two fuzzy PID (FPID) systems. FPID type I is designed using Mamdani's style FPID system and constitute coupled rules to define the overall FPID output. FPID type II is designed using a rule decoupled system, in which each PID action is described using a separate rule base.

FPID tuning is performed using the two-level tuning principle where the overall tuning is decomposed into two tuning levels, low-level and high-level. The low-level tuning is dedicated to devise linear gain parameters in the FPID system where as the high-level tuning is dedicated to adjust the fuzzy rule base parameters. The low-level tuning method adopts a novel linear tuning scheme for general decoupled PID controllers and the high-level tuning adopts a heuristic based method to change the nonlinearity in the fuzzy output.

The stability analysis using Nyquist array and Gershgorin band proves the robustness of the proposed method. The stability criterion is performed to define the hard limits for nonlinear tuning variables in the SAM system. The proposed FPID tuning technique guarantees the stability of the MIMO control system.

The applicability of the proposed methods in this research is demonstrated through several control simulations and real-time experiments. The results show FPID systems able to handle such a complex system more robustly than using linear systems and also the experiments validated the design method proposed in this thesis.

Acknowledgements

First, I would like to thank Dr. George Mann, Associate Professor in Faculty of Engineering and Applied Science for giving me an opportunity to pursue my higher studies under his supervision. I express my gratitude to him for providing excellent research environment, guidance, encouragement and friendly attitude during the course of the M. Eng program.

Many thanks to the Faculty of Engineering for providing excellent academic courses during course of studies. I would also like to thank my fellow members in INCA lab, Memorial University of Newfoundland for discussions and suggestions in various stages.

This work is undertaken as a part of PPSC (Pan-Atlantic Petroleum system. consortium) project funded from Atlantic Innovation fund. The fellowship and other funding assistance from Memorial University of Newfoundland is gratefully acknowledged.

Contents

1	Introduction	1
1.1	Overview of Multivariable Control	1
1.1.1	Internal Model Control (IMC)	3
1.1.2	Model Predictive Control (MPC)	4
1.1.3	Proportional Integral Derivative (PID)	5
1.1.4	Fuzzy Control	5
1.2	Research Motivation	6
1.3	Research Objective	8
1.4	Controlling Process	8
1.5	Systematic Design Procedure	10
1.6	Contributions resulted from this Thesis	11
1.7	Organization of the Thesis	11
2	Two-Level Tuning Principle	13
2.1	Introduction	13
2.2	Fuzzy PID (FPID) Configurations	14
2.2.1	High-Level Nonlinear Tuning Variables	15
2.2.2	Low-Level Linear Tuning Variables	16

3	Linear PID controller Tuning	19
3.1	Introduction	19
3.2	Background	21
3.3	System Description	23
3.4	Low-Level Tuning	24
3.4.1	Tuning 1 st loop	26
3.4.2	Tuning <i>i</i> th loop:	29
3.5	Stability Analysis	29
3.5.1	Direct Nyquist Array (DNA) Stability Theorem	29
3.5.2	Gain and Phase Margins Calculation	30
3.6	Control Simulation	33
3.6.1	Example 1	34
3.6.2	Example 2	37
3.7	Performance Analysis	40
4	Non Linear Fuzzy PID Controller Tuning	44
4.1	Introduction	44
4.2	Background	45
4.3	High-Level Tuning : Nonlinearity Tuning	46
4.3.1	Standard Additive Model (SAM)	46
4.3.2	SAM Theorem	49
4.3.3	Design of SAM; Identification of High-Level Tuning Variables	50
4.4	Nonlinearity Analysis of Fuzzy SAM output	53
4.5	Stability Analysis	56
4.5.1	Maximum values of PID parameters	56
4.6	Control Simulation	59

4.6.1	Example 1	59
4.6.2	Example 2	60
5	Real-Time Experiments	70
5.1	Introduction	70
5.2	System Modeling and Identification	71
5.2.1	Dynamic Modeling : Soil-cell	72
5.2.2	Identification : Soil-cell	74
5.3	Openloop Test	76
5.4	Implementation of Control Algorithms	78
6	Conclusion and Future Work	87
6.1	Conclusion	87
6.2	Future Work	90
	List of References	93
	A Design Sketches for Realtime Implementation	104
	Bibliography	104

List of Figures

1-1	Flow of the systematic design and tuning of FPID for MIMO systems	9
2-1	FPID configurations. (a) Type I: rule-coupled FPID, (b) Type II: rule de-coupled FPID	14
2-2	Nonlinear tuning variables measured at local control points for FPID configurations	16
3-1	Statically decoupled multivariable control	23
3-2	Nyquist diagram with the Gershgorin circle at the gain crossover frequency ω_g	31
3-3	Nyquist diagram with the Gershgorin circle at the phase crossover frequency ω_p	31
3-4	Schematic view of soil-cell (a) and finite element based model for soil-cell (b)	33
3-5	Example 1, Simulation of closed loop system with PID and BLT controllers	35
3-6	Example 1, Nyquist array and Gershgorin bands of system	36
3-7	Example 2, Simulation of closed loop system with PID and BLT controllers	38
3-8	Example 2, Nyquist array and Gershgorin bands of system	39

3-9	SIMULINK implementation of a PID control strategy for the multi-variable soil-cell temperature controller	43
4-1	Function approximator: Additive fuzzy system	47
4-2	General framework of additive fuzzy system	47
4-3	Nonlinear tuning variables measured at local control points of SAM .	51
4-4	Membership functions for if-part in SAM	51
4-5	Admissible area (grey) of nonlinearity diagram for SAM controller .	55
4-6	Stability region for θ_0 and α_0 . It is same for θ_1 and α_1	59
4-7	Example 1, Simulation of closed loop system with PID and FPID controllers	61
4-8	Example 2, Simulation of closed loop system with PID and FPID controllers	63
4-9	SIMULINK implementation of a FPID type 1 control strategy for the multivariable soil-cell temperature controller	66
4-10	SIMULINK implementation of a FPID type 1 controller	67
4-11	SIMULINK implementation of a FPID type 11 control strategy for the multivariable soil-cell temperature controller	68
4-12	SIMULINK implementation of a FPID type 11 controller	69
5-1	First-order dead time model approximation for a higher order process	73
5-2	Determination of first-order dead time model using process reaction curve method	75
5-3	First-order dead time model approximation for a higher order process	76
5-4	Real time experiments: Openloop test No. 1 of cell soil	79
5-5	Real time experiments: Openloop test No. 2 of cell soil	80
5-6	Real time experiments: Openloop test No. 3 of cell soil	81

5-7	Real time experiments: Closed loop tests of cell soil	83
5-8	SIMULINK implementation of a PID control strategy of the multivariable soil-cell temperature controller for real-time experimentations	84
5-9	SIMULINK implementation of a FPID type1 control strategy of the multivariable soil-cell temperature controller for real-time experimentations	85
5-10	SIMULINK implementation of a FPID type 11 control strategy of the multivariable soil-cell temperature controller for real-time experimentations	86
A.1	SIMULINK implementation of Pulse Width Modulator (PWM) of power suppliers for real-time experimentations	105
A.2	SIMULINK implementation of I/O interface for real-time experimentations	106

List of Tables

3.1	Performance characteristic indices of proposed PID method and BLT method for set point tracking in example 1	41
3.2	Performance characteristic indices of proposed PID method and BLT method for load disturbance in example 1	41
3.3	Tuning parameters of example 1 for PID and BLT controllers	41
3.4	Gain and Phase Margins of each loop of example 1	41
3.5	Performance characteristic indices of proposed PID method and BLT method for set point tracking in example 2	42
3.6	Performance characteristic indices of proposed PID method and BLT method for load disturbance in example 2	42
3.7	Tuning parameters of example 2 for PID and BLT controllers	42
3.8	Gain and Phase Margins of each loop of example 2	42
4.1	Nonlinearity variation indices for different fuzzy systems	56
4.2	Performance characteristic indices of proposed FPID methods and PID method for set point tracking in example 1	64
4.3	Performance characteristic indices of proposed FPID methods and PID method for load disturbance in example 1	64
4.4	Tuning parameters of example 1 for FPID controllers	64

4.5	Performance characteristic indices of proposed FPID methods and PID method for set point tracking in example 2	65
4.6	Performance characteristic indices of proposed FPID methods and PID method for load disturbance in example 2	65
4.7	Tuning parameters of example 2 for FPID controllers	65
5.1	Performance characteristic indices of proposed FPID methods and PID method for set point tracking	82
5.2	Tuning parameters of FPID and PID controllers for real time experiments	82
5.3	Gain and Phase Margins of each loop of the soil-cell	82

Acronyms

MIMO	=	Multiple Input Multiple output
SISO	=	Single Input Single Output
RHP	=	Right-Half complex Plane
IMC	=	Internal Model Control
PID	=	Proportional Integral Derivative
MPC	=	Model Predictive Control
DMC	=	Dynamic Matrix Control
GPC	=	Generalized Predictive Control
CARIMA	=	Controller Auto-Regressive Integrated Moving-Average
NMPC	=	Nonlinear Model Predictive Control
FLC	=	Fuzzy logic control
FPID	=	Fuzzy Proportional Integral Derivative
FPD	=	Fuzzy Proportional Derivative
FPI	=	Fuzzy Proportional Integral
FE	=	Finite Element
ZN	=	Ziegler and Nichols
SAM	=	Standard Additive Model
BLT	=	Biggest Log Modulus
ALG	=	Apparent Linear Gains
ANG	=	Apparent Nonlinear Gains

ELC = Equivalent Linear Controller
LLFLC = Linear-Like Fuzzy Logic Controller
TITO = Two Input Two Output
DNA = Direct Nyquist Array
INA = Inverse Nyquist Array
RGA = Relative Gain Array
RNA = Rosenbrock- Nyquist Array
MMG = Max-Min-Gravity
PSG = Product-Sum-Gravity
TSK = Takagi-Sugeno-Kang
NVI = Nonlinearity Variation Index
LAI = Linearity Approximation Index
GPP = Guaranteed-PID-Performance
RTD = Resistance Temperature Detector
ADC = Analog to Digital Converter
PC = Personal Computer
DAC = Digital to Analog Converter

Chapter 1

Introduction

1.1 Overview of Multivariable Control

There are many industrial control systems which are required to deal with multi-variable systems. The distillation columns is one good example used in the chemical and refining industry to achieve product purification. Multivariable control becomes a challenging task in the process industry especially when the process contains significant interaction among loops. In addition to the dynamic coupling existing in multi-input-multi-output (MIMO) systems, the general limitations that are applicable for single-input-single-output (SISO) systems also complicates the design procedure. Levien and Morari [1] have discussed three such limitations on process resilience.

- Non-minimum phase characteristics.
- Constraints on manipulated variables.
- Sensitivity to model uncertainty.

The non-minimum phase characteristics are caused by the presence of time delay and right-half complex plane (RHP) zeros of the process. The time delay is a

very common phenomenon in process industries , especially in chemical industries. The presence of time delay in a feedback control loop could be a serious barrier to good process performance. This problem is more complicated in the case of MIMO processes. The input-output loops of MIMO process usually have different time delays, and for a particular loop its output could be affected by all the inputs through different time delays. As a result, such a plant may then be represented by a multivariable transfer function matrix having multiple time delays around a operating point. It is well known that the presence of RHP zeros limit the achievable closed-loop performance. The most familiar characteristic of real RHP zeros is that they lead to an inverse response to a step change in input.

Almost all processes which appears in industry operate under input constraints since the manipulated variables can only vary between the upper and lower limits of the corresponding actuator. These physical constraints on inputs make the process nonlinear and design of controllers more complex.

In general, when a controller is designed using off-line simulations, a model of the process is considered. It is known that due to the modeling errors, there is always model-process mismatch. This model-process mismatch sometimes causes undesirable responses with unstable transient output. Therefore, the designed controller should be more robust to model uncertainty.

A large number of design methods addressing the above issues are available for SISO systems. However, there are few commonly used techniques for MIMO systems which address the above issues.

1.1.1 Internal Model Control (IMC)

The Internal model model (IMC) [2] is a model based control structure that provides a convenient way to tune and design a controller. Especially IMC based proportional integral derivative (PID) controllers are more popular. The IMC structure offers several advantages [3] as compared to the standard feedback control such as conventional PID. Those includes convenient analysis of non-minimum phase characteristics and controllability analysis in the presence of time delay and RHP zeros. The IMC control tuning usually simplifies to a single parameter, and offers a convenient design procedure for optimal performance.

The design of an IMC controller for a SISO process is quite standard. Revera *et. al.* [4] have introduced the IMC-based PID control for first-order SISO process. However, unlike in the scalar case, the design of an IMC controller for MIMO process is mathematically complex. This is tedious especially in the case of higher dimensional process or when the process constitutes non-minimum phase characteristics [5]. This non-minimum phase problem is usually solved by factorizing the process model into two parts; invertible and non-invertible [5]. The non-invertible part is diagonal and contains the time delay components and non-minimum phase zeros of the process model. However, the resulting closed-loop system still consists of unavoidable time delays and non-minimum phase zeros.

In the absence of disturbance and model-process mismatch, the IMC structure has the capacity to handle the manipulated variable saturation. This is mainly due to existence of an openloop structure of the overall system [3]. However, in practice there may be model process mismatch and disturbances. The conventional remedy is to compensate the effects of constraints by modifying the controller input when the output of the controller (manipulated variable) is saturated. In literature, the works

that discuss such performance limitations include [6], [7], [8], [9], [10], [11].

1.1.2 Model Predictive Control (MPC)

Model predictive control (MPC) refers to a class of computer control algorithms that utilize an explicit process model to predict the future response of a process over an extended time horizon. The MPC is more famous as one of the most attractive control technique especially among multivariable processes which appear in chemical, automotive and aerospace industries [12] [13] [14]. This real benefit of MPC is accrued mainly due to its explicit use of the process model and optimization technique to solve complex control problem such as non-minimum phase, constraints on manipulated variables, model uncertainty in multivariable processes [15] [16]. Especially, MPC has the capacity to easily handle the multivariable processes with long and varying time delays [3], [15], [16] in addition to inverse response behavior due to RHP zeros [17].

It is well known that model uncertainties cannot be avoided in practice, especially, in many chemical processes. There is a growing interest about this problem and many researchers are attempting to find solutions to compensate [18], [19], [20]. The parameter uncertainties are the main cause of performance degradation and instability. As a remedy they tend to apply different modeling techniques to predict output response of process and in some cases adaptive techniques also have been utilized. There are two types of notable original formulations of MPC in last three decades. The dynamic matrix control (DMC)(Cutler and Ramaker, 1980) [21] and the generalized predictive control (GPC)(Clarke, et al., 1987) [22]. The DMC uses a step response model to predict the future output response of process while GPC uses a controller with auto-regressive integrated moving-average (CARIMA) model.

However, As most of the industrial processes display non-linearity, linear MPC algorithm may not exhibit satisfactory dynamics performance. Researchers recently began to develop nonlinear model, such as fuzzy logic based model, neural network based model in order to predict future output in the nonlinear MPC (NMPC) algorithm [23], [24], [25], [26], [27], [28]. There is good discussion about literature survey of MPC techniques in [29].

1.1.3 Proportional Integral Derivative (PID)

It is well known that the PID controller is the most popular and widely used control system in industries. PID controller offers simple control structure and allows implementation using fewer number of variables. According to the survey conducted by Yamamoto and Hashimoto [30], PI/PID controllers are used in more than 90% of control loops in Japan. Due to its popularity, researchers attempted to develop the advanced control techniques such as optimal control, H_∞ , MPC, IMC in order to generate equivalent PID terms. In the second chapter, there is comprehensive study of PID controller applications in multivariable processes and equivalent representation of advanced control techniques.

1.1.4 Fuzzy Control

Fuzzy logic was introduced by Zadeh [31] and has been widely used in many engineering areas and consumer products and has gained much interest since the pioneer work of Mamdani [32], [33]. Fuzzy logic control (FLC) has emerged in recent years as promising way to approach nonlinear control problems [34]. Some applications of FLC for MIMO systems have been reported in [35].

The main challenge in fuzzy control design is in the tuning, particularly in choosing

correct fuzzy system and its associated fuzzy parameters. The *curse of dimensionality* during the rule explosion [36] is the main draw-back and as a result the fuzzy control designers are still unable to find an effective tuning algorithm. However, the recent increase in computing power enabled most designers to adopt numerical optimization techniques for generating optimum or near optimum solutions to fuzzy systems, such as genetic algorithm and neural network, where those techniques have the capacity to determine a large number of unknown parameters in fuzzy systems [37],[38] . However, those application are somewhat specific and unable to generalize for wider process specifications. Moreover, most of them are off-line optimization methods and cannot be used for real-time control. In many cases the optimizations have been performed using exact process model and any miss-match of the real the system does not guarantee stability or the overall performance.

1.2 Research Motivation

The common issues related to MIMO controller design includes; non-minimum phase characteristics, constraints on manipulated variables, sensitivity to model uncertainty on process resilience, the interactions which exist among different loop of multivariable processes. Among those the loop interaction is the most challenging issue in the area of multivariable control. When interactions are not severe one input signal mainly affects only a particular output. Under those circumstances, when the pairing of input-output is not a problem, it might be sufficient to assign a number of SISO control loops in order to control the system. This type of control is called the decentralized control of multivariable process and conventional SISO tuning techniques can be applied to obtain desired response of the process.

However, in many cases when a particular input signal is varied, it not only

effects one variable but also several other outputs in the MIMO systems. When the interactions among the openloops process are severe the conventional scalar control tuning techniques may results in a poor performances even leading to instability of the control system. As a solution to the interaction problem, a dynamic decoupler (compensator) can be used. The dynamic decoupler requires computation of the inverse process model. In many cases, the resulting dynamic decoupler may not be physically realizable [3]. Alternatively, this problem can be solved using static decoupler. The static decoupler is easy to design and implement since it requires less information about the process model and depends only on steady state conditions of the process output variables. The static decoupler is effective only at steady sates and the interaction among loops at high frequency will not be eliminated.

“The multivariable control becomes challenging task in process industry especially when the process has significant interactions among loops.”

In order to cope with this problem, the interactions should be the main design criteria when a controller is designed for a multivariable process system. The advanced control techniques have some difficulties in dealing with interactions among loops specially when band widths of those loops are limited. In some cases they are operated in supervisory mode [39]. Since PID controller is popular, design and tuning of PID controller is suggested. As a result most of PID controller operate in sub-optimal manner. Most of industrial processes are often nonlinear systems [40]. Then design of classical linear controller is generally based on linearized model around a steady state point. Hence the PID controller can not successfully control highly nonlinear plants [41].

Fuzzy PID controller (FPID) controllers have been successfully used in industrial processes and have often produced results superior to those of classical PID controller [42], [43], [44] including its simplified versions of fuzzy proportional derivative (FPD)

and fuzzy proportional integral (FPI) controller [45], [46], [47]. This real benefit of FLC is due to the nonlinearity that exist in the fuzzy output, the heuristic nature associated with simplicity and effectiveness of both linear and non-linear plants [35], [48]. The sub-optimal PID performance can be improved while incorporating non-linear FLC technique.

1.3 Research Objective

The main objective of this research is the design and tuning of FPID controller for multivariable process system. This research attempts to address the main problem of interactions among deferent loops which commonly appears on multivariable process system in industry.

1.4 Controlling Process

This research is focused on the conventional feedback strategy of a three inputs three outputs multivariable soil heating cell. First, the proposed FPID controllers tuning techniques are simulated for the finite element (FE) based 3×3 soil- heating processes [49]. Two transfer functions with different time delays are derived. A theoretical model is obtained using FE modeling [49]. The same model is altered by increasing time delay of the theoretical transfer function by two times. Finally, the proposed FPID controller techniques are applied to 3×3 soil-cell (real time experiments).

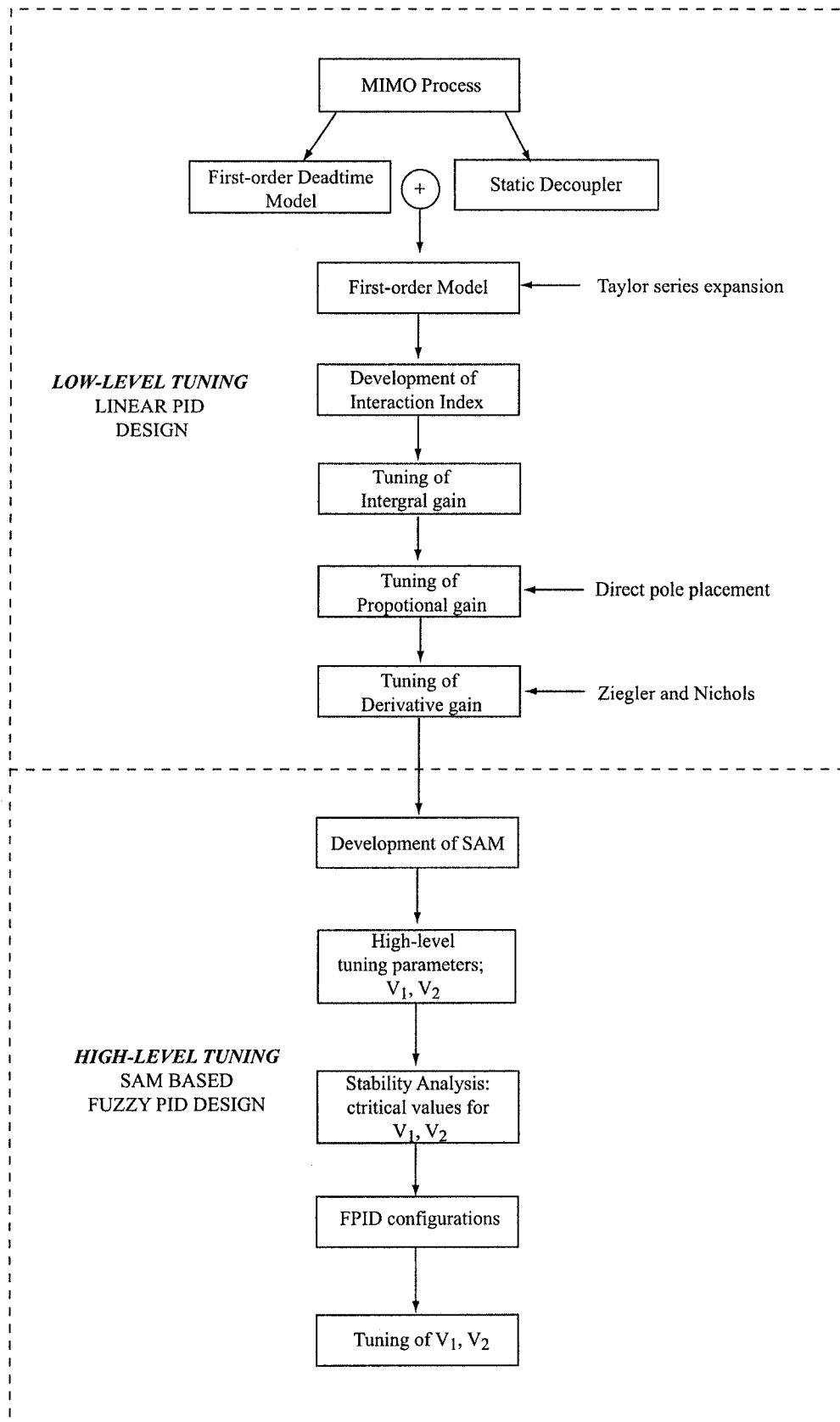


Figure 1-1: Flow of the systematic design and tuning of FPID for MIMO systems

1.5 Systematic Design Procedure

Fig. 1-1 shows the flow of design and tuning of FPID controller for the soil-cell. Following steps summaries the systematic design procedure.

1. Equivalent first-order delayed models are found for all higher order sub-processes by analyzing the response using plant reaction curve methods.
2. The static decoupler is obtained for MIMO process.
3. An equivalent first-order model for overall compensated system (first-order model with static decoupler) is obtained using truncated Taylor series approximation at low frequencies.
4. A measure of interaction is developed and integral gains are calculated for each loops at particular values of interaction indices .
5. Using direct pole placement method [50] and Ziegler/Nichols (ZN) [51] tuning formulae proportional and derivative gains of linear PID controllers are calculated for low-level tuning.
6. Standard Additive Model (SAM) is developed for MIMO process and high-level tuning parameters are identified in order to have optimum nonlinearity in the fuzzy output.
7. Different types of FPID configurations are considered for design of SAM.
8. Nonlinear tuning parameters (volumes of then-part fuzzy in SAM) are tuned for each FPID configuration so that overall system is stable.

1.6 Contributions resulted from this Thesis

Followings are the summary of outcomes in this research.

1. Extension of two-level tuning method for MIMO systems. The two-level tuning proposed in (Mann,99) is extended for a MIMO system. This is a novel attempt in multivariable control.
2. Development of novel linear PID tuning technique for MIMO systems. The linear tuning can be applied for any $n \times n$ process systems whereas other general methods have limitation to the 2×2 systems.
3. Investigation of Standard additive model (SAM) based fuzzy inference for MIMO systems. SAM based fuzzy inference allows nonlinear control. This is the first time application of SAM based fuzzy inference to multivariable systems
4. Development of generalized tuning technique for $n \times n$ multivariable FPID systems.

1.7 Organization of the Thesis

Chapter 2 provides an introduction of two-level tuning principle for FPID controllers. Two types of FPID controller are considered and detail analysis of two-level tuning technique for those are presented.

Chapter 3 describe a design of linear PID system for coupled multivariable process system. The interaction index is introduced to choose PID parameters. Stability analysis demonstrated through Nyquist array, Gershgorin band, gain and phase margins in order to prove robustness of proposed controller. The performance of the

proposed controller is evaluated using two control simulations. The results compare with well-known biggest log modulus (BLT) [52] technique for multivariable process.

Chapter 4 shows a non-linear FPID controller tuning technique for multivariable process system. SAM inference is presented and advantages of SAM is discussed with other commonly used fuzzy systems in the view of nonlinearity analysis. High-level tuning parameters are identified for SAM based FPID controller. Stability of the controller is analyzed in order to select correct values for high-level tuning parameters. Two types of SAM based FPID controller are investigated. The performance of the proposed FPID controller techniques are evaluated using two control simulations and compared with its counterpart; linear PID controller tuning technique which is presented in chapter 3.

Chapter 5 describes real time experiments of temperature control of a soil-cell. The objective of experiments is to control temperatures at three different locations of soil-cell using three different heaters. The soil-cell is modeled using first dead time models and identified using step response via process reaction curve. The different controller techniques; PID, FPID type I and FPID type II are implemented using dSAPCE controller board, SIMULINK, MATLAB and other hardware instruments like heaters, power suppliers etc. The performance of different controller techniques have been evaluated

Chapter 6 summarize the work presented in this thesis and provides suggestion for further research.

Chapter 2

Two-Level Tuning Principle

2.1 Introduction

In general the FPID design is a two-level tuning problem [53]. While low-level tuning addresses the linear gain and overall stability, the high-level tuning provides nonlinear control to enable superior performance. In a rule-coupled fuzzy system, such as Mamdani-Zadeh based system, the inputs (error and its derivative) are coupled to produce a combined fuzzy PI output [53]. The coupled nature of the inputs generally makes the nonlinear output a complex function. As a result it is difficult for one to isolate linear gains from the nonlinear output. In order to facilitate the two-level tuning, apparent linear gains (ALG) and apparent nonlinear gains (ANG) are defined. While the ALG terms are related to the overall performance and stability of the system the ANG terms provides the nonlinearity that is necessary in the fuzzy output. In the past for SISO systems, some have attempted to provide tuning rules for linear gains [54], [55], [56]. However the nonlinear tuning was not sufficiently or explicitly described. In [57], the design of conventional FPID is identified as a two-level tuning problem and described as a way of obtaining ALG terms for conventional

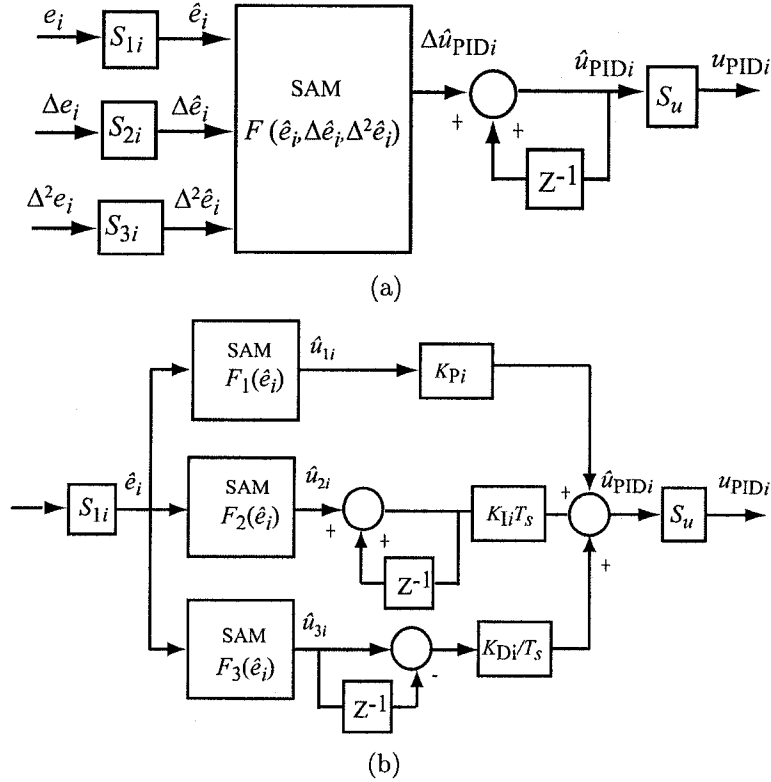


Figure 2-1: FPID configurations. (a) Type I: rule-coupled FPID, (b) Type II: rule de-coupled FPID

FPID type controllers. However, the non-linearity tuning was not sufficiently or explicitly described for implementing a two-level tuning. In the following section a systematic procedure is developed to devise two-level tuning methodology for general FPID controllers for MIMO systems.

2.2 Fuzzy PID (FPID) Configurations

Two types of FPID configurations are considered as shown in Fig.2-1. The type I is a conventional Mamdani's type FPID and has three inputs and it produces an incremental FPID signal. The type II uses SISO rule inference to provide decoupled and

independent tuning for the three actions in the PID signal [58]. Using suitable scale factors (S_{wi}), where $w = 1, 2, 3$, the feedback error terms (e_i) and its corresponding normalized error variables (\hat{e}_i) at n^{th} sampling instance can be expressed as

$$\begin{aligned}\hat{e}_i(n) &= S_{1i} e_i(n) \\ \Delta\hat{e}_i(n) &= S_{2i}\Delta e_i(n) \\ \Delta^2\hat{e}_i(n) &= S_{3i}\Delta^2 e_i(n).\end{aligned}\tag{2.1}$$

All FLC input variables are normalized to a compact region $[-1,1]$. The error variables are normalized by using the condition $\hat{e}_{wi} = \max(-1, \min(1, S_{wi}e_{wi}))$. The defuzzified controller output after the fuzzy inference is denoted by \hat{u} . Similarly the FLC output is normalized by using the condition $\hat{u} \equiv u/u_{max}$.

2.2.1 High-Level Nonlinear Tuning Variables

The nonlinear tuning variables are selected to affect ANG terms at any given local control point in the control surface. Since PID gains are proportional to the slopes of the control surface, the slope angles of the tangents drawn at a given point on the nonlinear control surface are considered to be the nonlinear tuning variables. For simplicity, two slope angles drawn at two selected points (see Fig. 2-2) on control surface are considered as nonlinear tuning variables.

In order to isolate slope angles from their associated outputs of FPID type I controller, the slopes are measured in the planes of individual error axes. The measurement of these angles with respect to a two-dimensional control surface is shown in Fig. 2-2(a). Fig. 2-2(b) shows a control curve that has been projected into a chosen error variable. In general, for a three- input coupled rule base the slope angles can

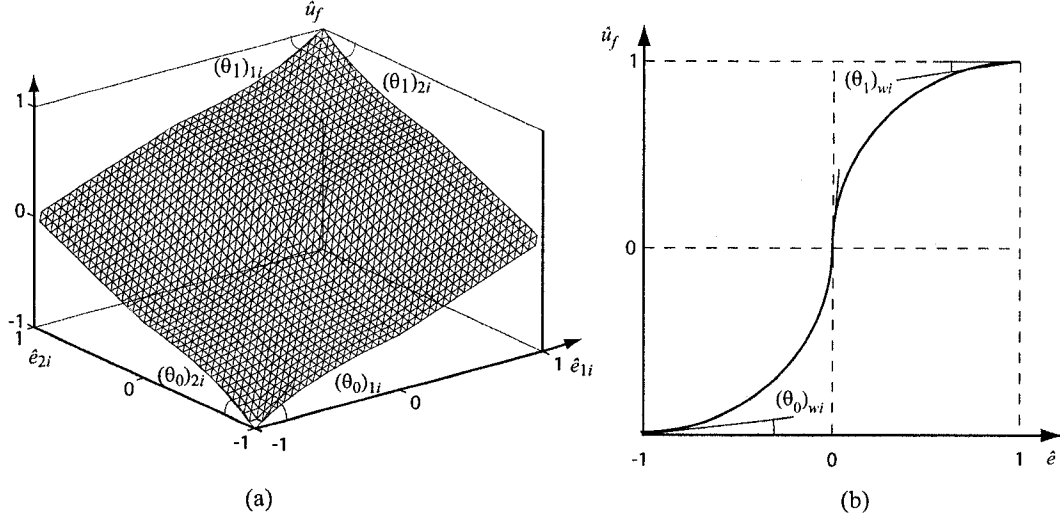


Figure 2-2: Nonlinear tuning variables measured at local control points for FPID configurations

be described by

$$\begin{aligned}
 (\theta_0)_{wi} &= \left(\frac{\partial \hat{u}_f}{\partial \hat{e}_{wi}} \right)_{\hat{e}_{wi}=-1} \\
 (\theta_1)_{wi} &= \left(\frac{\partial \hat{u}_f}{\partial \hat{e}_{wi}} \right)_{\hat{e}_{wi}=1}
 \end{aligned} \tag{2.2}$$

Where $\hat{u}_f = \hat{u}(\hat{e}_p = 0)$, $p = 1, 2, 3$ $p \neq w$. The fuzzy system designed for the PID control should allow independent variations of θ_0 and θ_1 within the range $[0 \ 90^\circ]$.

2.2.2 Low-Level Linear Tuning Variables

The composed FPID control action for FPID type I is given by

$$u_{\text{PID}i} = S_{ui} \sum_{k=0}^n \Delta \hat{u}_{\text{PID}i}. \tag{2.3}$$

Assuming the fuzzy integral action and derivative actions are in the form given by,

$$\hat{u}_I(n) = \sum_{k=0}^n \hat{u}_w(k)$$

and $\hat{u}_D(n) = \hat{u}_w(n) - \hat{u}_w(n-1)$, the FPID action for FPID type II can be expressed as

$$u_{\text{PID}i} = S_{ui} [K_{Pi} \hat{u}_{1i} + K_{Ii} T_s \sum_{k=0}^n \hat{u}_{2i}(k) + \frac{K_{Di}}{T_s} (\hat{u}_{3i}(n) - \hat{u}_{3i}(n-1))] \quad (2.4)$$

where K_{Pi} , K_{Ii} and K_{Di} are the linear PID gains for i^{th} loop and T_s is the sampling time. When a fuzzy system is set to produce a linear function, the FLC will become a linear type PID controller and is defined as an equivalent linear controller (ELC) [59]. Using the ELC output the i^{th} loop linear PID output can be arranged in the following form;

$$u_{\text{PID}i}^l(n) = K_{Pai} e_i(n) + K_{Iai} \sum_{k=0}^n e_i(k) T_s + K_{Dai} \Delta e_i(n) / T_s \quad (2.5)$$

where K_{Pai} , K_{Iai} and K_{Dai} are defined as the ALG terms of the FLC system. A FLC having linear rule base and uniform partition of universe of discourse of all variables is named as a linear-like fuzzy logic controller (LLFLC) [59]. The ELC defined for the LLFLC is used for deriving the linear tuning variables. Then the ELC output for type I is given by

$$\Delta \hat{u}_{\text{PID}i}^l = [\hat{e}_i + \Delta \hat{e}_i + \Delta^2 \hat{e}_i]. \quad (2.6)$$

From (2.1),(2.5) and (2.6), the ALG terms can be found as

$$\begin{aligned}
K_{Pa_i} &= S_u S_{2i} \\
K_{Ia_i} &= S_u S_{1i} / T_s \\
K_{Da_i} &= S_u S_{3i} T_s.
\end{aligned} \tag{2.7}$$

Similarly, ELC output for type II is given by

$$\hat{u}_{1i}^l = \hat{u}_{2i}^l = \hat{u}_{3i}^l = \hat{e}_i. \tag{2.8}$$

From (2.1),(2.5) and (2.8), the ALG terms can be found as

$$K_{Pa_i} = K_{pi}, \quad K_{Ia_i} = K_{Ii} \quad \text{and} \quad K_{Da_i} = K_{Di}. \tag{2.9}$$

The gain analysis provides two-levels of tuning for PID control. The adjustment of K_{Pa} , K_{Da} and K_{Ia} refers to a general PID tuning with the control surface normalized to a linear form in the normalized output space. The ANG terms refers the effect of changing the nonlinearity of the FPID output in the nonlinearity output space. This ALG and ANG decomposition allows the use two-level of tuning for fuzzy PID controllers.

Chapter 3

Linear PID controller Tuning

3.1 Introduction

Design and tuning of PID controller for MIMO process is presented in this chapter. It is well known that the conventional PID controller is still the most popular and widely used controller in industries. The simple control structure allows easy design and tuning. Most of industrial processes are often nonlinear systems [40], [60]. Then design of classical linear controller is generally based on linearized model around a steady state point. Hence the PID controller often provide sub-optimal performances in nonlinear plants [41],[60]. Therefore, FPID controller is proposed and is tuned using the two-level tuning technique which is described in the previous chapter. The aim of this chapter is to identified the ALG terms for two-level tuning.

This chapter is organized as follows. First, the detailed literature review of conventional PID controller for MIMO process is presented. Where it is identified that the available tuning techniques for MIMO processes have not sufficiently addressed the main problem of interactions among loops. Although there are few development in the past where some considerations were given on interaction, they are strict for

two input two output (TITO) processes [61], [39] and difficult to extend for general $n \times n$ MIMO processes. Secondly, the decoupling is performed while using a static decoupler, which has the effect of reducing interactions within individual loops. At steady state, the system with the static decoupler can be treated as number of SISO systems. Using truncated Taylor series expansion, a first-order model is obtained for the system with static decoupler at low frequencies. Each loop is assigned with a PID controller. The PID controller is designed in three steps. First, an interaction index is defined to reflect the low frequency interactions caused by a given loop to other loops in the system. The maximum interaction index is then chosen to define the integral gain. The proportional and derivative gains are then selected using direct pole placement method and ZN tuning rule respectively so that the closed-loop performance is improved.

Thirdly, stability analysis is performed for overall closed loop system using direct Nyquist array (DNA) stability theorem. The DNA theorem uses openloop frequency response characteristics of the system. The gain and phase margins are calculated for the MIMO process systems using method described by [62].

Finally, The proposed PID controller algorithm is simulated using two control simulations. A Nyquist array and Gershgorin bands for the system is drawn in order to justify the operation of controller for any frequency. The stability analysis suggest the controller can be safely operated with safe gain and phase margins. The performance, based on set point tracking and load disturbance rejection capability, of proposed algorithm is compared against the well known BLT technique, proposed by Luyben.

3.2 Background

In literature, the PID tuning methods applicable for MIMO systems can be divided in to four main categories.

In the first category, the best input-output pairing configurations are selected and individual PID controllers are subsequently designed while considering the diagonal transfer functions of the MIMO process model. The gains may be selected using well known ZN tuning rule. The ZN parameters are detuned by a factor in order to guarantee stability. Niederlinski [63] used tuning heuristics to modify the ZN parameters corresponding to individual PID controllers. In an other development of this category, the BLT tuning rule is used. In the BLT technique the pairing problem is assumed to have been solved. The method proposes a technique to choose the de-tuning factor for ZN based PID parameter. For SISO systems, the log modulus is defined as the magnitude of the closed-loop servo-transfer function and it expresses in decibels. The SISO definition is then extended to define the biggest log modulus and this number is directly used to calculate the de-tuning factor for ZN parameters. Recently, Dan and Dale [64] proposed a new definition to the ultimate gain and ultimate frequency which accounts the off diagonal transfer functions. The technique is developed using the Gershgorin bands of Nyquist plot. In case of interactions the method proposes a decoupler and the PID controllers are tuned by using modified ZN method. The de-tuning factor is arbitrarily chosen.

Unlike in the first category, the second category avoids using any SISO based tuning values, such as ZN. Instead the PID parameters are chosen entirely using the Nyquist stability criteria. First, a compensator (decoupler) is designed for dynamically coupled systems. Using the DNA the decentralized PID controllers are then designed. Rosenbrock [65] pioneered to introduce the Inverse Nyquist Array (INA)

analysis for MIMO control designs. Recently, Ho *et. al.* [62] introduced a method to shape the Gershgorin band. First, gain and phase margins for individual loops of the MIMO process are specified. Using the Gershgorian band the equivalent gain and phase margins of diagonal transfer functions of the openloop processes are then calculated. While knowing those gain and phase margins the PID design problem is solved while treating each loop as an equivalent SISO problems and PID parameters are thus obtained.

In the third category the PID tuning problem is solved using a closed loop interaction measure. The measure may be obtained either using steady state or dynamic measures. Bristol [66] has proposed a method called the relative gain array (RGA) to determine the interaction measure and this study was limited to steady state conditions. Witcher and McAvoy [67] extended the RGA method to accommodate the transient or dynamic process conditions. Astrom *et. al.* [39] then introduced a decoupled PID tuning rule based on the interaction measures and the study was limited to a two dimensional (2×2) process. The PID controller is designed in such a way that it will minimize the interaction index of an individual loop. Recently, Lee and Edgar [68] considered error matrix of complimentary sensitivity functions between process and diagonal process to define the dynamic interaction measure. IMC based controller is then designed with specific value of closed loop time constant so that the dynamic interaction is minimized.

In fourth category, the advanced control techniques such as optimal control, H_∞ and MPC have being utilized to find the equivalent PID terms [69]. MPC is the most widely applied advanced control technique in process industries [3]. As a result predictive type PID controllers received more attention in this area of research. Moradi *et. al.* [69] have introduced a predictive PID controller based on GPC. Most of IMC-based PID controller proposed in literature are not decentralized PID controllers.

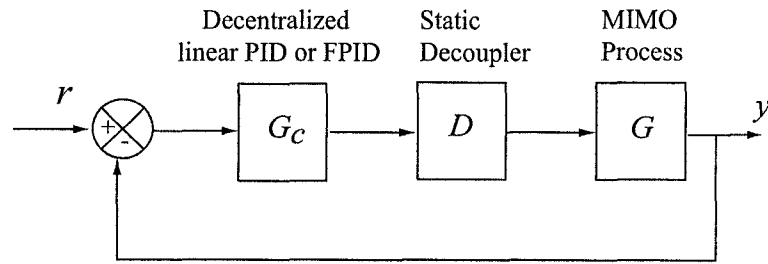


Figure 3-1: Statically decoupled multivariable control

Rivera *et. al.* [4] introduced IMC- based PID control technique for first-order SISO process. Lieslehto *et. al.* [8] proposed a heuristic tuning method for IMC-based PID controllers for MIMO process with minimum phase elements. Although they are being classified as PID designs, the true functionality is similar to the related advanced control system, such as MPC, and the PID terms represent only the equivalent form rather than self PID control. In other words, the control structure constitutes a non PID form and requires additional computing blocks, such as model identifications and predictions for real time control.

Although the advanced process control techniques is becoming popular for the MIMO system, PI/PID control is still dominant in process industries [9]. Under such circumstances, it is very important to develop a PID tuning method which can be applied to MIMO process. It is very clear that the available techniques have limitations to extend for general MIMO systems, mainly due to the complex nature.

3.3 System Description

The conventional feedback strategy of a n inputs n outputs multivariable system with a static decoupler and PID controller is shown in Fig. 3-1 where the multivariable system is assumed as a linear and open-loop stable system. Then, the transfer function of this MIMO system is described by,

$$G(s) = \begin{bmatrix} g_{11}(s) & g_{12}(s) & \dots & g_{1n}(s) \\ g_{21}(s) & g_{22}(s) & \dots & g_{2n}(s) \\ \vdots & \vdots & \ddots & \vdots \\ g_{n1}(s) & g_{n2}(s) & \dots & g_{nn}(s) \end{bmatrix}. \quad (3.1)$$

The open-loop SISO transfer function between i^{th} output and j^{th} input when all other inputs are zero is denoted by g_{ij} where $i, j = 1, 2, \dots, n$. The static decoupler D for the above system can be described using (3.2).

$$D = G^{-1}(0) \quad (3.2)$$

Where it is assumed that $G(0)$ is non-singular.

3.4 Low-Level Tuning

The PID controller matrix is expressed as,

$$G_c(s) = \text{diag}\{c_1(s), \dots, c_n(s)\}. \quad (3.3)$$

Where

$$c_i(s) = K_{P_i} + \frac{K_{I_i}}{s} + K_{D_i}s$$

and K_{P_i} , K_{I_i} and K_{D_i} are proportional, integral and derivative gains of the i^{th} PID controller. For the above system, shown in Fig. 3-1, the overall compensated system i.e. process model and static decoupler can be written as,

$$L(s) = G(s)D. \quad (3.4)$$

Where $G(s)$ is the MIMO process modeled assuming an open-loop stable first-order plus dead time model and D is the static de-coupler. Using the truncated Taylor series expansion, the above transfer function $L(s)$ is approximated to a first-order model. Since higher order terms in the Taylor series expansion are made to zero, this approximation is valid only at low frequencies. The approximated system is thus given by,

$$L(s) \approx \begin{bmatrix} \frac{1}{T_{11}s+1} & K_{12}s & \dots & K_{1n}s \\ K_{21}s & \frac{1}{T_{22}s+1} & \dots & K_{2n}s \\ \vdots & \vdots & \ddots & \vdots \\ K_{n1}s & K_{n2}s & \dots & \frac{1}{T_{nn}s+1} \end{bmatrix}. \quad (3.5)$$

Where T_{ii} represents the time constant of the i^{th} SISO loop and

$$K_{ij} ; i \neq j$$

represents off diagonal parameters which represent different loop interactions during steady state. It is clear that at low frequencies the off-diagonal terms are proportional to the frequency (s). Hence the system can be approximately decoupled if the bandwidth of decentralized PID controllers are low enough.

The open-loop transfer function of the system shown in Fig. 3-1 is written as,

$$Q(s) = G(s)DG_c(s) = L(s)G_c(s)$$

$$Q(s) = \begin{bmatrix} q_{11}(s) & q_{12}(s) & \dots & q_{1n}(s) \\ q_{21}(s) & q_{22}(s) & \dots & q_{2n}(s) \\ \vdots & \vdots & \ddots & \vdots \\ q_{n1}(s) & q_{n2}(s) & \dots & q_{nn}(s) \end{bmatrix} \quad (3.6)$$

where

$$q_{ij}(s) = \begin{cases} K_{ij}s(K_{Pi} + \frac{K_{Ii}}{s} + K_{Di}s) & ; i \neq j \\ \frac{K_{Pi} + \frac{K_{Ii}}{s} + K_{Di}s}{T_{ii}s+1} & ; i = j. \end{cases} \quad (3.7)$$

The close-loop relation for this system is expressed as,

$$\mathbf{y} = [I + Q(s)G_c(s)]^{-1}Q(s)G_c(s)\mathbf{r}. \quad (3.8)$$

Where \mathbf{r} and \mathbf{y} are input and out put vectors respectively. Then, the closed transfer matrix $H(s)$ between \mathbf{y} and \mathbf{r} can be written as,

$$H(s) = [I + Q(s)G_c(s)]^{-1}Q(s)G_c(s)$$

$$H(s) = \begin{bmatrix} h_{11}(s) & h_{12}(s) & \dots & h_{1n}(s) \\ h_{21}(s) & h_{22}(s) & \dots & h_{2n}(s) \\ \vdots & \vdots & \ddots & \vdots \\ h_{n1}(s) & h_{n2}(s) & \dots & h_{nn}(s) \end{bmatrix}. \quad (3.9)$$

3.4.1 Tuning 1st loop

When all other loops are open, the elements in first column of $H(s)$ can be written as,

$$h_{i1}(s) = \frac{q_{i1}(s)}{1 + q_{11}(s)} = q_{i1}(s)S_1$$

where $S_1 = (1 + q_{11}(s))^{-1}$ is defined as sensitivity function of the first loop [50]. Thus, for a step input change in the first loop, the interactions to other loops at low frequencies can be computed as,

$$\begin{aligned}
h_{i1}(s) &= \lim_{s \rightarrow 0} q_{i1}(s)S_1 \\
&= \lim_{s \rightarrow 0} K_{i1}s(K_{P1} + \frac{K_{I1}}{s} + K_{D1}s)S_1 \\
&= K_{i1}K_{I1}S_1.
\end{aligned}$$

Then the upper bound of interaction is given by,

$$|h_{i1}(s)| \leq \max_{i \neq 1}(|K_{i1}|) |K_{I1}| (S_1)_{\max} \quad (3.10)$$

where $(S_1)_{\max}$ is the maximum value of S_1 and $\max(|K_{i1}|)$ is the maximum absolute value of $K_{i1}; i \neq 1$. Hence we can introduce interaction index of first loop as,

$$I_1 = \max_{i \neq 1}(|K_{i1}|) |K_{I1}| (S_1)_{\max}. \quad (3.11)$$

The value of K_{I1} can be calculated at particular value of $(S_1)_{\max}$ so that the interaction index, I_1 is kept as low as possible. Then, the rest of interactions can also be reduced according to the inequality (3.10). The proportional gain, K_{P1} of PID controller is computed using time constant of the first-order approximated process and the designed integral gain. The derivative gain, K_{D1} is chosen from ZN formula as,

$$T_{D1} = \frac{1}{4}T_{I1}. \quad (3.12)$$

Where T_{D1} and T_{I1} are derivative and integral time constants for PID controller at the first loop. Then,

$$K_{D1} = \frac{K_{P1}^2}{4K_{I1}}. \quad (3.13)$$

In order to find K_{P1} , In this analysis we use direct pole placement method [70] as follows. The closed loop transfer function of the first loop with reduced first-order model and PID controller is given by,

$$h_{11} = \frac{\frac{K_{D1}s^2 + K_{P1}s + K_{I1}}{T_{11} + K_{D1}}}{s^2 + \left(\frac{1 + K_{P1}}{T_{11} + K_{D1}}\right)s + \frac{K_{I1}}{T_{11} + K_{D1}}}. \quad (3.14)$$

Considering second order dynamics of the numerator in (3.14), the cross over frequency of first loop can be written as,

$$\omega_{o1} = \sqrt{K_{I1}/(T_{11} + K_{D1})}$$

and the proportional gain is given by,

$$K_{P1} = 2\zeta_1\omega_{o1}(T_{11} + K_{D1}) - 1. \quad (3.15)$$

Where ζ_1 is the damping constant of second order system. From (3.13) and (3.15),

$$K_{P1} = \frac{1 \pm \zeta_1 \sqrt{K_{I1}^2 - 4\zeta_1^2 K_{I1}^3 T_{11} + 4K_{I1} T_{11}^2}}{4K_{I1}^2 \zeta_1^2 - 1}. \quad (3.16)$$

The same procedure is repeated for other loops and tuned while keeping interaction index as minimum.

3.4.2 Tuning i^{th} loop:

This section introduce generalized interaction index for $n \times n$ MIMO process system as follows.

$$I_i = \max_{i \neq j} (|K_{ij}|) (|K_{Ii}|) (S_i)_{\max} \quad (3.17)$$

where

$$(S_i)_{\max} = \max(1 + q_{ii}(s))^{-1}$$

is the maximum value of i^{th} loop sensitivity function and the reasonable range of $(S_i)_{\max}$ is 1.3 to 2 [70]. The $\max(|K_{ij}|)$ is the maximum absolute value of $K_{ij}; i \neq j$. The integral and proportional gains of each loop can be evaluated as,

$$K_{Ii} = \frac{I_i}{\max_{i \neq j} (|K_{ij}|) (S_i)_{\max}} \quad (3.18)$$

and

$$K_{Pi} = \frac{1 \pm \zeta_i \sqrt{K_{Ii}^2 - 4\zeta_i^2 K_{Ii}^3 T_{ii} + 4K_{Ii} T_{ii}^2}}{4K_{Ii}^2 \zeta_i^2 - 1}. \quad (3.19)$$

By selecting suitable value for ζ_i , K_{Pi} can be calculated. Then,

$$K_{Di} = \frac{K_{Pi}^2}{4K_{Ii}}. \quad (3.20)$$

3.5 Stability Analysis

3.5.1 Direct Nyquist Array (DNA) Stability Theorem

An analytical expression for the i^{th} Gershgorin band of $Q(s)$ is given by

$$q_{ii}(j\omega) + R_i(\omega)e^{j\theta}, \quad \theta \in [0, 2\pi], \quad \forall \omega.$$

Where

$$R_i(\omega) = \sum_{i,i \neq j} |q_{ij}(j\omega)| \quad \text{for } i = 1, 2, \dots, n \quad (3.21)$$

is radius of i^{th} Gershgorin circle. Then, DNA stability theorem [71],[72],[62] is expressed as follows.

When the Gershgorin bands based on the diagonal elements $q_{ii}(s)$ of $Q(s)$ exclude the point $(-1 + j 0)$ and the i^{th} Gershgorin band encircle the point $(-1 + j 0)$, N_i times anticlockwise, then the closed-loop system is stable if , and only if,

$$\sum_{i=1}^n N_i = p_0$$

where p_0 is the number of unstable poles of $Q(s)$. In this work it is assumed that the open-loop stable process, $Q(s)$ since most of industrial process are open-loop stable systems [73]. Then, $p_0 = 0$ for this stability analysis. Hence, if the Gershgorin bands do not encircle, nor include, the critical point $(-1, j0) \forall i$ the closed-loop system is stable.

3.5.2 Gain and Phase Margins Calculation

Ho *et. al.* [62] has given the definitions for gain and phase margins of MIMO system process as follows. Fig. 3-2 shows a Nyquist diagram with Gershgorin circle at the gain crossover frequency (defined as ω_{gi}) of i^{th} loop. The Gershgorin circle intersects the unit circle at A. At the phase cross over frequency (defined as ω_{pi}), the Gershgorin circle intersects the negative real axis at C as shown in Fig. 3-3. Then the phase and gain margins for the MIMO system are defined as ,

$$\phi'_i = \pi + \arg(\text{AOB}) \quad \text{and} \quad (3.22)$$

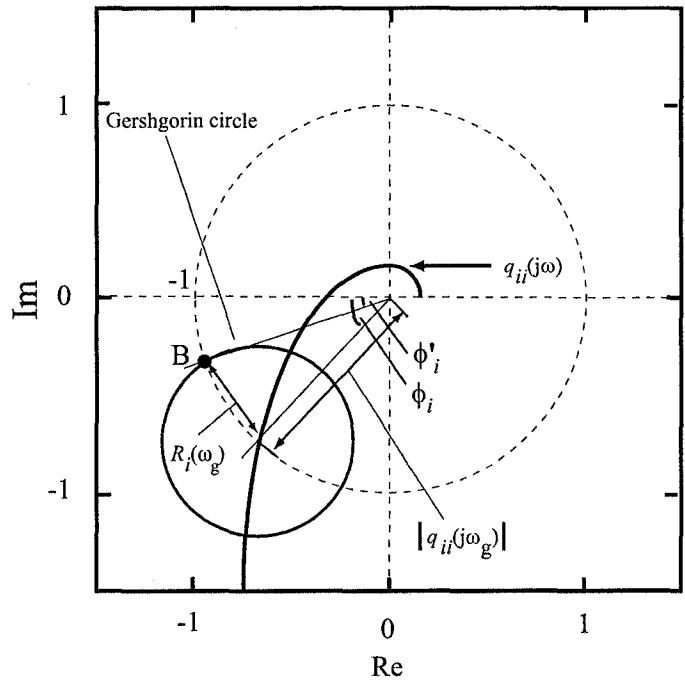


Figure 3-2: Nyquist diagram with the Gershgorin circle at the gain crossover frequency ω_g

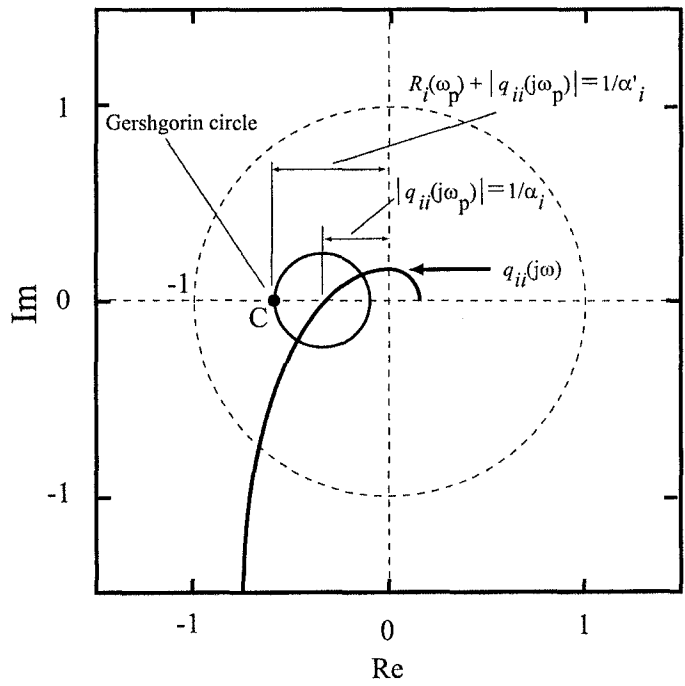


Figure 3-3: Nyquist diagram with the Gershgorin circle at the phase crossover frequency ω_p

$$\alpha'_i = \frac{1}{|\text{OC}|}. \quad (3.23)$$

In order to grantee stability, according to the DNA theorem, the Gershgorin bands should be shaped based on predefined values of ϕ'_i and α'_i so that it excludes and does not encircle the point $(-1 + j 0)$. As a rule of thumb [62], ϕ'_i and α'_i should satisfy the following conditions,

$$30^0 \leq \phi'_i \leq 60^0 \quad \text{and} \quad (3.24)$$

$$2 \leq \alpha'_i \leq 5. \quad (3.25)$$

The ϕ_i in Fig. 3-2 and α_i in Fig. 3-3 are phase and gain margins in the SISO system respectively. Then from Fig. 3-2 the following expression can be derived for ϕ_i

$$\begin{aligned} \phi_i &= \phi'_i + 2 \arcsin \left(\frac{\sum_{i,i \neq j} |q_{ij}(j\omega_{gi})|}{2 |q_{ii}(j\omega_{gi})|} \right) \\ &= \phi'_i + 2 \arcsin \left(\frac{\sum_{i,i \neq j} |g_{ij}(j\omega_{gi})|}{2 |g_{ii}(j\omega_{gi})|} \right). \end{aligned} \quad (3.26)$$

From the Fig. 3-3, α_i

$$\begin{aligned} \alpha_i &= \alpha'_i \left(1 + \frac{\sum_{i,i \neq j} |q_{ij}(j\omega_{pi})|}{2 |q_{ii}(j\omega_{pi})|} \right) \\ &= \alpha'_i \left(1 + \frac{\sum_{i,i \neq j} |g_{ij}(j\omega_{pi})|}{2 |g_{ii}(j\omega_{pi})|} \right). \end{aligned} \quad (3.27)$$

The equivalent gain and phase margins for MIMO system are calculated using (3.26) and (3.27).

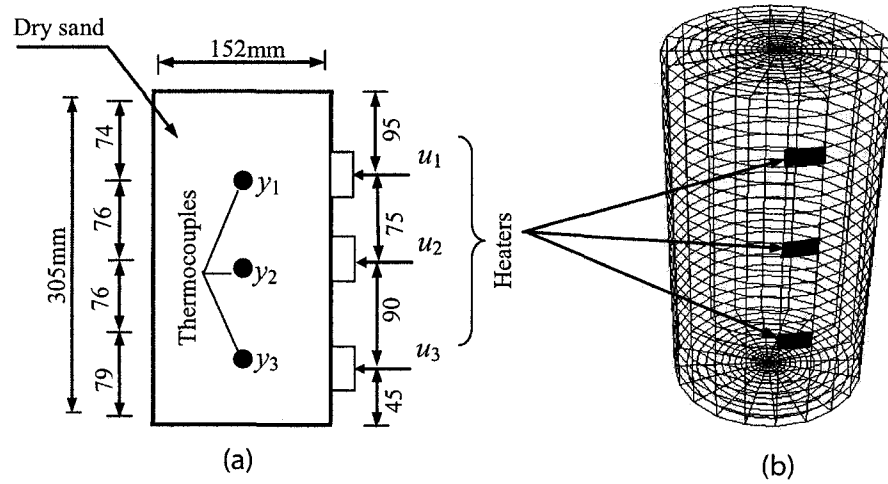


Figure 3-4: Schematic view of soil-cell (a) and finite element based model for soil-cell (b)

3.6 Control Simulation

The proposed PID controllers tuning techniques are applied for a multivariable process with the FE based 3×3 soil- heating processes which is shown in Fig. 3-4. [49]. Here, two transfer functions are derived. The first one is obtained directly from FE method and the second one is obtained by increasing time delay given in FE based model by a factor of two. In addition, the equivalent delayed first-order models for all the higher order sub-processes are obtained by analyzing the response using “plant reaction curve methods” [74]. Then equivalent first-order models with dead time are used to design of PID controllers. Since the models and the processes are mismatch the controllers are more robust for uncertainty. The BLT tuning method also simulated to confirm the superiority of the PID controllers techniques.

3.6.1 Example 1

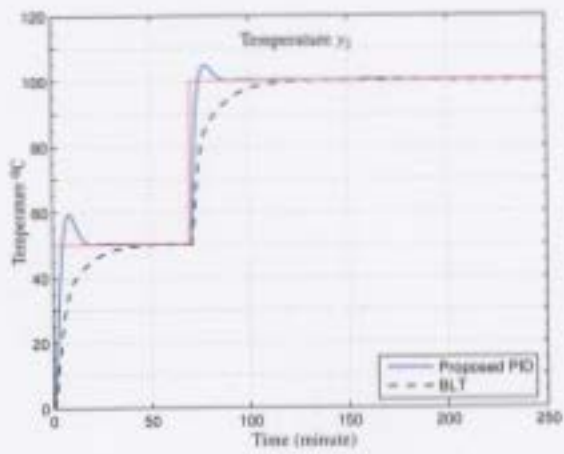
The dynamics of transfer function between heat input (w) and temperature output ($^{\circ}$ C) is described by;

$$\begin{bmatrix} \frac{0.0288e^{-0.6s}}{6.605s^2+5.14s+1} & \frac{0.0119e^{-1.2s}}{97.02s^2+19.7s+1} & \frac{0.00028e^{-3.6s}}{23.52s^2+9.7s+1} \\ \frac{0.0141e^{-1.2s}}{10.11s^2+6.36s+1} & \frac{0.0295e^{-0.6s}}{5.523s^2+4.7s+1} & \frac{0.0035e^{-1.8s}}{23.52s^2+9.7s+1} \\ \frac{0.0015e^{-3.6s}}{17.56s^2+8.38s+1} & \frac{0.0143e^{-1.8s}}{6.605s^2+5.14s+1} & \frac{0.0282e^{-0.6s}}{7.29s^2+5.4s+1} \end{bmatrix}. \quad (3.28)$$

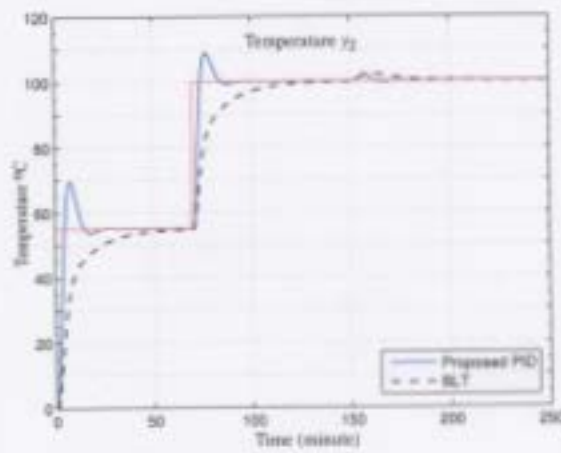
The equivalent first-order model from plant reaction curve is given by;

$$\begin{bmatrix} \frac{0.0288e^{-1.85s}}{4.35s+1} & \frac{0.0119e^{-6s}}{16.05s+1} & \frac{0.00028e^{-5.95s}}{8.1s+1} \\ \frac{0.0141e^{-2.85s}}{6.6s+1} & \frac{0.0295e^{-1.85s}}{3.9s+1} & \frac{0.0035e^{-4.25s}}{7.95s+1} \\ \frac{0.0015e^{-5.65s}}{6.6s+1} & \frac{0.0143e^{-3.05s}}{4.2s+1} & \frac{0.0282e^{-1.9s}}{4.5s+1} \end{bmatrix}. \quad (3.29)$$

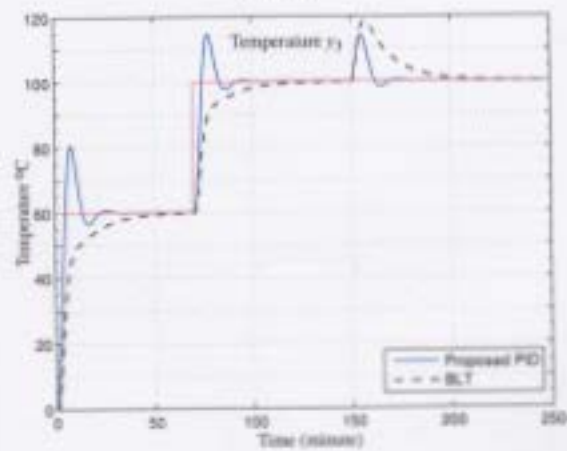
The set points were increased by 50 $^{\circ}$ C, 55 $^{\circ}$ C and 60 $^{\circ}$ C at the beginning of the simulation. Once the outputs reached the initial set points, all variables were changed to 100 $^{\circ}$ C at 70 minute. In order to measure load disturbance rejection capability, a step load disturbance was given to the third input (y_3) of the process. Fig. 3-5 shows responses of this system to step input(reference) and step load disturbance. The system with PID controller has fast set-point tracking and better load disturbance rejection though it has more overshoots compared to the BLT. Tables 3.1 and 3.2 show the comparisons of performance indices of proposed method with BLT method. The controller tuning parameters for individual loop are shown in table 3.3. The gershgorin bands for closed loop system is shown in Fig. 3-6 and the gain and phase margins are shown table 3.4.



(a) y_1



(b) y_2



(c) y_3

Figure 3-5: Example 1, Simulation of closed loop system with PID and BLT controllers

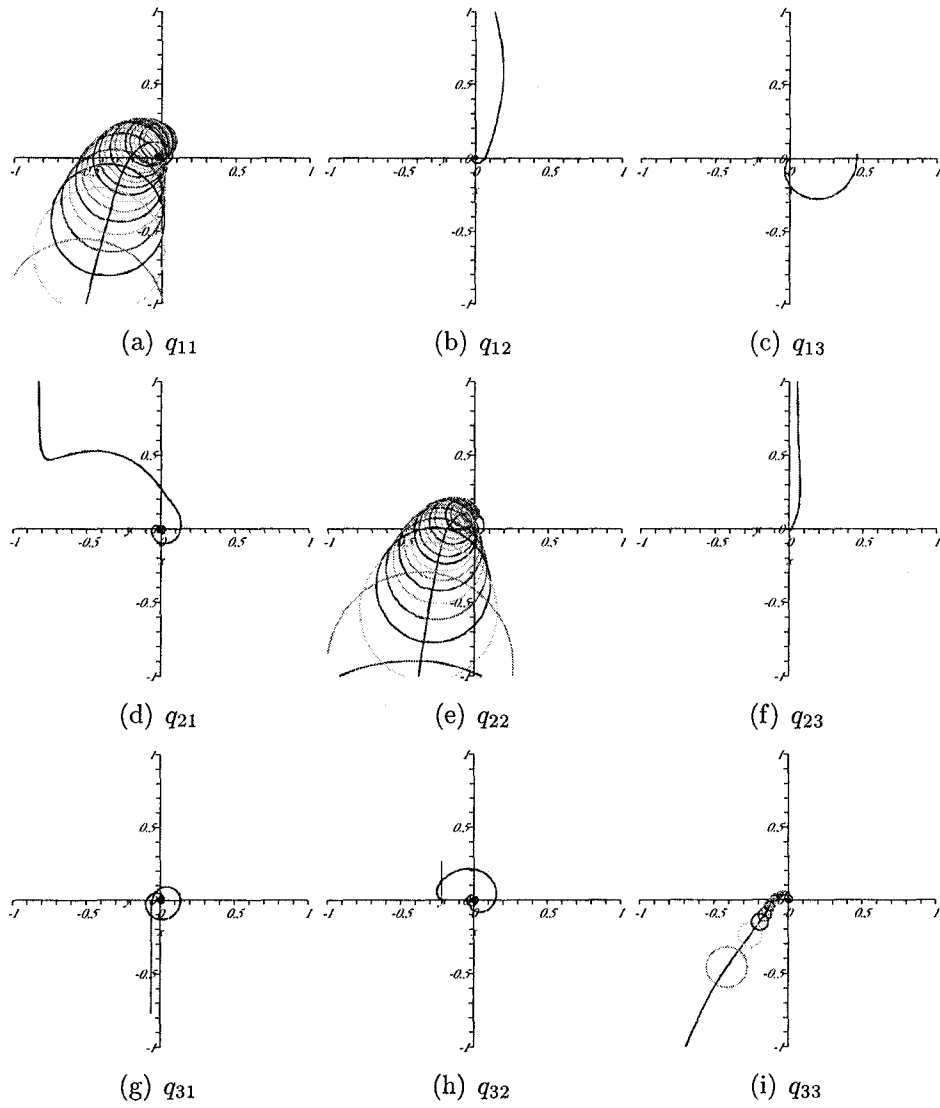


Figure 3-6: Example 1, Nyquist array and Gershgorin bands of system

3.6.2 Example 2

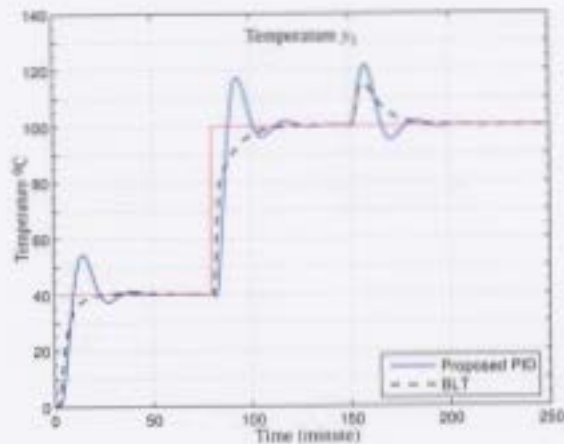
In this example a new transfer function is derived by increasing the time delay two times of each subsystem. The dynamics of this process is described by;

$$\begin{bmatrix} \frac{0.0288e^{-1.2s}}{6.605s^2+5.14s+1} & \frac{0.0119e^{-2.4s}}{97.02s^2+19.7s+1} & \frac{0.00028e^{-7.2s}}{23.52s^2+9.7s+1} \\ \frac{0.0141e^{-2.4s}}{10.11s^2+6.36s+1} & \frac{0.0295e^{-1.2s}}{5.523s^2+4.7s+1} & \frac{0.0035e^{-3.6s}}{23.52s^2+9.7s+1} \\ \frac{0.0015e^{-7.2s}}{17.56s^2+8.38s+1} & \frac{0.0143e^{-3.6s}}{6.605s^2+5.14s+1} & \frac{0.0282e^{-1.2s}}{7.29s^2+5.4s+1} \end{bmatrix}. \quad (3.30)$$

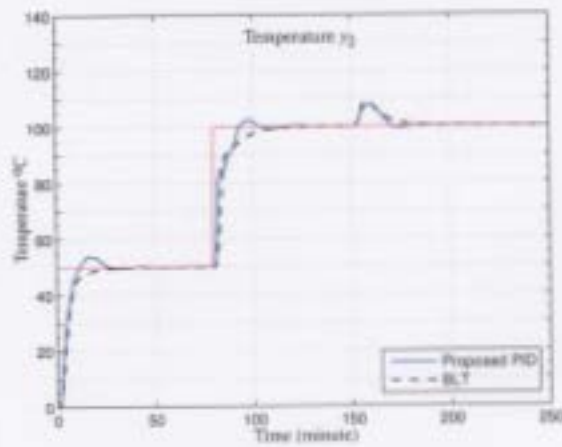
The equivalent first-order model obtained from plant reaction curve is given by;

$$\begin{bmatrix} \frac{0.0288e^{-2.45s}}{4.35s+1} & \frac{0.0119e^{-7.45s}}{16.05s+1} & \frac{0.00028e^{-9.7s}}{8.1s+1} \\ \frac{0.0015e^{-3.5s}}{6.6s+1} & \frac{0.0295e^{-2.4s}}{3.9s+1} & \frac{0.0035e^{-6.05s}}{7.95s+1} \\ \frac{0.0015e^{-9.5s}}{6.6s+1} & \frac{0.0143e^{-4.9s}}{4.2s+1} & \frac{0.0282e^{-2.5s}}{4.5s+1} \end{bmatrix}. \quad (3.31)$$

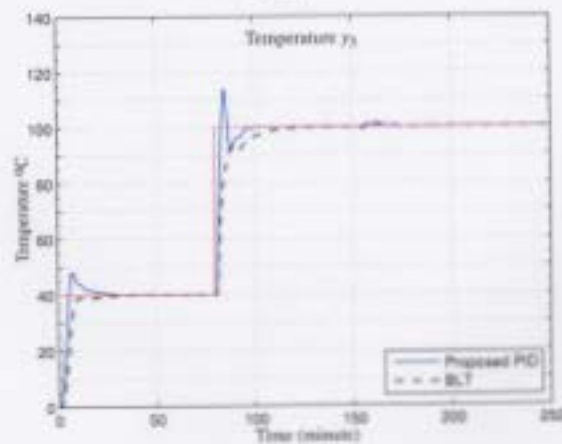
The set points were increased by 40°C, 50°C and 40°C at the beginning of the simulation. Once the outputs reached the initial set points, all variables were changed to 100°C at 80. In order to measure load disturbance rejection capability, a step load disturbance was given to the first input (y_1) of the process. Fig. 3-7 shows responses of this system to step input(reference) and step load disturbance. The system with PID controller has fast set-point tracking though it has bit overshoots compared to BLT. However, all the system show same capability of load disturbance rejection. Tables 3.5 and 3.6 shows the comparisons of performance indices of proposed method with BLT method. The controller tuning parameters for individual loop are shown in table 3.7. The gershgorin bands for closed loop system is shown in Fig. 3-8 and the gain and phase margins are shown table 3.8.



(a) y_1



(b) y_2



(c) y_3

Figure 3-7: Example 2, Simulation of closed loop system with PID and BLT controllers

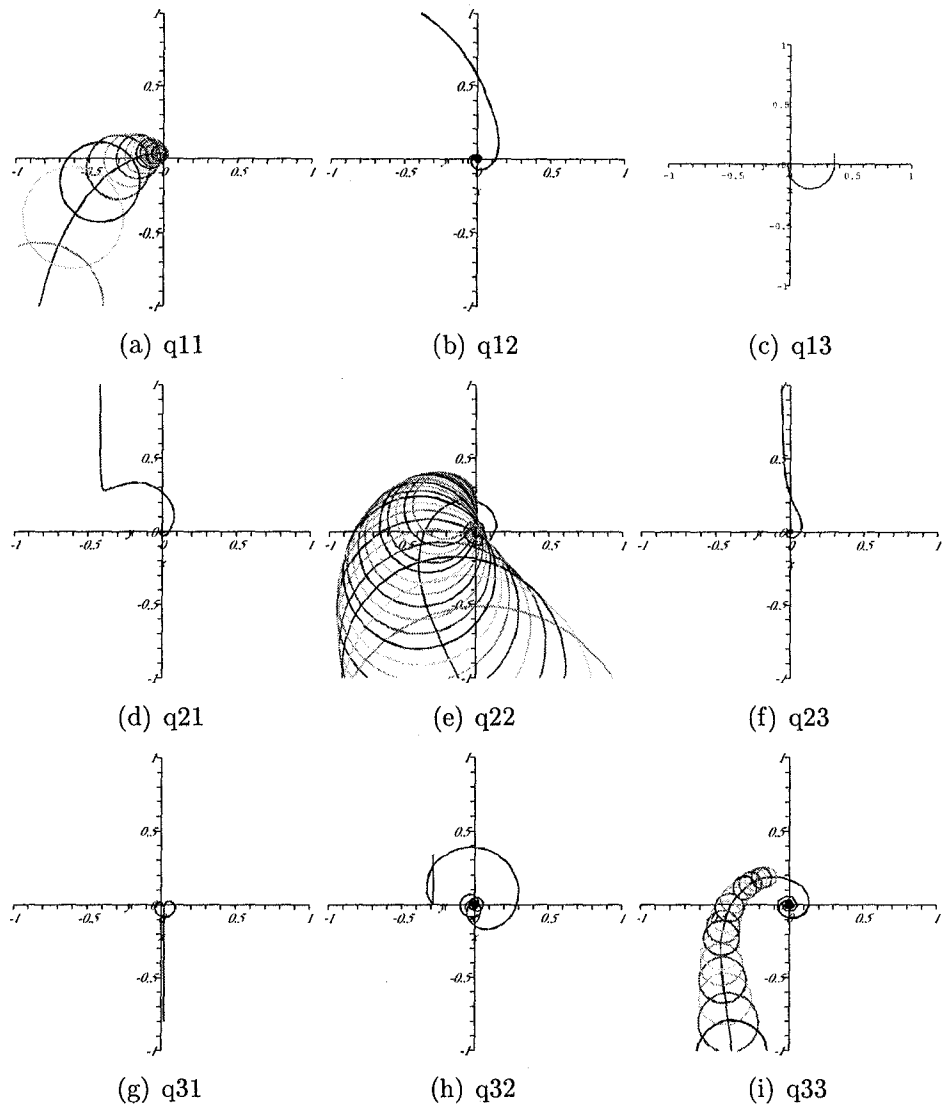


Figure 3-8: Example 2, Nyquist array and Gershgorin bands of system

3.7 Performance Analysis

The proposed algorithm is developed while minimizing the loop interactions at low frequencies which leads to first-order model reduction. Hence, in order to justify the operation of this controller for any frequency, a stability analysis has been then preformed. Nyquist array and Gershgorin bands for the two soil heating examples are drawn for any frequency. In simulations the second order plant has been modeled using plant reaction curve and model/plant mismatch has been already considered. Therefore the results justify the robustness of the proposed method. The gain and phase margins for individual loop are shown in table 3.4 and 3.8 for both examples respectively. The results reveal that gain and phase margins for both the examples are within the specified limits as proposed in Ho *et. al.* [62]. Therefore both the examples confirm to the DNA stability theorem.

Output	Set Point Tracking					
	Rise Time (minute)		Overshoot %		Setting Time (minute)	
	PID	BLT	PID	BLT	PID	BLT
y_1	5	17	19	0	15	27
y_2	5	13	25	0	14	32
y_3	5	8	33	0	19	30

Table 3.1: Performance characteristic indices of proposed PID method and BLT method for set point tracking in example 1

Output	Load Disturbance			
	Overshoot %		Setting Time (minute)	
	PID	BLT	PID	BLT
y_1	2.6	0.64	0	0
y_2	5	4.36	0	0
y_3	28	46	10	34

Table 3.2: Performance characteristic indices of proposed PID method and BLT method for load disturbance in example 1

Loop No	PID			BLT		
	P	I	D	P	I	D
(1)	2.61	0.61	2.79	1.13	0.12	1.00
(2)	2.03	0.57	1.82	0.97	0.11	0.90
(3)	1.70	0.52	1.40	1.14	0.12	1.08

Table 3.3: Tuning parameters of example 1 for PID and BLT controllers

loop No	Gain Margin	Phase Margin
1	2.2	32°
2	2.6	31°
3	8.1	41°

Table 3.4: Gain and Phase Margins of each loop of example 1

Output	Set Point Tracking					
	Rise Time (minute)		Overshoot %		Setting Time (minute)	
	PID	BLT	PID	BLT	PID	BLT
y_1	10	11.6	37	0	30	15
y_2	9	10.3	8	0	22	14
y_3	5	8.4	20	0	6	9

Table 3.5: Performance characteristic indices of proposed PID method and BLT method for set point tracking in example 2

Output	Load Disturbance			
	Overshoot %		Setting Time (minute)	
	PID	BLT	PID	BLT
y_1	34	31	14	26
y_2	12	18	13	20
y_3	1	4	0	0

Table 3.6: Performance characteristic indices of proposed PID method and BLT method for load disturbance in example 2

Loop No	PID			BLT		
	P	I	D	P	I	D
(1)	0.56	0.25	0.32	1.33	0.17	1.63
(2)	1.45	0.23	2.29	1.22	0.16	1.46
(3)	2.34	0.39	3.54	1.35	0.17	1.69

Table 3.7: Tuning parameters of example 2 for PID and BLT controllers

loop No	Gain Margin	Phase Margin
1	3.2	24°
2	3.0	40°
3	8.0	56°

Table 3.8: Gain and Phase Margins of each loop of example 2

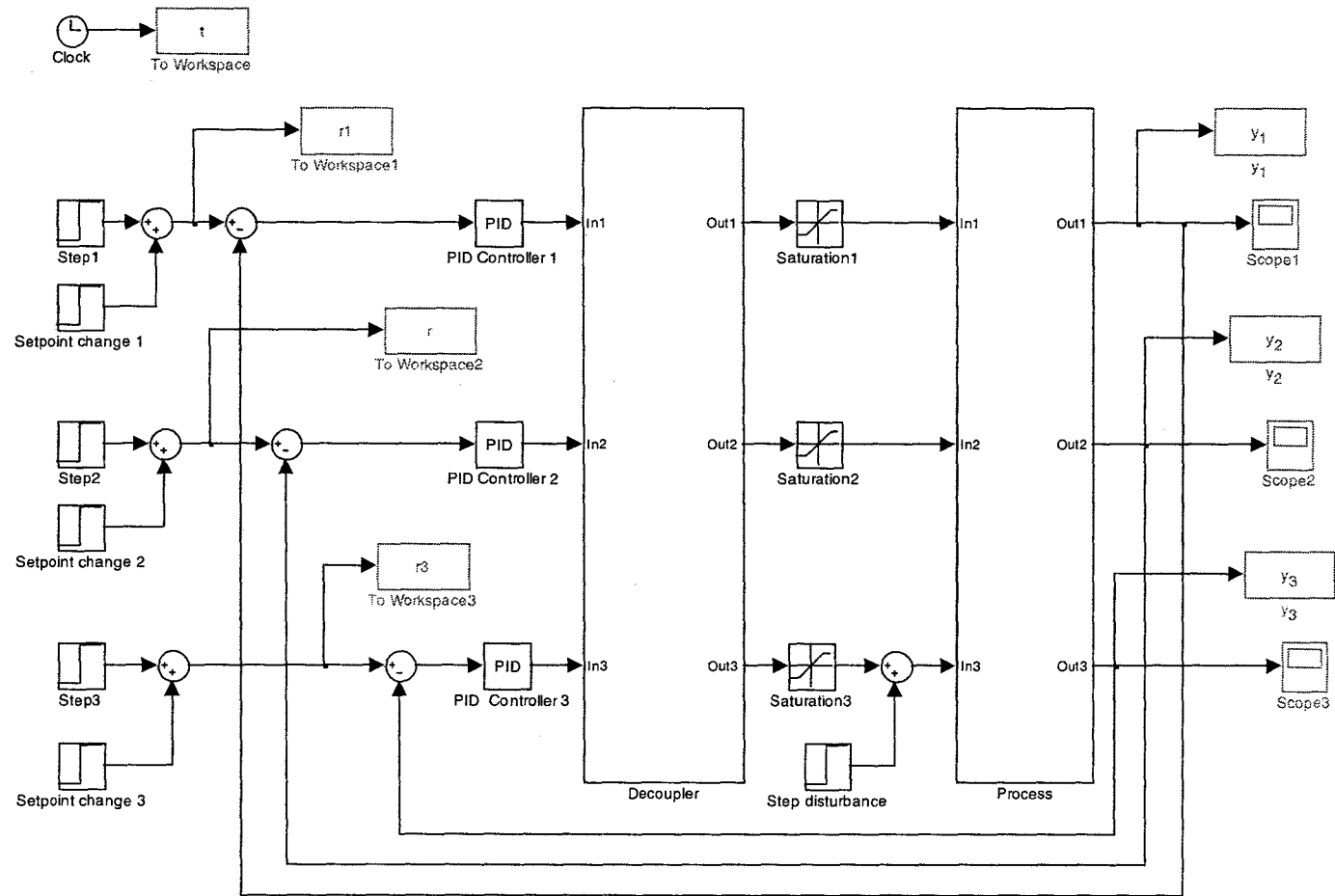


Figure 3-9: SIMULINK implementation of a PID control strategy for the multivariable soil-cell temperature controller

Chapter 4

Non Linear Fuzzy PID Controller Tuning

4.1 Introduction

Fuzzy high-level control of a MIMO process is presented in this chapter in the view SAM fuzzy inference. While the previous chapter presented the way of finding ALG terms (K_p , K_d , and K_i), the objective of this chapter is to find ANG terms for two level tuning of FPID controller.

This chapter investigates application of SAM based FPID controller for multivariable processes in the view of designing ANG terms for high-level tuning. This chapter is organized as follows: First, conventional SAM theorem is described. Secondly, a comprehensive study of two types of FPID configurations are presented. The type I is a conventional Mamdani's type FPID and has three inputs and it produces an incremental FPID signal. The type II uses SISO rule inference to provide decoupled and independent tuning for the three actions in the PID signal. Thirdly, design of SAM is described in the view of FPID controllers for MIMO processes. In this section, high-

level tuning variables which effect nonlinearity of fuzzy output are identified. Finally, the validity of proposed FPID control algorithm is justified with two simulations.

4.2 Background

Some successful applications of FLC have been achieved since the introduction of the first fuzzy controller in 1974. There is a huge volume of FPID applications which are available in the literature where the control has been performed for variety of processes, including nonlinear systems. Almost all of these applications belongs to SISO process systems. Only in a very few applications the MIMO systems processes have been considered. Chieh and Pey [75] used pre-compensator to decouple the MIMO process and it is based on Rosenbrock- Nyquist Array (RNA) method. In the design the FPID parameters have been chosen arbitrary. Gamero and Medrano [48] used FPID controller to control a biotechnology process. They have used dynamic decoupler in order to reduce loop interactions. The controller is based on a two- dimensional Mamdani type fuzzy rule base which uses the feedback error and its rate as inputs. The application of dynamic decoupler for multivariable process is sometimes not physically realizable [3]. Dynamic decoupler is also shown to be more sensitive to plant and process mismatch and therefore is less popular in process control. In another application, Rahmati *et. al.* [42] used FPID controller for HVAC plant. They have presented similarity between conventional digital PID control algorithm and Takagi-Sugeno based FPID control. Recently, Shaoyuan *et. al.* [76] presented coordinated control strategy for boiler- turbine control using fuzzy reasoning and auto-tuning techniques. Self-organizing FPID controller is presented by Hassan *et. al.* [77] for robot arm. In these applications fuzzy logic controllers are used at supervisory level for self tuning of conventional PID gains at the lower level.

4.3 High-Level Tuning : Nonlinearity Tuning

4.3.1 Standard Additive Model (SAM)

FLC is a rule-based controller and it does not require a very precise mathematical model of the processes under control. The FLC uses fuzzy linguistic variables (if-then rules) to solve the complex system control problems. This model freedom improves the modeling power of FLC. These input(error) maps output(control action). An additive fuzzy system (controller) fire all rules in parallel to some degree. Then the system weights and average then-part fuzzy set to infer output fuzzy set [78], [79]. Finally, the system defuzzifies the output fuzzy set using centroid or other operation which maps input to fuzzy output. Simply, an additive fuzzy system is a function approximator and the SAM is the simplest form of an additive fuzzy system. Bart Kosko was the pioneer to introduce SAM [36]. According to Kosko, an additive FLC divides the global conditional mean in to a convex sum of local conditional means while the conventional centroids type FLC computes the conditional mean as output. The then-part fuzzy set of the SAM consist of centroid and area or volume. The SAM theorem, [36] which is described in next section allow to compute these volumes and centroids in advance.

Consider fuzzy rules of the form

$$\text{IF } X = A_\alpha \text{ THEN } Y = B_\beta$$

where X and Y be nonempty sets. When λ and ζ be nonempty index sets, the $A_\alpha : \alpha \in \lambda$ and $B_\beta : \beta \in \zeta$ represent input fuzzy set of X and output fuzzy sets of Y respectively. An additive fuzzy system stores m number of above fuzzy rules. These rules describe fuzzy subsets or fuzzy patches in the Cartesian product space $X \times Y$ as

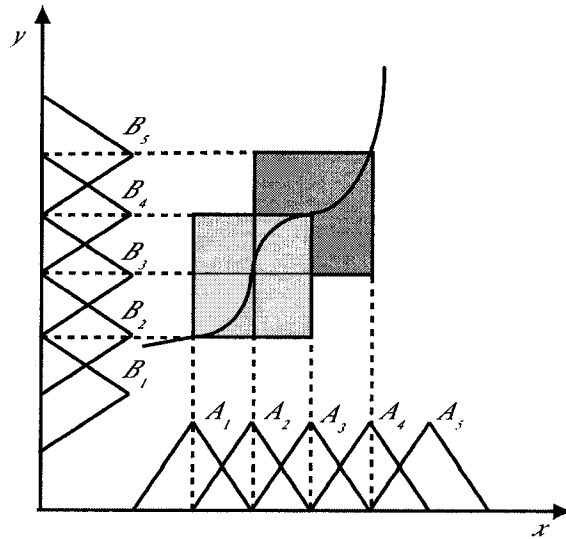


Figure 4-1: Function approximator: Additive fuzzy system

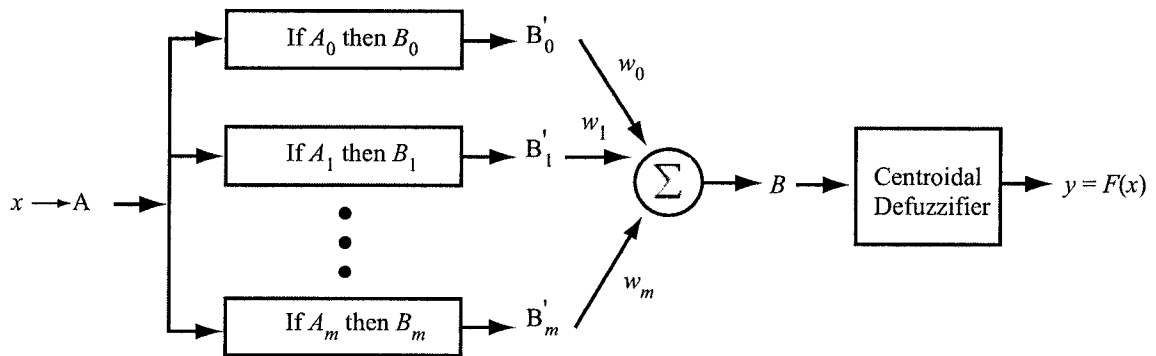


Figure 4-2: General framework of additive fuzzy system

shown in the Fig.4-1. Hence an additive fuzzy system (collection of IF-THEN rules) approximates a function $F : X \rightarrow Y$.

The general framework for a feed forward additive fuzzy system is shown in Fig. 4-2. The each input x fires the if-part of all m rules to some degree in parallel. Then the system weights (using rule weight w_m) the then-part to give the new fuzzy sets B'_β and then sums these to form the output sets B as,

$$B = \sum_{\beta=1}^m w_{\beta} B'_{\beta}(x). \quad (4.1)$$

The weights w_j is used to reflect rule credibility or frequency and then it gives an extra term for a learning system to tune. In practice the rule weights are assumed to be equal to unity: $w_1 = \dots = w_m = 1$ The SAM is a special case of the additive model framework.

The inference of the SAM algorithm is as follows,

1. The fired then-part set B'_{β} is the fit product $a_{\beta}(x)B_{\beta}$. Where the fit value $a_{\beta}(x)$ (a_{β} is called membership function) express the degree to which the input x belongs to the if-part fuzzy set A_{α} . Then the output set can be expressed as,

$$B = \sum_{\beta=1}^m w_{\beta} a_{\beta}(x) B_{\beta}(x). \quad (4.2)$$

2. The system output $F(x)$ computes as centroid of output set $B(x)$ when it defuzzifies $B(x)$ to scalar or vector.

$$F(x) = \text{Centroid} \left(\sum_{\beta=1}^m w_{\beta} a_{\beta}(x) B_{\beta}(x) \right) \quad (4.3)$$

The centroid gives the structure of a conditional expectation to the fuzzy system F and it acts as an optimal nonlinear approximator in the mean-squared sense.

4.3.2 SAM Theorem

Suppose the fuzzy system $F : R^n \rightarrow R^p$ is a standard additive model as 4.3. Then $F(x)$ is a convex sum of the m then-part set centroids:

$$\begin{aligned} F(x) &= \frac{\sum_{\beta=1}^m w_{\beta} a_{\beta}(x) V_{\beta} C_{\beta}}{\sum_{\beta=1}^m w_{\beta} a_{\beta}(x) V_{\beta}} \\ &= \sum_{\beta=1}^m p_{\beta}(x) C_{\beta} . \end{aligned} \quad (4.4)$$

The convex coefficients or discrete probability weights $p_1(x), \dots, p_m(x)$ depends on the input x through the ratios

$$p_{\beta}(x) = \frac{w_{\beta} a_{\beta}(x) V_{\beta}}{\sum_{k=1}^m w_k a_k(x) V_k} . \quad (4.5)$$

V_{β} is the finite positive volume (or area if $p = 1$ in the range space R^p) and C_{β} is the centroid of then-part set B_{β} :

$$V_{\beta} = \int_{R^p} b_{\beta}(y_1, \dots, y_p) dy_p > 0 \quad (4.6)$$

$$C_{\beta} = \frac{\int_{R^p} y b_{\beta}(y_1, \dots, y_p) dy_1 \dots dy_p}{\int_{R^p} b_{\beta}(y_1, \dots, y_p) dy_1 \dots dy_p} . \quad (4.7)$$

The popular scalar case of $p = 1$ reduces (4.6) and (4.7) to

$$V_{\beta} = \int_{-\infty}^{\infty} b_{\beta}(y) dy \quad (4.8)$$

$$C_\beta = \frac{\int_{-\infty}^{\infty} y b_\beta(y) dy}{\int_{-\infty}^{\infty} b_\beta(y) dy}. \quad (4.9)$$

Then SAM theorem allows us to calculate these volumes and centroids (or local conditional means) in advance. They change only when the system learns or tunes its rules or when a user varies them in the system. Each input x requires to compute only the m_β fit values, $a_\beta(x)$, and then update the ratio in (4.4). The consequent fuzzy sets B_β can take the form of triangular or trapezoidal or bell type curves where area and centroids of those shapes can easily be computed. The SAM structure (4.4) lets us replace all then-part fuzzy sets (consequent) B_β with rectangle or non fuzzy sets R_β that have the same volume V_β and centroid c_β without rather changing the output value $F(x)$.

4.3.3 Design of SAM; Identification of High-Level Tuning Variables

Consider two control regions in the controller output space. The first region is when the normalized error variables are $-1 \leq \hat{e}_i < 0$. The local control in this region affects steady state, load disturbance and overshoot properties. The second region is when $0 \leq \hat{e}_i \leq 1$. The control in this region affects the speed of response during the transient, undershoot and steady state properties. The aim is now to realize independent adjustment of FLC parameters in the view of changing ANG terms at the chosen control points. The membership functions (a_i) for the if-part fuzzy in SAM is defined as triangle functions as shown in the Fig. 4-4. The slope angle θ for type II (see figure 4-3(b)) can be described by,

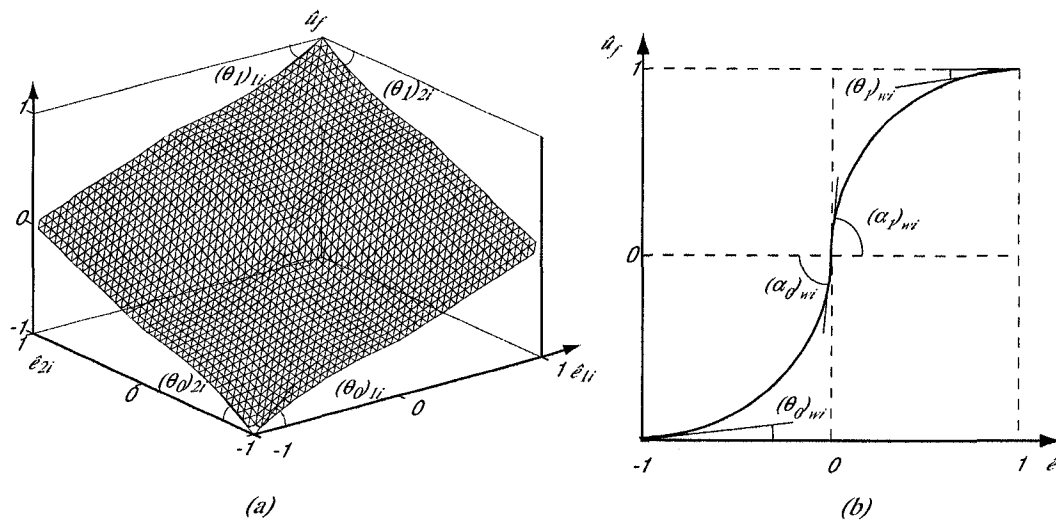


Figure 4-3: Nonlinear tuning variables measured at local control points of SAM

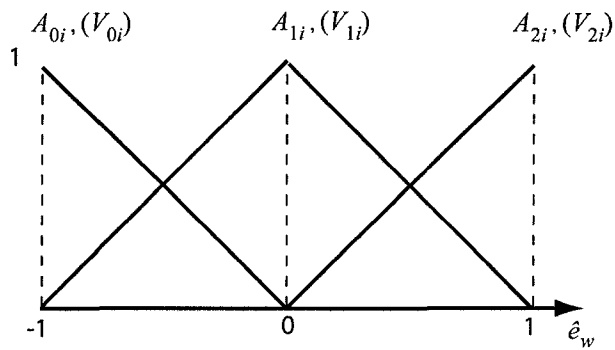


Figure 4-4: Membership functions for if-part in SAM

$$\theta = \begin{cases} \arctan \left(\frac{V_{0i}(2\hat{e}_i V_{0i} C_{0i} - 2C_{0i} V_{1i} \hat{e}_i - C_{0i} V_{1i} + V_{1i} C_{1i})}{(\hat{e}_i V_{0i} - \hat{e}_i V_{1i} - V_{1i})^2} \right) \\ \text{for } -1 \leq \hat{e}_i < 0 \\ \arctan \left(-\frac{V_{2i} V_{1i} (-C_{2i} + C_{1i})}{(V_{1i} \hat{e}_i - V_{1i} - V_{2i} \hat{e}_i)^2} \right) \\ \text{for } 0 \leq \hat{e}_i \leq 1 \end{cases} \quad (4.10)$$

In this analysis, the then-part centroids C_{wi} are selected as,

$$C_{0i} = -1, C_{1i} = 0 \text{ and } C_{2i} = 1. \quad (4.11)$$

The overall gain of the system can also be changed by ANG. Therefore, in order to maintain stability the maximum and minimum ANG terms are evaluated and they should be controlled while follow the stability theory. In the SAM this occurs at $\hat{e}_i = -1$, $\hat{e}_i = 0$ and $\hat{e}_i = 1$. Thus, the slope angle at selected four points (see figure4-3) are,

$$(\theta_0)_{wi} = \arctan(V_{1i}/V_{0i}) \quad (4.12)$$

$$(\alpha_0)_{wi} = \arctan(V_{0i}/V_{1i}) \quad (4.13)$$

$$(\theta_1)_{wi} = \arctan(V_{1i}/V_{2i}) \quad (4.14)$$

$$(\alpha_1)_{wi} = \arctan(V_{2i}/V_{1i}) \quad (4.15)$$

It is clear, the pairs $\{(\theta_0)_{wi}, (\alpha_0)_{wi}\}$ and $\{(\theta_1)_{wi}, (\alpha_1)_{wi}\}$ form right angle. i.e There are two independent angle over the control surface of SAM corresponding to two regions $-1 \leq \hat{e}_i < 0$ and $0 \leq \hat{e}_i \leq 1$. $(\theta_0)_{wi}$ and $(\theta_1)_{wi}$ are selected as two independent slope angles which can be controlled within the range of $[0 - 90^0]$.

In order to find two independent angles, the then-part volume for second membership

function is selected as unity: $V_{1i} = 1$.

Then,

$$\theta_0 = \arctan(1/V_0) \quad (4.16)$$

$$\theta_1 = \arctan(1/V_2) \quad (4.17)$$

Hence the terms V_0 and V_2 are the nonlinear tuning variable for the SAM.

4.4 Nonlinearity Analysis of Fuzzy SAM output

The superiority of fuzzy control over linear control is mainly due to the nonlinear mapping in the inference system. This will permit the system to change the controller gains adaptively with the change of error. In a properly designed fuzzy controller the high-level tuning generally provides the improved control performance. In fact there are many other fuzzy systems available, such as Zadeh-Mamdani's "max-min-gravity" (MMG), Mizumoto's "product-sum-gravity" (PSG) and "Takagi-Sugeno-Kang" (TSK) schemes to achieve the same nonlinear mapping. However, the properly designed fuzzy system should allow the controller to have a greater degree of nonlinearity variation to accommodate better control. The work shown in [80] compares different fuzzy systems against nonlinearity. The nonlinearity measures identify admissible area drawn in a nonlinearity variation diagram.

The study of nonlinearity variations is quite novel at present. As described below two quantitative indices [81], [82], [80] which demonstrate how to implement a systematic design for nonlinearity variation is considered.

- 1) Nonlinearity Variation Index (NVI):

Suppose any design parameters related to fuzzy structures are called nonlinear tuning parameters. By increasing the number of these parameters will increase the nonlinearity variations, but this will make the nonlinearity evaluation difficult. For simplicity and without losing generality, it is considered the simplest rules (say, two or three in this work) and two nonlinear tuning parameters for the comparative study. Since a one-input fuzzy controller only involves a control curve design, the nonlinearity analysis will be based on a two-dimensional space. The θ_0 and θ_1 are the angles in radians corresponding to the curve slopes ($\frac{\partial \hat{u}_f}{\partial \hat{e}_{wi}}$) at $\hat{e}=-1$ and $\hat{e}=1$ respectively.

To examine the nonlinearity variations approximately, the admissible area (or curve) of the nonlinearity diagram on the θ_0 and θ_1 plane is drawn. The θ_0 and θ_1 are called nonlinearity examination parameters. A point within the admissible area (or on the admissible curve) means that the control curve corresponding to the chosen point and can be produced by the controller. The larger the admissible area, the greater the flexibility of the system in generating the nonlinear functions. The NVI is defined in a dimensionless form as,

$$\text{NVI}(N_v, N_t, N_e) = \frac{\text{admissible region in } N_e \text{ dimensional space}}{\text{whole region in } N_e \text{ dimensional space}} \quad (4.18)$$

where N_v, N_t and N_e are the total number of input variable, non linear tuning parameters and non liner examination parameters, respectively.

2) Linearity Approximation Index (LAI):

A conservative design strategy for a FPID controller is proposed [82]: A FPID controller should be able to perform a linear, or approximately linear, PID function such that the system performance is no worse than its conventional counterpart. If the controller is able to generate a perfect linear function, it is a guaranteed-PID-performance (GPP) system. Along the line of this strategy, a safe performance bound

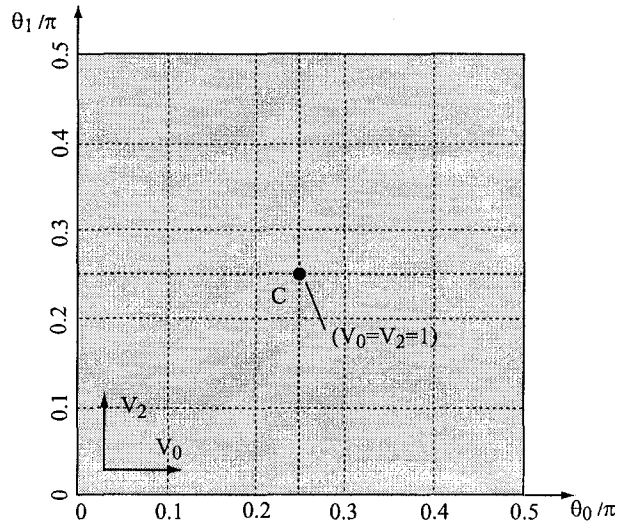


Figure 4-5: Admissible area (grey) of nonlinearity diagram for SAM controller

is produced for the FPID system from the performance analysis of its counterpart that has the same PID connective structure. For examining the system on this aspect, an LAI is given by,

$$\text{LAI} = 1 - \frac{\max |\hat{u}_f(\hat{e}) - \bar{u}_f(\hat{e})|}{\max |\bar{u}_f(\hat{e})|} \quad (4.19)$$

where $\bar{u}_f(\hat{e})$ is a linear function which is imposed to pass through the origin point, $\bar{u}_f(\hat{e})(\hat{e} = -1)$ and the ending point $\bar{u}_f(\hat{e})(\hat{e} = 1)$. This index, representing the most linearity approximation that can be produced by the controller, is normalized within a range of $[0, 1]$. When LAI=1, it corresponds to a perfect linear PID controller. The larger the value of LAI, the higher degree of linear approximation the FPID controller produces. This index is a quantitative measure of confidence in using a GPP bound calculated from the linear PID controller.

Fig. 4-5 shows the nonlinearity variation diagram for SAM which is designed in previous section. Since the angle θ_0 and θ_1 can independently changed it has full contour of admissible area. The point C, corresponding to the linear function

Fuzzy system	NVI(1,2,2)	LAI
MMG	0.755	0.974
PSG	Admissible line	1
TSK	0.695	1
SAM	1	1

Table 4.1: Nonlinearity variation indices for different fuzzy systems

approximation of SAM and it is located at $\theta_0 = \theta_1 = \pi/4$. The table 4.1 summarize the nonlinearity evaluation indices for different fuzzy systems (most popular) along with SAM. As it can be seen in the table 4.1, the SAM scheme produces the highest score in terms of nonlinearity variations.

4.5 Stability Analysis

4.5.1 Maximum values of PID parameters

In order to grantee the stability we can specify the predefined gain margin α'_i and phase margin ϕ'_i of MIMO process so that it satisfy (3.24) and (3.25). The Limits of PID parameters can then be calculated for i^{th} loop. Following four equations can be used to calculate the four unknowns, ω_{pi} , ω_{gi} , K_{Pi} and K_{Ii} in i^{th} loop.

$$\alpha_i = \frac{1}{|g_{ii}(j\omega_{pi})c_i(j\omega_{pi})|} \quad (4.20)$$

$$\arg[g_{ii}(j\omega_{pi})c_i(j\omega_{pi})] = -\pi \quad (4.21)$$

$$\phi_i = \pi + \arg[g_{ii}(j\omega_{gi})c_i(j\omega_{gi})] \quad (4.22)$$

$$|g_{ii}(j\omega_{gi})c_i(j\omega_{gi})| = 1 \quad (4.23)$$

Substituting from (3.26) and (3.27) in (4.20)-(4.23),

$$f_{1,i} = \alpha'_i |c_i(j\omega_{pi})| \{ |g_{ii}(j\omega_{pi})| + \sum_{i,i \neq j} |q_{ij}(j\omega_{pi})| \} - 1 = 0 \quad (4.24)$$

$$f_{2,i} = \arg[g_{ii}(j\omega_{pi})c_i(j\omega_{pi})] + \pi = 0 \quad (4.25)$$

$$\begin{aligned} f_{3,i} &= \pi + \arg[g_{ii}(j\omega_{gi})c_i(j\omega_{gi})] - \phi'_i - 2 \arcsin \left(\frac{\sum_{i,i \neq j} |g_{ij}(j\omega_{gi})|}{2 |g_{ii}(j\omega_{gi})|} \right) \\ &= 0 \end{aligned} \quad (4.26)$$

$$f_{4,i} = |g_{ii}(j\omega_{gi})c_i(j\omega_{gi})|^2 - 1 = 0 \quad (4.27)$$

Then it can be defined

$$K_{Pi \max} \text{ and } K_{Ii \max} \quad (4.28)$$

as maximum values of PI parameters at a given ϕ'_i and α'_i . From (3.13),

$$K_{Di \max} = \frac{K_{Pi \max}^2}{4K_{Ii \max}}. \quad (4.29)$$

The Newton-Raphson methods can be used to solve (4.24)-(4.27) as follows,

$$\begin{bmatrix} \frac{\partial f_{1,i}}{\partial K_{Pi}} \Big|_{K_{Pi}^{(r)}} & \frac{\partial f_{1,i}}{\partial K_{Ii}} \Big|_{K_{Ii}^{(r)}} & \frac{\partial f_{1,i}}{\partial \omega_{pi}} \Big|_{\omega_{pi}^{(r)}} & \frac{\partial f_{1,i}}{\partial \omega_{gi}} \Big|_{\omega_{gi}^{(r)}} \\ \frac{\partial f_{2,i}}{\partial K_{Pi}} \Big|_{K_{Pi}^{(r)}} & \frac{\partial f_{2,i}}{\partial K_{Ii}} \Big|_{K_{Ii}^{(r)}} & \frac{\partial f_{2,i}}{\partial \omega_{pi}} \Big|_{\omega_{pi}^{(r)}} & \frac{\partial f_{2,i}}{\partial \omega_{gi}} \Big|_{\omega_{gi}^{(r)}} \\ \frac{\partial f_{3,i}}{\partial K_{Pi}} \Big|_{K_{Pi}^{(r)}} & \frac{\partial f_{3,i}}{\partial K_{Ii}} \Big|_{K_{Ii}^{(r)}} & \frac{\partial f_{3,i}}{\partial \omega_{pi}} \Big|_{\omega_{pi}^{(r)}} & \frac{\partial f_{3,i}}{\partial \omega_{gi}} \Big|_{\omega_{gi}^{(r)}} \\ \frac{\partial f_{4,i}}{\partial K_{Pi}} \Big|_{K_{Pi}^{(r)}} & \frac{\partial f_{4,i}}{\partial K_{Ii}} \Big|_{K_{Ii}^{(r)}} & \frac{\partial f_{4,i}}{\partial \omega_{pi}} \Big|_{\omega_{pi}^{(r)}} & \frac{\partial f_{4,i}}{\partial \omega_{gi}} \Big|_{\omega_{gi}^{(r)}} \end{bmatrix} \begin{bmatrix} \delta_{1i}^{(r)} \\ \delta_{2i}^{(r)} \\ \delta_{3i}^{(r)} \\ \delta_{4i}^{(r)} \end{bmatrix} = \begin{bmatrix} f_{1,i}^{(r)} \\ f_{2,i}^{(r)} \\ f_{3,i}^{(r)} \\ f_{4,i}^{(r)} \end{bmatrix} \quad (4.30)$$

For each iteration, K_{P_i} , K_{I_i} , ω_{p_i} and ω_{g_i} are updated as follows,

$$\begin{bmatrix} K_{P_i}^{(r+1)} \\ K_{I_i}^{(r+1)} \\ \omega_{p_i}^{r+1} \\ \omega_{g_i}^{r+1} \end{bmatrix} = \begin{bmatrix} K_{P_i}^{(r)} \\ K_{I_i}^{(r)} \\ \omega_{p_i}^r \\ \omega_{g_i}^r \end{bmatrix} + \begin{bmatrix} \delta_{1i}^{(r)} \\ \delta_{2i}^{(r)} \\ \delta_{3i}^{(r)} \\ \delta_{4i}^{(r)} \end{bmatrix} \quad (4.31)$$

Since PID gains are proportional to the slopes of the control surface shown in Fig. 4-3, we can find maximum values of slopes angle corresponding to $K_{P_i \max}$, $K_{I_i \max}$ and $K_{D_i \max}$.

For instance, let the proportional SAM based fuzzy controller for i^{th} has high-level tuning parameters: V_0 and V_2 . From (4.16):(4.17) following expression can be derived

$$\begin{aligned} V_{0 \min} = V_{2 \min} &= K_{P_i} / K_{P_i \max} \\ V_{0 \max} = V_{2 \max} &= K_{P_i \max} / K_{P_i} \end{aligned} \quad (4.32)$$

Then limiting angles for θ_0 , α_0 , θ_1 and α_1 can expressed as,

$$\theta_{0 \max} = \alpha_{0 \max} = \theta_{1 \max} = \alpha_{1 \max} = \arctan(K_{P_i \max} / K_{P_i}) \quad \text{and} \quad (4.33)$$

$$\theta_{0 \min} = \alpha_{0 \min} = \theta_{1 \min} = \alpha_{1 \min} = \arctan(K_{P_i} / K_{P_i \max}) \quad (4.34)$$

If $\{K_{P_i \max} / K_{P_i} \geq 1.571\}$, the fuzzy controller has independent variations of θ_0 and θ_1 within the range $[0 \ 90^\circ]$. Otherwise, it has feasible stability region as shown in Fig. 4-6.

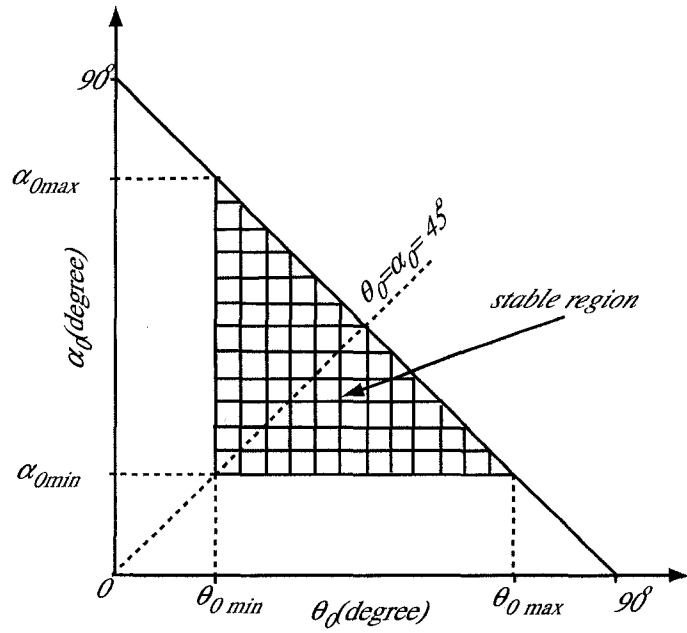


Figure 4-6: Stability region for θ_0 and α_0 . It is same for θ_1 and α_1

4.6 Control Simulation

Here, two examples which are previously simulated in the last chapter are re-simulated with FPID controllers.

4.6.1 Example 1

The dynamics of transfer function between heat input (W) and temperature output ($^{\circ}C$) is described by;

$$\begin{bmatrix} \frac{0.0288e^{-0.6s}}{6.605s^2+5.14s+1} & \frac{0.0119e^{-1.2s}}{97.02s^2+19.7s+1} & \frac{0.00028e^{-3.6s}}{23.52s^2+9.7s+1} \\ \frac{0.0141e^{-1.2s}}{10.11s^2+6.36s+1} & \frac{0.0295e^{-0.6s}}{5.523s^2+4.7s+1} & \frac{0.0035e^{-1.8s}}{23.52s^2+9.7s+1} \\ \frac{0.0015e^{-3.6s}}{17.56s^2+8.38s+1} & \frac{0.0143e^{-1.8s}}{6.605s^2+5.14s+1} & \frac{0.0282e^{-0.6s}}{7.29s^2+5.4s+1} \end{bmatrix} \quad (4.35)$$

The equivalent first-order model from plant reaction curve is given by;

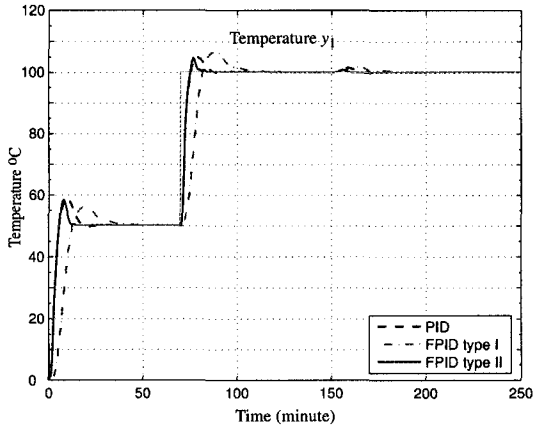
$$\begin{bmatrix} \frac{0.0288e^{-1.85s}}{4.35s+1} & \frac{0.0119e^{-6s}}{16.05s+1} & \frac{0.00028e^{-5.95s}}{8.1s+1} \\ \frac{0.0141e^{-2.85s}}{6.6s+1} & \frac{0.0295e^{-1.85s}}{3.9s+1} & \frac{0.0035e^{-4.25s}}{7.95s+1} \\ \frac{0.0015e^{-5.65s}}{6.6s+1} & \frac{0.0143e^{-3.05s}}{4.2s+1} & \frac{0.0282e^{-1.9s}}{4.5s+1} \end{bmatrix}. \quad (4.36)$$

The set points were increased by 50°C, 55°C and 60°C at the beginning of the simulation. Once the outputs reached the initial set points, all variables were changed to 100°C at 70 minute. In order to measure load disturbance rejection capability, a step load disturbance was given to the third input (y_3) of the process. Fig. 4-7 shows responses of this system to step input(reference) and step load disturbance. The system with FPID type II controller has less over shoot and better load disturbance rejection. Tables 4.2 and 4.3 show the comparisons of performance indices. The controller tuning parameters for individual loop are shown in table 4.4.

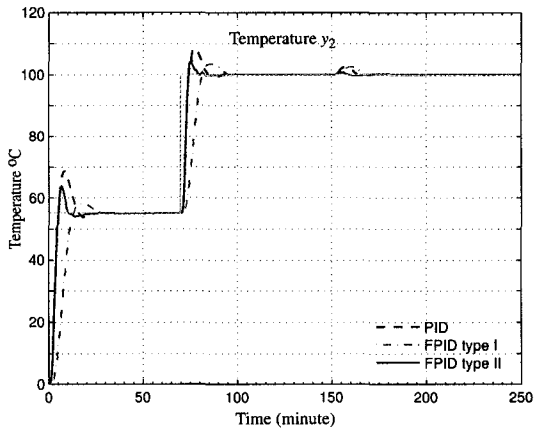
4.6.2 Example 2

In this example a new transfer function is derived by increasing the time delay two times of each subsystem. The dynamics of this process is described by;

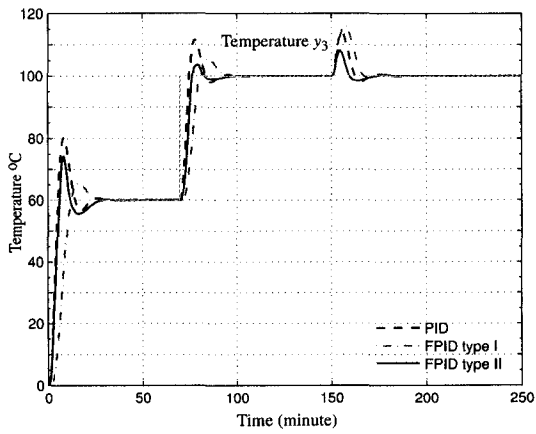
$$\begin{bmatrix} \frac{0.0288e^{-1.2s}}{6.605s^2+5.14s+1} & \frac{0.0119e^{-2.4s}}{97.02s^2+19.7s+1} & \frac{0.00028e^{-7.2s}}{23.52s^2+9.7s+1} \\ \frac{0.0141e^{-2.4s}}{10.11s^2+6.36s+1} & \frac{0.0295e^{-1.2s}}{5.523s^2+4.7s+1} & \frac{0.0035e^{-3.6s}}{23.52s^2+9.7s+1} \\ \frac{0.0015e^{-7.2s}}{17.56s^2+8.38s+1} & \frac{0.0143e^{-3.6s}}{6.605s^2+5.14s+1} & \frac{0.0282e^{-1.2s}}{7.29s^2+5.4s+1} \end{bmatrix}. \quad (4.37)$$



(a) y_1



(b) y_2



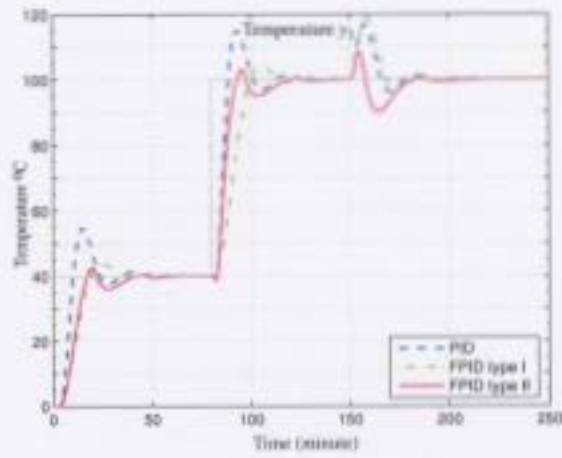
(c) y_3

Figure 4-7: Example 1, Simulation of closed loop system with PID and FPID controllers

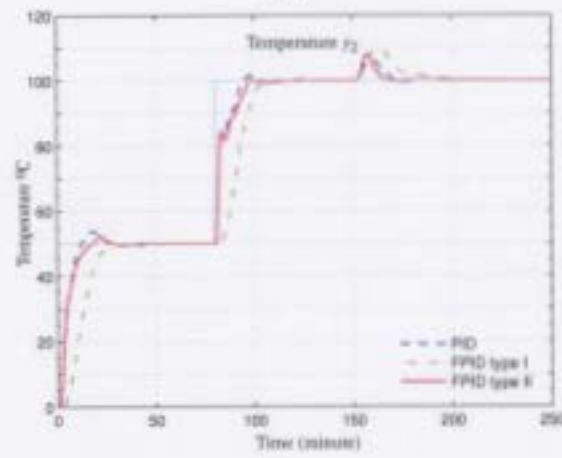
The equivalent first-order model obtained from plant reaction curve is given by;

$$\begin{bmatrix} \frac{0.0288e^{-2.45s}}{4.35s+1} & \frac{0.0119e^{-7.45s}}{16.05s+1} & \frac{0.00028e^{-9.7s}}{8.1s+1} \\ \frac{0.0015e^{-3.5s}}{6.6s+1} & \frac{0.0295e^{-2.4s}}{3.9s+1} & \frac{0.0035e^{-6.05s}}{7.95s+1} \\ \frac{0.0015e^{-9.5s}}{6.6s+1} & \frac{0.0143e^{-4.9s}}{4.2s+1} & \frac{0.0282e^{-2.5s}}{4.5s+1} \end{bmatrix}. \quad (4.38)$$

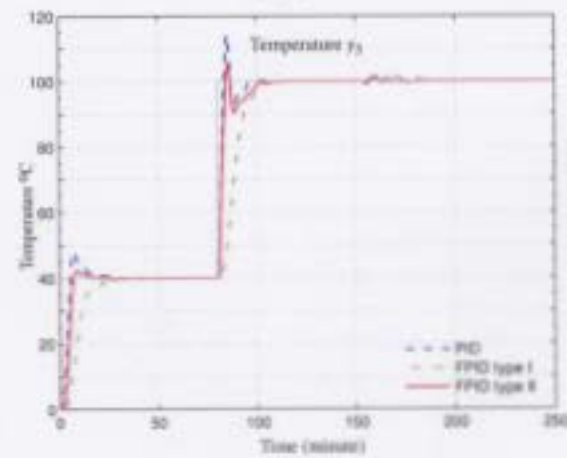
The set points were increased by 40°C, 50°C and 40°C at the beginning of the simulation. Once the outputs reached the initial set points, all variables were changed to 100°C at 80. In order to measure load disturbance rejection capability, a step load disturbance was given to the first input (y_1) of the process. Fig. 4-8 shows responses of this system to step input(reference) and step load disturbance. The system with FPID type II controller has less over shoot though it show bit slow response compared to linear PID system. However, all the systems show same capability of load disturbance rejection. Tables 4.5 and 4.6 shows the comparisons of performance indices. The controller tuning parameters for individual loop are shown in table 4.7.



(a) y_1



(b) y_2



(c) y_3

Figure 4-8: Example 2, Simulation of closed loop system with PID and FPID controllers

Output	Set Point Tracking								
	Rise Time (minute)			Overshoot %			Setting Time (minute)		
	PID	FPID1	FPID2	PID	FPID1	FPID2	PID	FPID1	FPID2
y_1	5	11	5	19	11	17	15	26	11
y_2	5	11	5	25	6	16	14	20	9
y_3	5	11	6	33	8	25	19	14	20

Table 4.2: Performance characteristic indices of proposed FPID methods and PID method for set point tracking in example 1

Output	Load Disturbance					
	Overshoot %			Setting Time (minute)		
	PID	FPID1	FPID2	PID	FPID1	FPID2
y_1	2.6	3.6	1.6	0	0	0
y_2	5	5	1	0	0	0
y_3	28	32	75	10	13	7

Table 4.3: Performance characteristic indices of proposed FPID methods and PID method for load disturbance in example 1

Loop No	PID			FPID1		FPID2					
	P	I	D	v_1	v_3	P		I		D	
						v_1	v_3	v_1	v_3	v_1	v_3
(1)	2.61	0.61	2.79	0.7	0.9	2.2	1.3	2.3	1.5	1.8	1.1
(2)	2.03	0.57	1.82	0.9	1.1	4.0	1.4	3.5	1.6	3.8	1.4
(3)	1.7	0.52	1.40	0.9	1.0	2.0	0.6	1.8	0.8	2.3	1.3

Table 4.4: Tuning parameters of example 1 for FPID controllers

Output	Set Point Tracking								
	Rise Time (minute)			Overshoot %			Setting Time (minute)		
	PID	FPID1	FPID2	PID	FPID1	FPID2	PID	FPID1	FPID2
y_1	10	17	15	37	10	7	30	30	35
y_2	9	20	11	8	0	6	22	23	22
y_3	5	15	6	20	0	6	6	22	7

Table 4.5: Performance characteristic indices of proposed FPID methods and PID method for set point tracking in example 2

Output	Load Disturbance					
	Overshoot %			Setting Time (minute)		
	PID	FPID1	FPID2	PID	FPID1	FPID2
y_1	34	38	17	14	16	23
y_2	12	19	16	13	20	10
y_3	1	2	3	0	0	0

Table 4.6: Performance characteristic indices of proposed FPID methods and PID method for load disturbance in example 2

Loop No	PID			FPID1		FPID2					
	P	I	D	v_1	v_3	P		I		D	
						v_1	v_3	v_1	v_3	v_1	v_3
(1)	0.56	0.25	0.32	1.1	0.8	5.5	0.35	4.2	0.5	3.5	0.2
(2)	1.45	0.23	2.29	0.8	1.0	1.1	0.80	1.3	0.9	1.1	1.8
(3)	2.34	0.39	3.54	0.9	1.2	1.5	0.50	1.8	0.2	0.9	0.6

Table 4.7: Tuning parameters of example 2 for FPID controllers

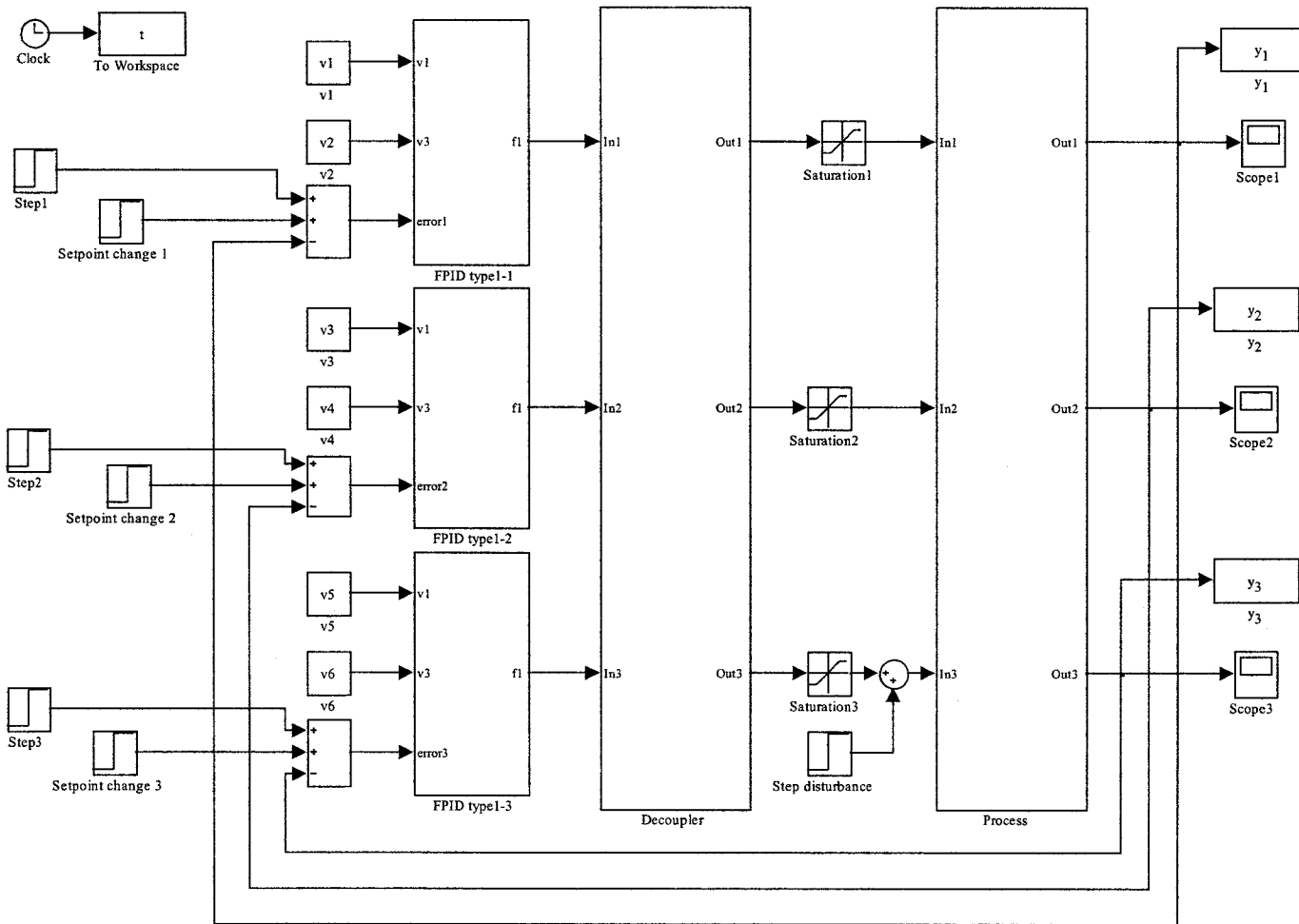


Figure 4-9: SIMULINK implementation of a FPID type 1 control strategy for the multivariable soil-cell temperature controller

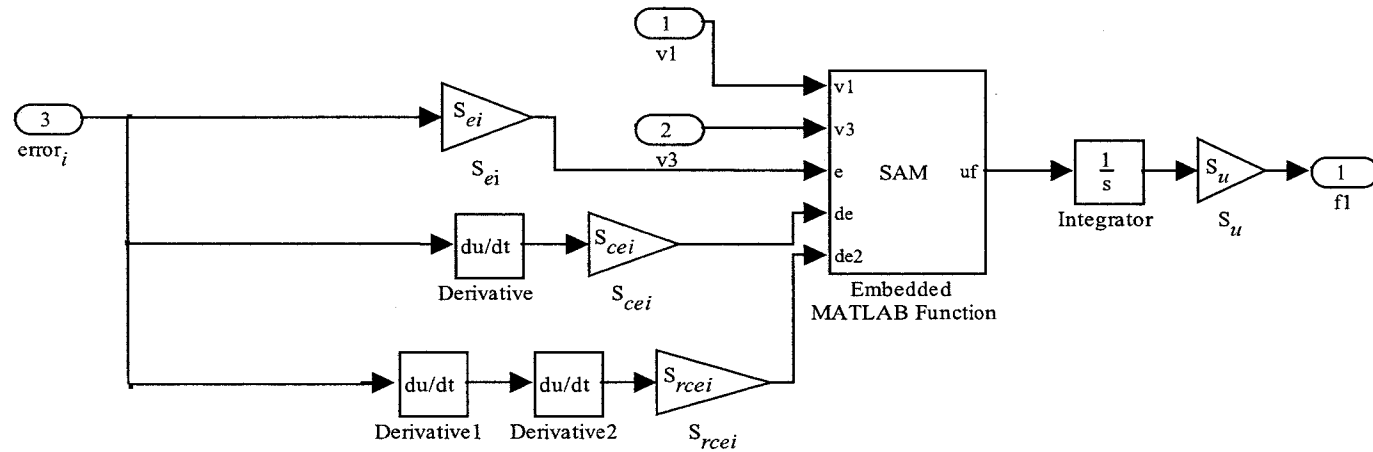


Figure 4-10: SIMULINK implementation of a FPID type 1 controller

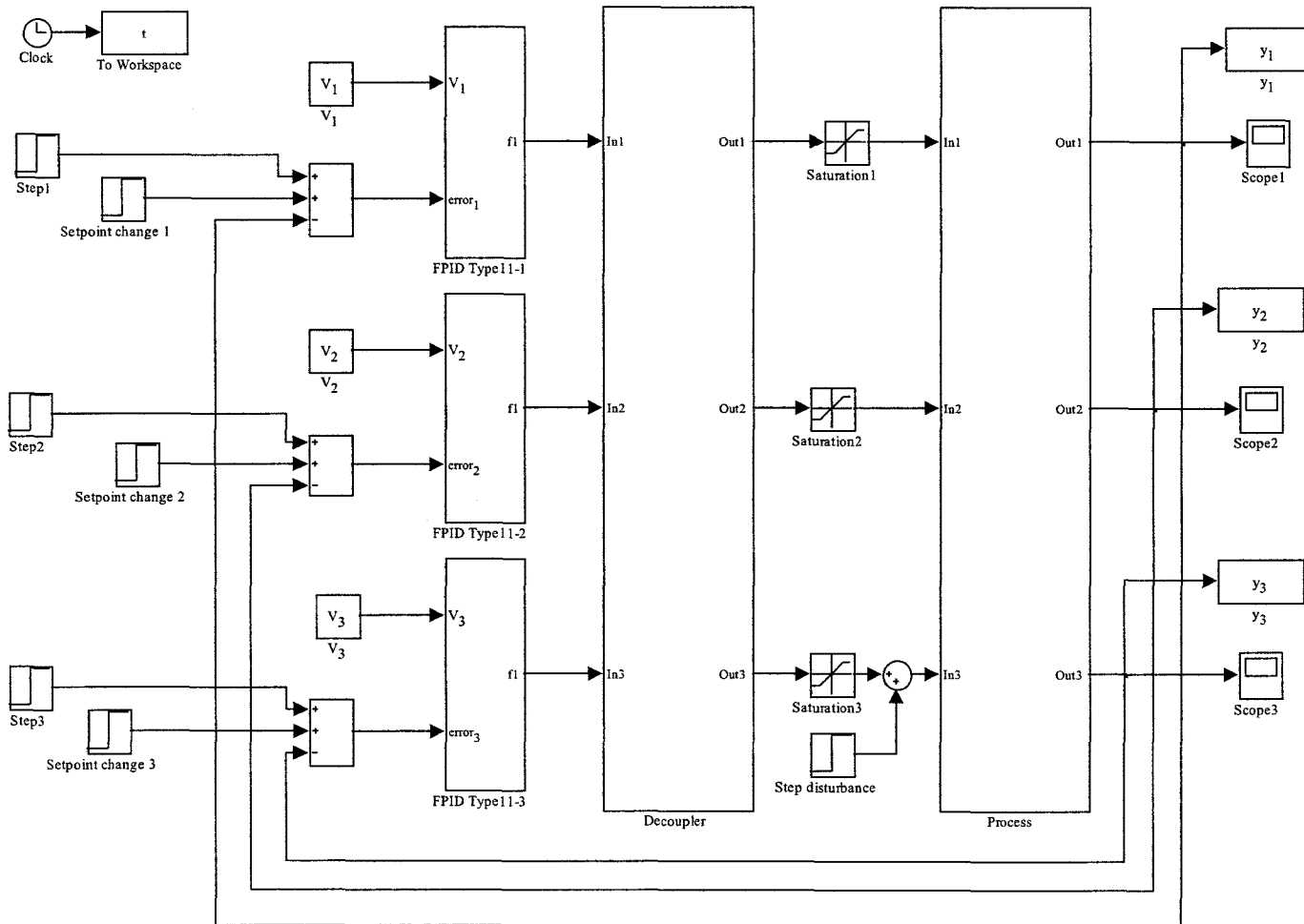


Figure 4-11: SIMULINK implementation of a FPID type 11 control strategy for the multivariable soil-cell temperature controller

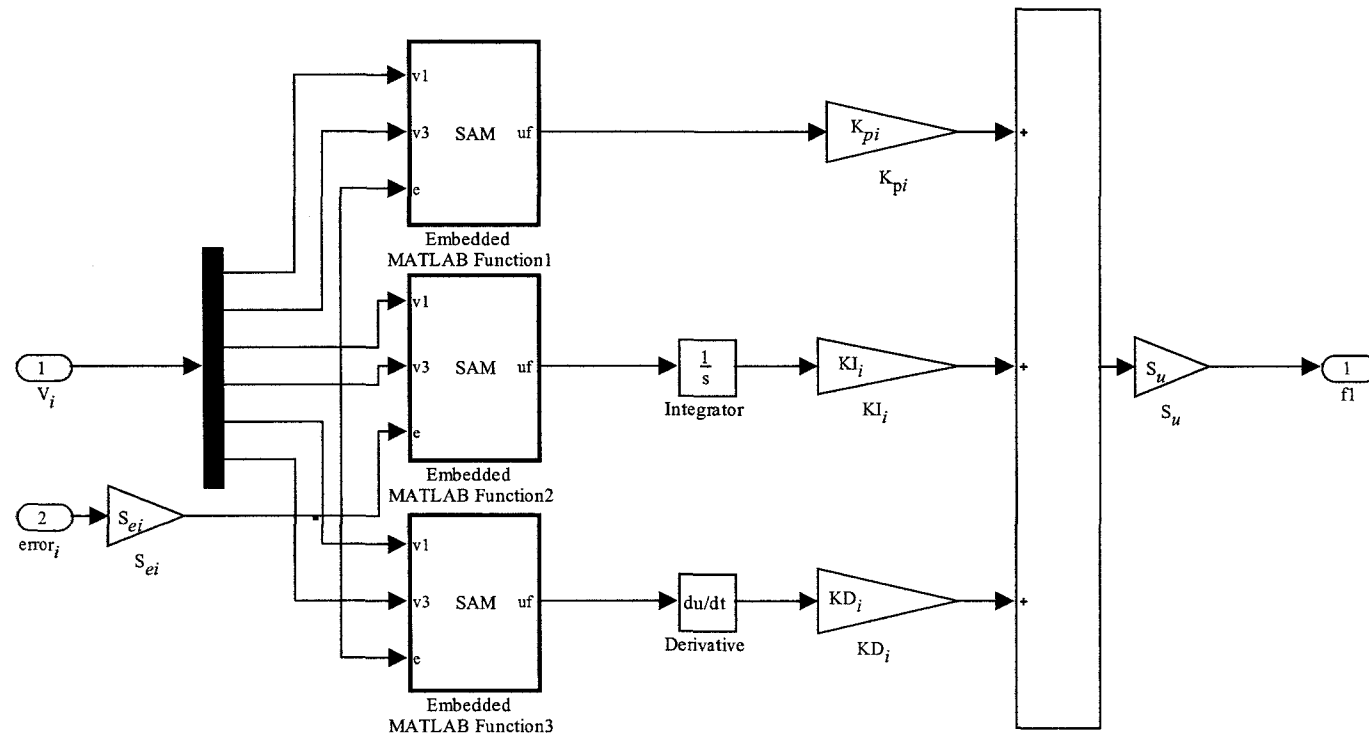


Figure 4-12: SIMULINK implementation of a FPID type 11 controller

Chapter 5

Real-Time Experiments

5.1 Introduction

This chapter describes real time experiments of temperature control of a soil-cell. The objective of experiments is to control temperatures at three different locations of soil-cell using three different heaters. The system identification is performed for soil-cell via classical step response method. Openloop tests (step response) are carried out for the soil- cell process and transfer function matrix is developed using plant reaction curve method [74]. Different type of control algorithm are executed for temperature control in the soil-cell in order to maintain desired temperatures in three different locations.

This chapter is organized as follows. First, overview of system modeling and identification is presented. The soil-cell is modeled with first-order dead time models and identified using conventional step response method. The plant reaction curve methods is used to identified the openloop transfer functions of soil-cell using open loop tests data.

5.2 System Modeling and Identification

The system modeling and identification play one of major roles in control engineering. The identified model can be used for output prediction, system design and control in diverse engineering applications [83]. In order to successfully model and identify a system, Ljung [84] pointed out three major procedures;

1. Model structure selection.
2. Model order estimation.
3. Parameterizations.

In this chapter, the selection of model structure and the order is discussed under the modeling of the system and parameterizations is discussed under the system identification.

There are two basic types of modeling problems. They are dynamic modeling of measured input/output and stochastic modeling problems. In each of these cases, a modeling consists basically of mathematical equations which can be used to understand the behavior of the system. The first type of modeling is the model estimation process of capturing system dynamics using measured data (inputs and outputs) [84], [85]. The relationship between outputs and the inputs can be formulated through a set of mathematical equations. In general, there are two ways to determine these equations. By writing set of equilibrium equations based on mass and energy balance and other physical laws, the relationship between outputs and inputs can be determined for given a system. A more common method is to use an empirical model approach (black box method). The empirical modeling is more common in engineering practice than its counterpart due to easiness of formulate the relationship between outputs and inputs.

The stochastic modeling arises when there is uncertainty about system inputs which causes the system outputs. For example, in large number of problems concerned with environmental, social and engineering systems, although the outputs are easily observed, it not possible to observe or measure the causes or the inputs. In this chapter, the dynamics modeling of measure input/output is described relating to soil-cell since outputs and inputs of the soil-cell are already identified.

5.2.1 Dynamic Modeling : Soil-cell

Although, in practice, most industrial processes are nonlinear (like soil-cell), linear models for such processes are often used due to their simplicity [40]. In this case, a high order process can be considered as a linear process for small changes when it is operated around its steady states [74].

In literature, [86] and [87] indicate that first-order models of process dynamics may frequently be sufficient for multivariable process control applications. And this assumption is well observed in classical control. The reason for first-order model selection is that most industrial processes are composed of many dynamics elements, usually first-order [40]. Hence the overall process would be of an order equal to number of elements and this high order process would be difficult to use for design and tuning of a controller. However, it is possible to approximate the process dynamics of such higher order process by a model with one time constant and a dead time as shown in [88].

Consider a process having N (positive integer) first-order elements in series. This type of process can be represented by,

$$G(s) = \frac{1}{(1 + \frac{\tau s}{N})^N} \quad (5.1)$$

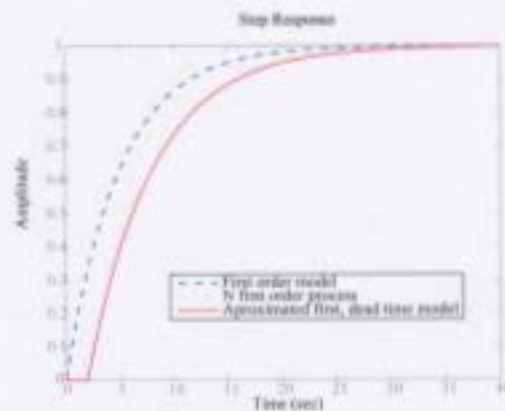


Figure 5-1: First-order dead time model approximation for a higher order process

Where $\frac{1}{N}$ is the time constant. When the N changes from 1 to ∞ the step response shifts from exact first-order to dead plus first-order as shown in Fig.5-1. In this case lower time constants contribute to the process dead time while larger time constants effect dynamics of the process. Hence it is possible to approximate a higher order process (having monotonically increasing response) to a simplified first-order with dead model and this simplified model then can be used to design and tuning of the controller.

By considering above facts, the soil-cell is modeled with first order processes and dead time elements. The dynamics of transfer function between heat input (W) and temperature output ($^{\circ}C$) of soil-cell then represented by,

$$G(s) = \begin{bmatrix} g_{11}(s) & g_{12}(s) & g_{13}(s) \\ g_{21}(s) & g_{22}(s) & g_{23}(s) \\ g_{31}(s) & g_{32}(s) & g_{33}(s) \end{bmatrix}. \quad (5.2)$$

The open-loop SISO transfer function between i^{th} temperature output and power input of j^{th} heater when all other heaters are switched off is denoted by g_{ij} where $i, j = 1, 2, 3$ and g_{ij} is modeled by,

$$g_{ij} = \frac{K_{ij}}{(1 + \tau_{ij}s)} \exp^{-s(\tau_d)_{ij}} . \quad (5.3)$$

Where τ_{ij} is time constant and $(\tau_d)_{ij}$ is dead time of the process. The off-diagonal transfer functions of soil-cell model represent the interaction among output temperatures caused by different heaters (power output) while diagonal transfer functions represent the direct effect of heaters (power output) to the corresponding temperature outputs

5.2.2 Identification : Soil-cell

The parameterizations is next step to perform once the correct model is defined for the soil-cell. i.e. choosing the correct values for K , τ and τ_d of each transfer function in (5.3). In general, parameterizations can be divided in to two categories. They are "on-line" and "off-line" system identifications.

The on-line system identification is common in especially adaptive control and it is necessary to identify the system in a fairly short time. Then the data are processed to estimate the parameters of the model while maintaining cost function. The best example of on-line system identification method is recursive least-square technique [89], [90].

The off-line identification requires a collections of data (inputs and outputs) for long period of time. Then, in off-line identification, there is a greater flexibility choosing a technique without any restriction on computing time. This may enhance the accuracy of the estimated model. There are well-known off-line classical techniques as step response, impulse response and frequency response. As their name imply these techniques use different kind of input to system and examined the outputs of the system. Among them the simplest input which can be applied to the process is a

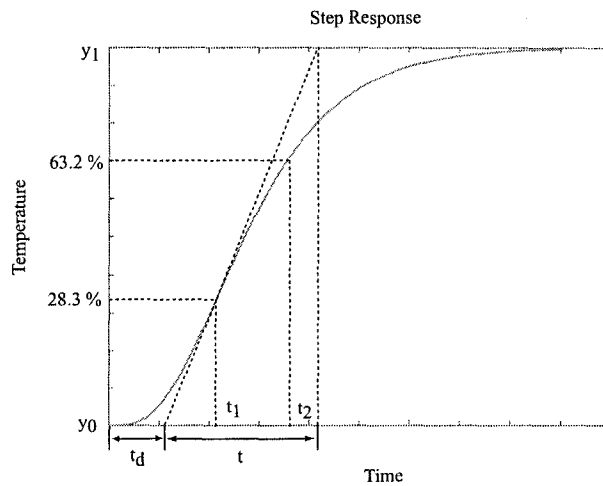


Figure 5-2: Determination of first-order dead time model using process reaction curve method

step input. In practice this may be one the scenarios of sudden switching on (or off) of input voltage or current, sudden opening (or closing) of input valve, so on.

In this research the step response technique is utilized to identify the first-order dead-time model (K , τ and τ_d) of the soil-cell since it can be done easily with sudden switching on of the heaters one by one at a time and measuring corresponding temperatures. These real time openloop experiments are well described in section 5.3

As described in [74], the plant reaction curve method is used to determine the process parameters. Fig. 5-2 shows the step response or reaction curve for a higher order process (monotonically increasing). At a steady state of the process out y_0 , the step input of Δu is applied to manipulated input of the process. The process response is then observed and recorded until it reaches a new steady state y_1 . By measuring the times to reach 28.3 per cent(t_1) and 63.2 per cent(t_2) of its steady state value $\Delta y (= y_0 - y_1)$ the process parameters can be obtained. Then the following expressions are used to calculate the parameters of first-order dead time model.

$$K = \frac{\Delta y}{\Delta u}$$

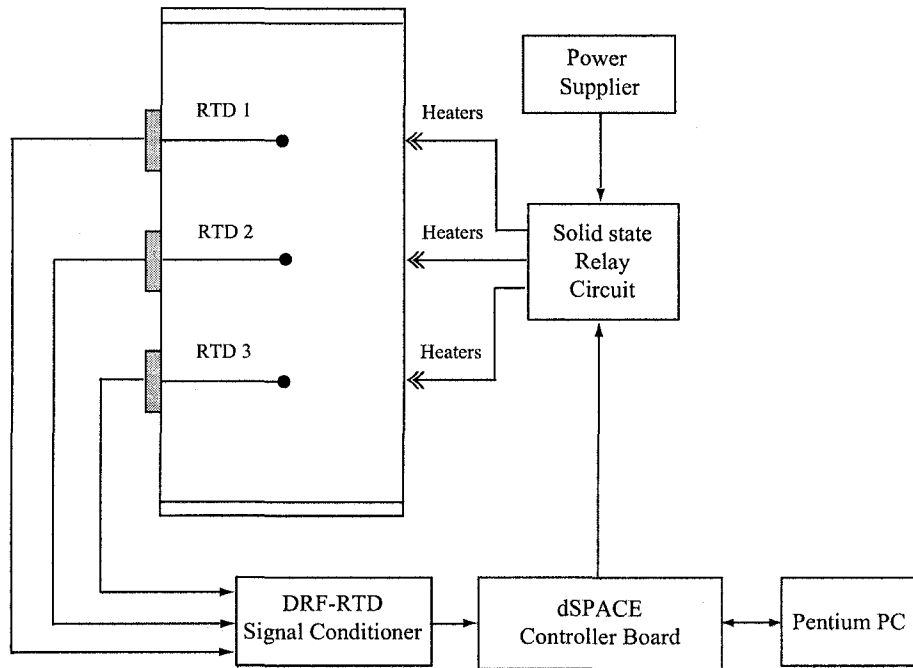


Figure 5-3: First-order dead time model approximation for a higher order process

$$\begin{aligned}\tau &= 1.5(t_2 - t_1) \\ \tau_d &= 1.5\left(t_1 - \frac{t_2}{3}\right)\end{aligned}\quad (5.4)$$

5.3 Openloop Test

The hardware setup which is used to implement real time experiments is shown in Fig. 5-3. The Thermofoil type heaters (each $7.1\Omega/10V$ DC) from Minco Products, Inc. are used in the soil-cell. The heaters are placed at three different levels (equiv distance) on two sides (opposite to each other) of the soil-cell. At each level two heaters are connected in parallel and therefore maximum power available (14W) is two times of a single heater coil. Three RDT (Resistance Temperature Detector)(each $100\ \Omega$, -200 to 600°C) from Omega Engineering are used to measure the output temperatures at three different levels of the soil-cell. The tip of each RTD is placed at the center of each

level so that they measure the center (point) temperature. The outputs of the RTD are fed to the signal conditioner. The RTD and signal conditioner is set up to convert 0-200°C to 0-10V. The dSPACE controller (DS1103) is configured directly to read this voltage out from the signal conditioner. Using three separate analog to digital converter (ADC) channels (1Hz sampling) on DS1103 PPC controller board of the dSPACE controller, this voltage output is read. The important fact about dSPACE controller is, the MATLAB and SIMULINK program can directly be downloaded to realtime processor (rti1103). Finally this voltage output is directly read and stored as temperature of the soil-cell with ControlDesk interface on personal computer (PC).

The controller algorithm, written in rti1103 processor calculate the duty cycle for each solid state relay and send to each relay circuit via three separate digital to analog converter (DAC) channels on dSPACE controller board. The switching period is set to 5 minutes. Thus the power at each heater sets can be varied from 0 to 14W depending on duty cycle which is calculated by control algorithm.

In the first part of real time experiments three openloop tests were carried out to determine the parameters of the first-order dead time models described in (5.3). The step input was applied to the soil-cell, i.e. sudden switched on a particular heater set up and the rest of heater setup were kept switched off for entire period of openloop test. Once the temperatures at three locations arrived new steady states, the heater setup was switched off. This procedure was repeated with for other two openloop tests and step input was applied to another heater setup alternatively. The temperature responses are plotted with respect to room temperature. The first-order dead time models are found using plant reaction curve method as described in previous section. Fig. 5-4:5-6 show temperature responses and its corresponding models for the openloop tests.

Then the dynamics of open transfer function between full duty (= 14W) of each

input and temperature output ($^{\circ}\text{C}$) of the soil-cell is described by,

$$G(s) = \begin{bmatrix} g_{11}(s) & g_{12}(s) & g_{13}(s) \\ g_{21}(s) & g_{22}(s) & g_{23}(s) \\ g_{31}(s) & g_{32}(s) & g_{33}(s) \end{bmatrix}$$

where

$$\begin{aligned} g_{11}(s) &= \frac{13.42e^{-54s}}{168s + 1} \\ g_{12}(s) &= \frac{5e^{-487s}}{397.5s + 1} \\ g_{13}(s) &= 0 \\ g_{21}(s) &= \frac{3.019e^{-184s}}{258s + 1} \\ g_{22}(s) &= \frac{19.8e^{-99s}}{462s + 1} \\ g_{23}(s) &= \frac{4.1e^{-271s}}{313.5s + 1} \\ g_{31}(s) &= 0 \\ g_{32}(s) &= \frac{2.25e^{-553s}}{358.5s + 1} \\ g_{33}(s) &= \frac{12.5e^{-55.5s}}{178.5s + 1} \end{aligned} \tag{5.5}$$

5.4 Implementation of Control Algorithms

Three different type of control algorithms; PID, FPID type I and FPID type II are implemented for soil-cell. The room temperature was around 22°C for all experiments. The initial set point temperature for loop 1 and 3 was 28°C and for loop 2 was 32°C .

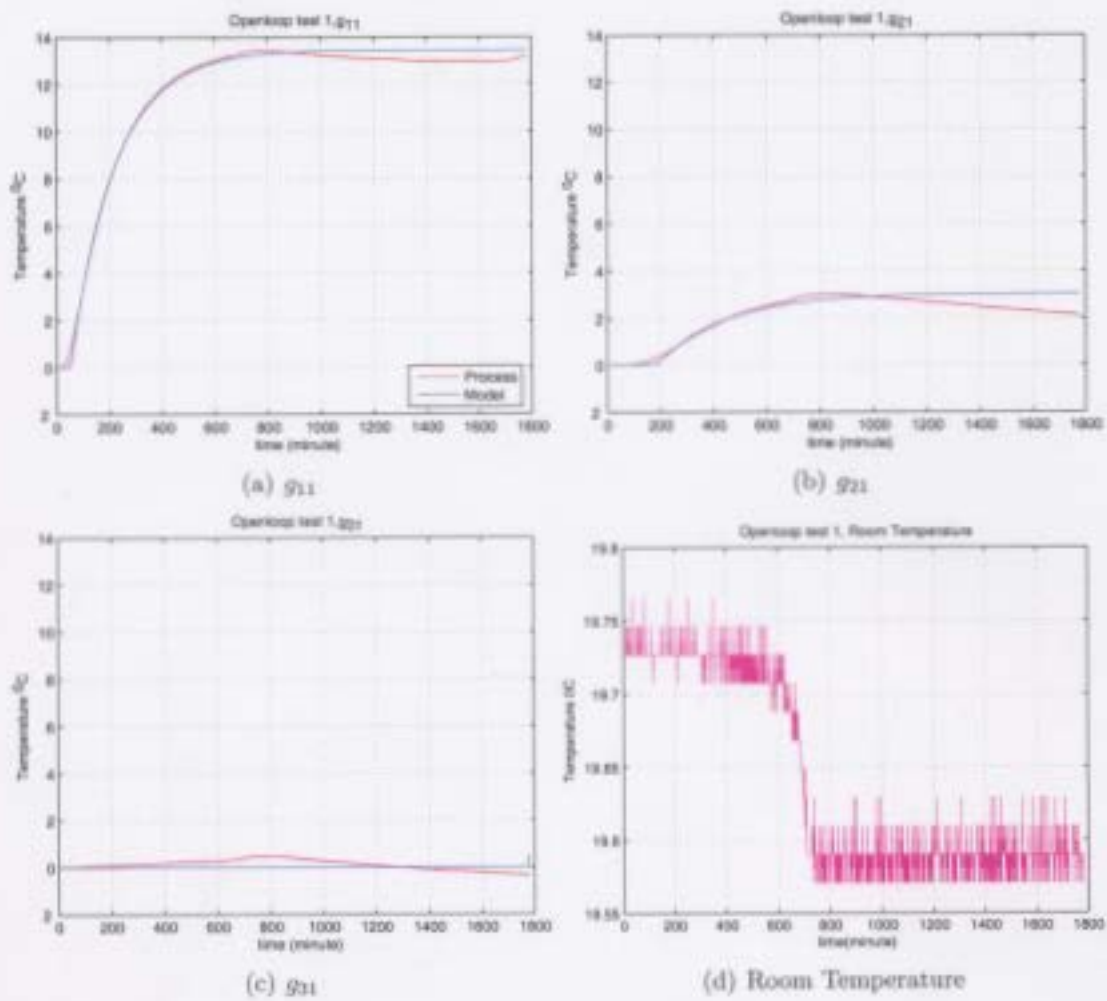


Figure 5-4: Real time experiments: Openloop test No. 1 of cell soil

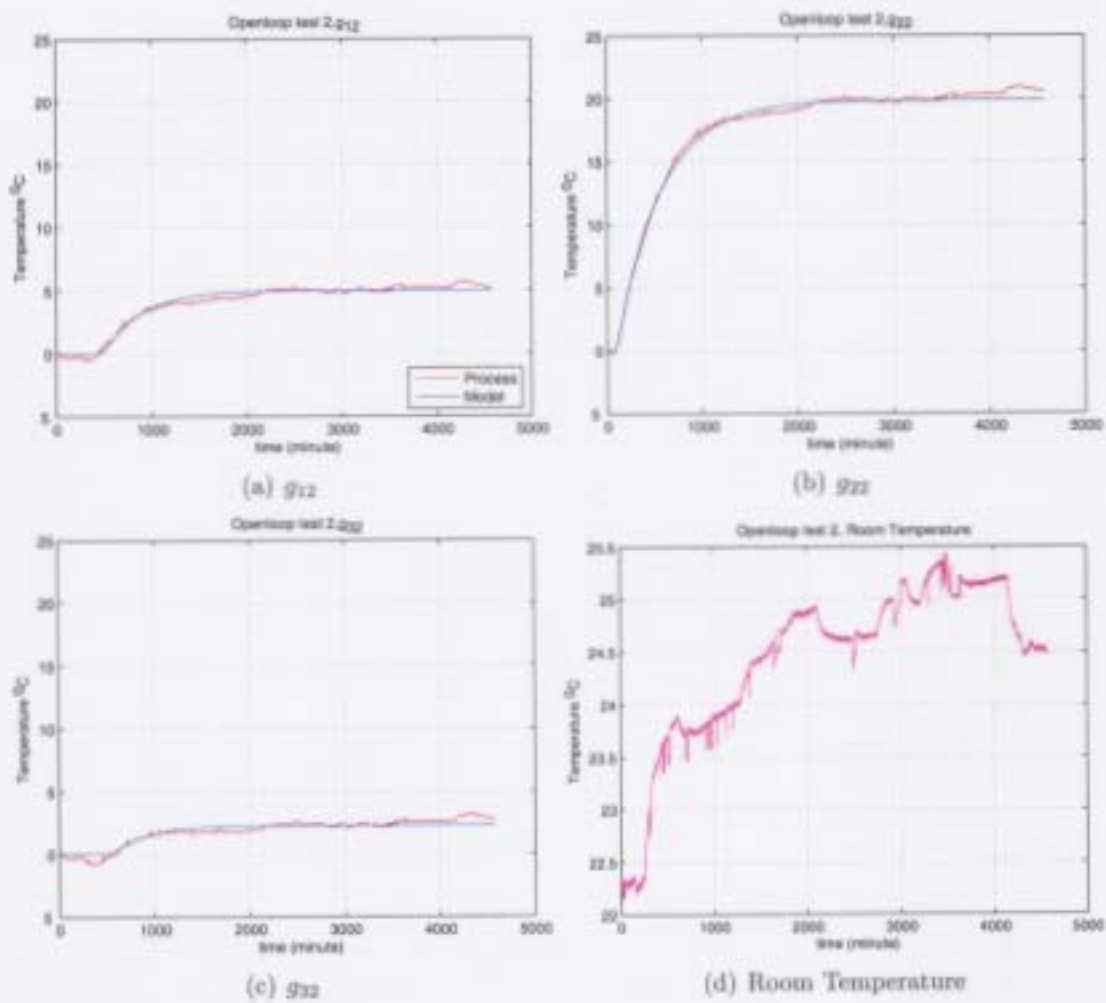


Figure 5-5: Real time experiments: Openloop test No. 2 of cell soil

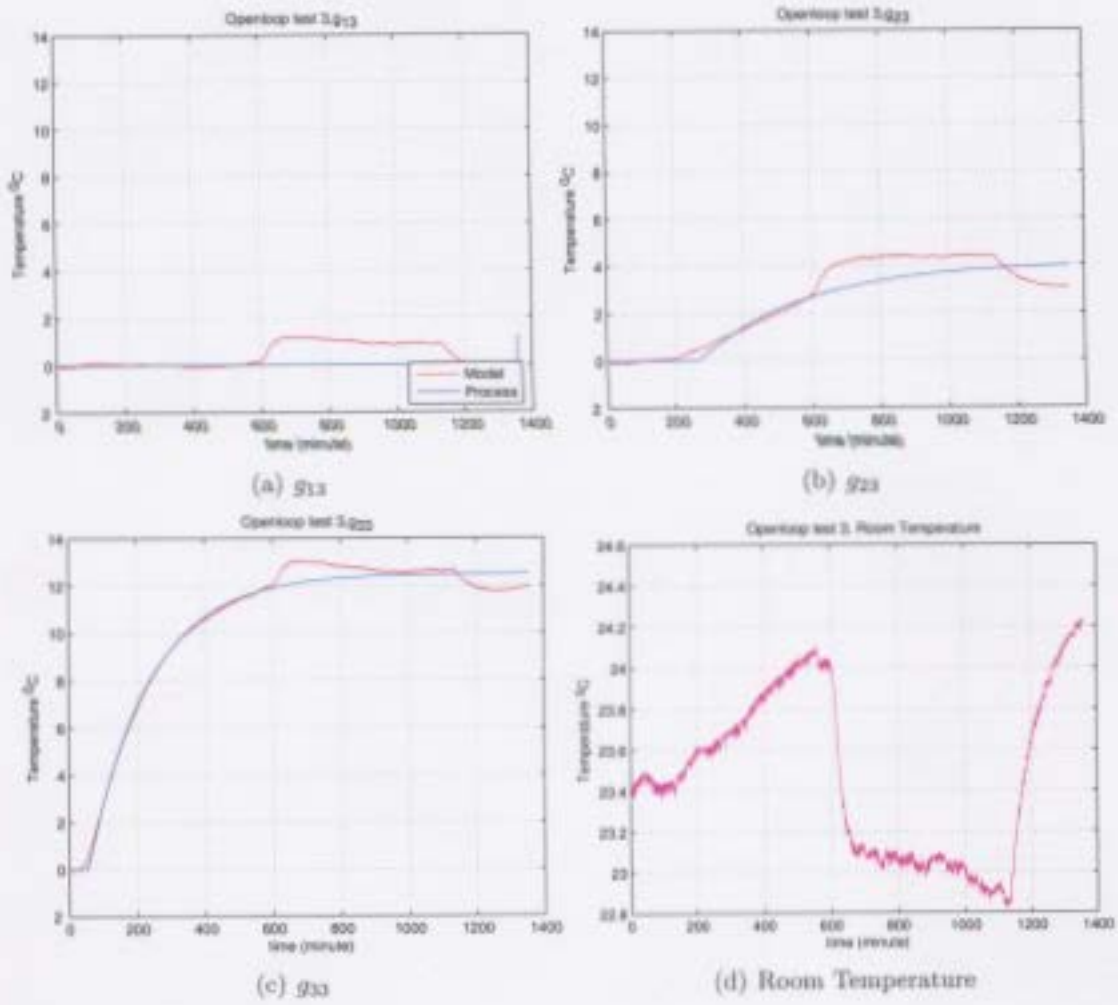


Figure 5-6: Real time experiments: Openloop test No. 3 of cell soil

Output	Set Point Tracking								
	Rise Time (minute)			Overshoot %			Setting Time (minute)		
	PID	FPID1	FPID2	PID	FPID1	FPID2	PID	FPID1	FPID2
y_1	740	1700	445	16.7	10.0	11.7	2300	3670	1000
y_2	730	1080	260	10.0	9.0	3.0	3750	2500	960
y_3	700	1590	425	17.7	11.7	15.8	2050	3550	1000

Table 5.1: Performance characteristic indices of proposed FPID methods and PID method for set point tracking

Loop No	PID			FPID1		FPID2					
	P	$I \times 10^{-5}$	$D \times 10^{-6}$	v_1	v_3	P		I		D	
						v_1	v_3	v_1	v_3	v_1	v_3
(1)	0.16	2.5	9.5	0.5	0.8	1.8	1.5	2.5	1.8	2.1	1.3
(2)	0.18	1.4	8.4	0.9	1.0	3.1	1.1	2.6	1.1	3.9	0.9
(3)	0.15	2.4	9.5	0.6	1.0	2.3	0.9	1.9	1.2	1.8	1.2

Table 5.2: Tuning parameters of FPID and PID controllers for real time experiments

loop No	Gain Margin	Phase Margin
1	2.4	40°
2	3.6	35°
3	5.5	45°

Table 5.3: Gain and Phase Margins of each loop of the soil-cell

After the all outputs reached their set point values, the set point temperatures were changed 34°C for loop 1 and 3, and 42°C for loop 3 at 4000 min respectively. The Fig. 5-7 show responses of each system.

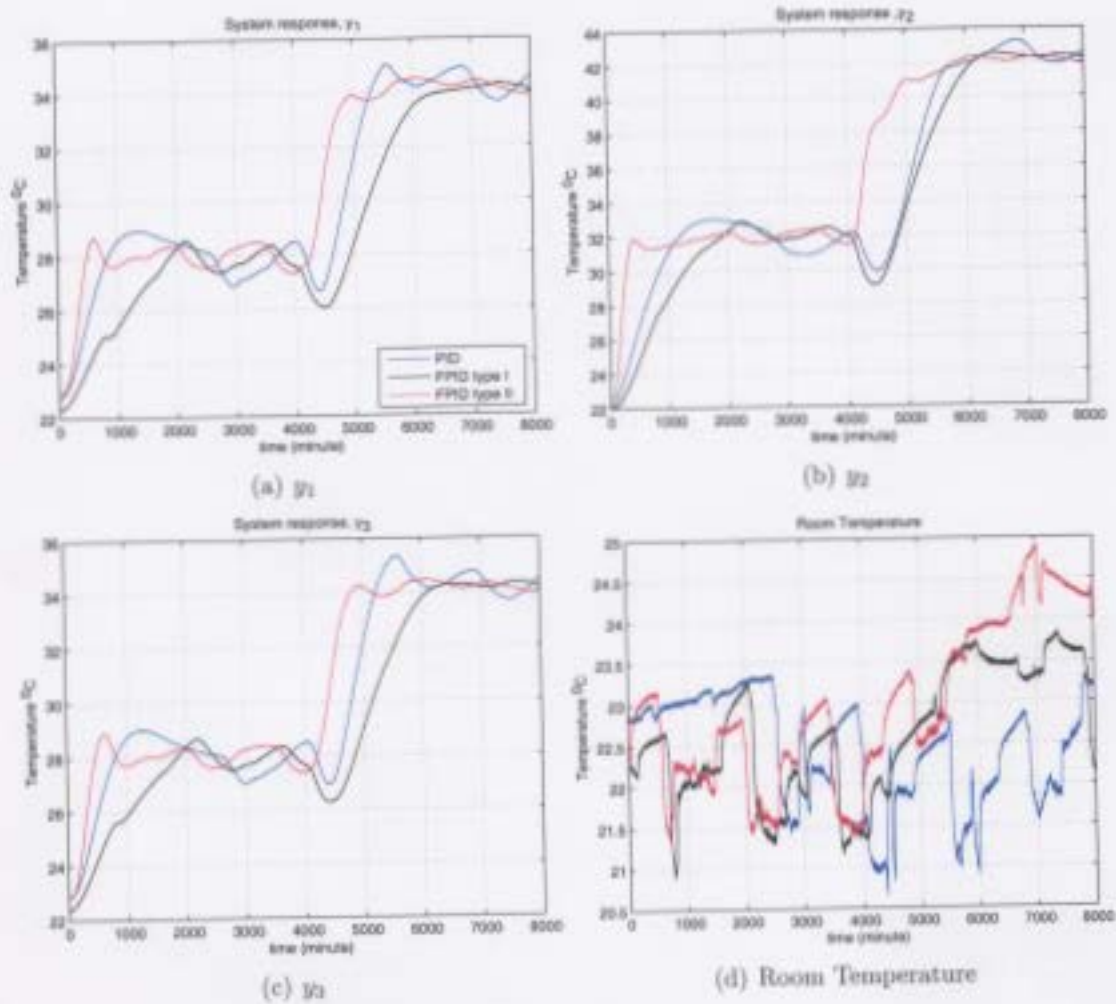


Figure 5-7: Real time experiments: Closed loop tests of cell soil

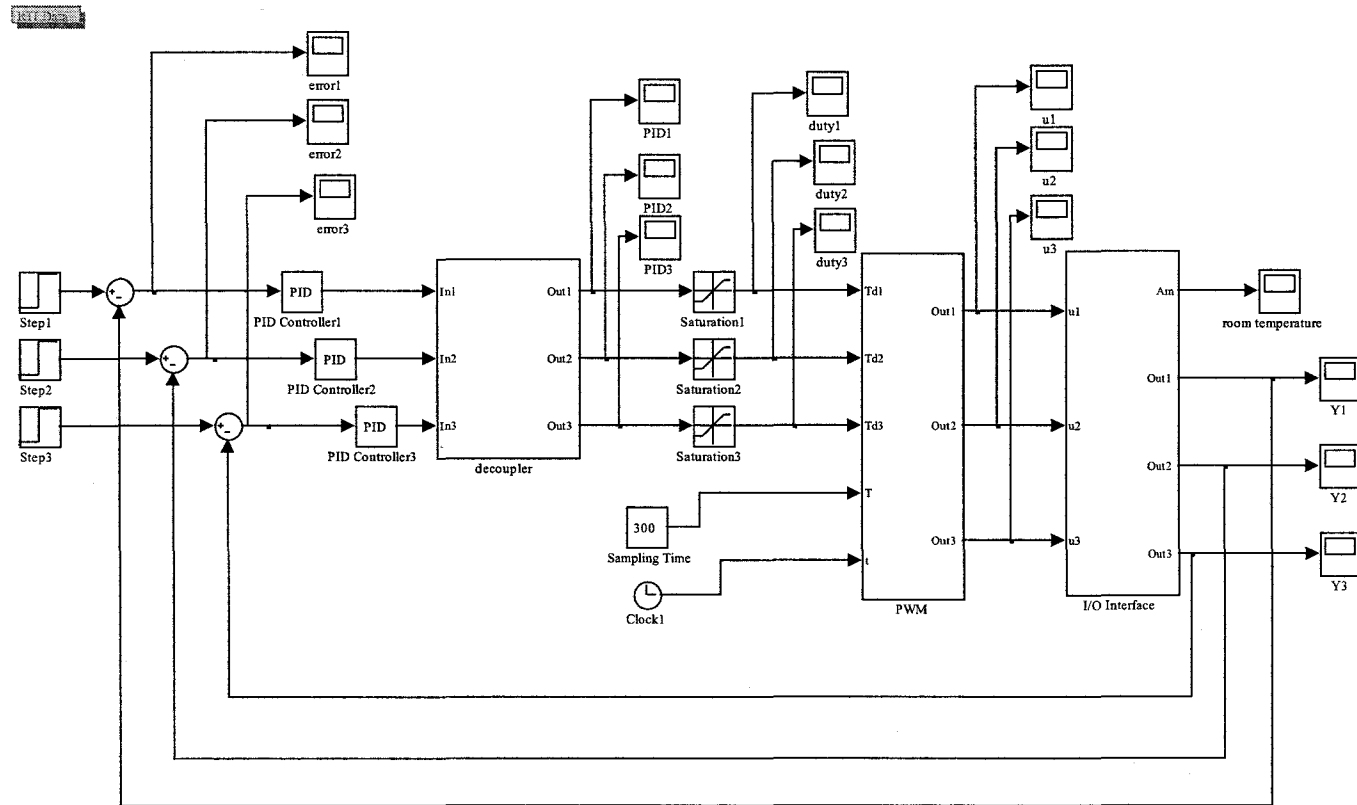


Figure 5-8: SIMULINK implementation of a PID control strategy of the multivariable soil-cell temperature controller for real-time experimentations

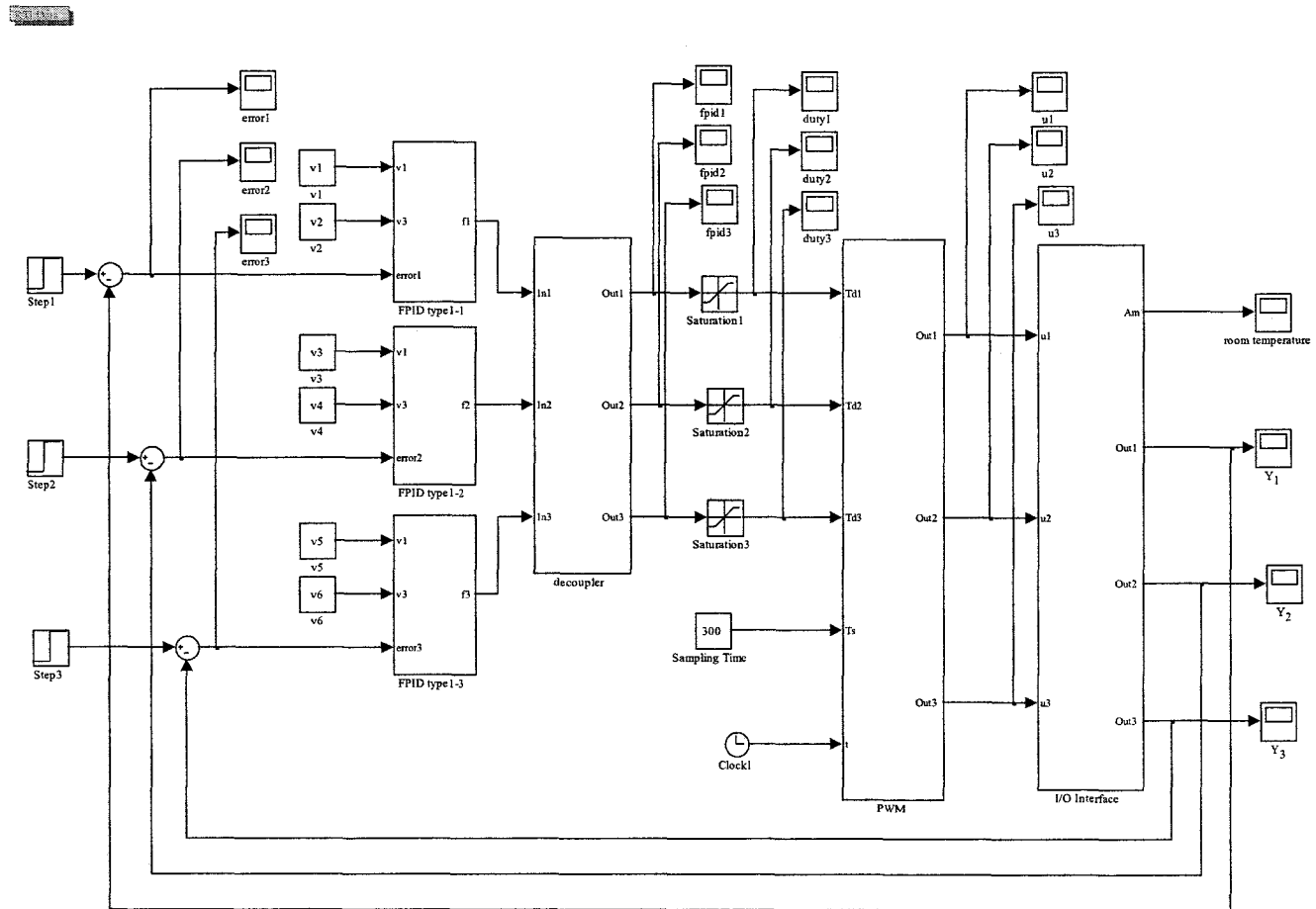


Figure 5-9: SIMULINK implementation of a FPID type1 control strategy of the multivariable soil-cell temperature controller for real-time experimentations

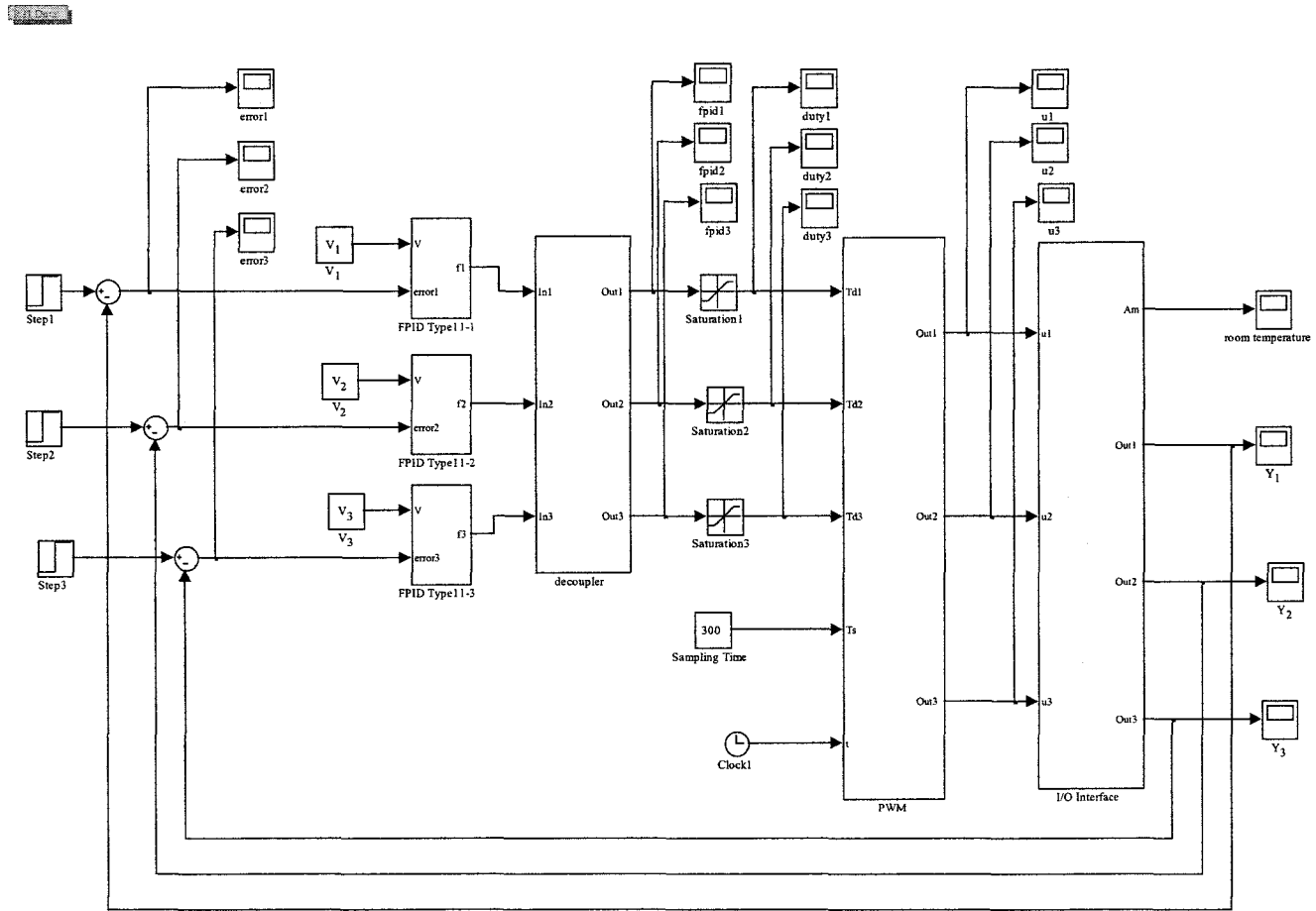


Figure 5-10: SIMULINK implementation of a FPID type 11 control strategy of the multivariable soil-cell temperature controller for real-time experimentations

Chapter 6

Conclusion and Future Work

6.1 Conclusion

The main objective of this thesis was to develop technique for the design and tuning of FPID controller for multivariable process system. This research attempt to address main problem of interactions among different loops which commonly appears in multivariable process systems in industry. Two types of FPID configurations were considered for designing FPID controllers. The type I was a conventional Mamdani's type and it used rule-coupled inference to produce an incremental FPID signal. The type II used rule decouple inference to provide independent tuning for the three actions in the PID signal. The tuning of both FPID configurations was achieved while using the two-level tuning principle which was presented in chapter 2. The low-level tuning dealt with linear gains whereas the high-level tuning adjusted the fuzzy rule base parameters. The low-level tuning method adopted a novel linear tuning scheme for general decoupled PID controllers and the high-level tuning adopted a heuristic method to change the nonlinearity in the fuzzy output.

In chapter 3, formulation of low-level tuning strategy was presented. For low-level

tuning a novel PID tuning technique for MIMO process had been developed. The proposed method was based on an interaction index. The proposed method can be used for any $n \times n$ dimensional MIMO process systems and guarantees closed loop stability. The decoupling was performed while using a static decoupler, which has the effect of reducing interactions within individual loops. The linear PID parameters were calculated for each loop by using interaction index, pole placement and ZN tuning rules. The superiority of proposed low-level tuning technique was evaluated using control simulations and compared against well known multivariable tuning technique, BLT.

In chapter 4, formulation of high-level tuning strategy was presented. Through nonlinearity analysis via NVI and LAI parameters of different fuzzy systems, SAM was selected to design high-level FPID controller. Two points of out of SAM fuzzy inference were selected to change the nonlinearity out of fuzzy system. However, change of nonlinearity at more than two points could have been done with cost of higher parameters complexity. For both configurations, FPID type I and FPID type II, high-level tuning parameters; V_0 and V_1 were identified. Tuning of those parameters have been performed using two heuristics; increase of V_0 decreases the undershoot of response and increase of V_1 increases the overshoot of the response. Stability analysis of overall system was performed through gain margin and phase margin of MIMO system. The superiority of proposed FPID techniques were evaluated using control simulations and compared against its linear counterpart.

In order to prove validity of proposed control algorithm real time experiments have been conducted. A prototype of three input three output soil heating cell was constructed for experiments. The objective of the experiments was to control temperatures at three different locations of soil-cell using three different heaters. The main challenging task of this experiment was the presence of interactions among three loops

in the soil-cell. Due to the interaction, the heat input of particular heater affected not only corresponding output but other output as well. This was clearly seen in openloop tests which were conducted to identify the soil-cell. Since the proposed algorithm is based on interaction index, which is a measure of maximum interaction given by a particular loop to other loops, the issue of loop interactions was well handled in the realtime experiments and could be able to have different temperatures at different level as desired. Due to the long time constant of soil-cell, the experiments had been conducted for long period of time. During this period of experiments, the system has undergone different temperature variations of the environment. This was another challenging task for experiments to provide better performance. However, the proposed algorithm was more robust to those external disturbances and has shown better performance. Based on the analysis of simulation and realtime experiments results it can be concluded that the proposed multivariable FPID type 2 scheme has better capability to exhibit satisfactory performances against its counterparts.

Followings are the summary of outcomes in this research.

1. Extension of two-level tuning method for MIMO systems. The two-level tuning proposed in (Mann,99) is extended for a MIMO system. This is a novel attempt in multivariable control.
2. Development of novel linear PID tuning technique for MIMO systems. The linear tuning can be applied for any $n \times n$ process systems whereas other general methods have limitation to the 2×2 systems.
3. Investigation of Standard additive model (SAM) based fuzzy inference for MIMO systems. SAM based fuzzy inference allows better nonlinear control against other inference. Application of SAM based fuzzy inference to multivariable systems is novel.

4. Development of generalized tuning technique for $n \times n$ multivariable FPID systems.

6.2 Future Work

Followings summarize the future research work:

- In formulation of decoupled PID controller technique, the overall compensated (static decoupler and process model) was modeled using first-order system at low frequency. Alternatively, the compensated system can be modeled using higher-order model in order to deal with any frequency.
- In this thesis tuning of high-level parameters for SAM was performed using heuristics. However, it is good to study the systematic tuning of those parameters considering performance indices of multivariable system.
- Moreover, online adaptation of those high-level tuning parameters has to be performed in order to cope with the discrepancy of model/process mismatch.

Publications during the course of the M. Eng program

Conference Papers

1. E. Harinath and G. K. I. Mann, "Standard Additive Model (SAM) based fuzzy PID controller for MIMO process," *Proceedings, The 16th Annual IEEE Newfoundland Electrical and Computer Engineering Conference*, St. John's, Canada, Nov. 2006.
2. E. Harinath and G. K. Mann, "Decoupled fuzzy PI Controller Tuning Scheme for Multivariable Processes," *IEEE World Congress on Computational Intelligence, WCCI 2006*, July 16 to 21, 2006 Sheraton Vancouver Wall Centre Hotel, BC, Canada
3. E. Harinath and G. K. Mann, "Tuning of Decoupled PI Controllers For Multi-variable Process Systems," *Proceedings, The 15th Annual IEEE Newfoundland Electrical and Computer Engineering Conference*, St. John's, Canada, Oct. 2005.
4. E. Harinath and G. K. Mann, "IMC-Based PI controller Design for a Multi-variable Soil Heating System," *Proceedings, The 15th Annual IEEE Newfoundland Electrical and Computer Engineering Conference*, St. Johns, Canada, Oct. 2005.
5. Md. Arifujjaman, E. Harinath, X. Fang and M.T. Iqbal, "Design and Comparison of different controllers for a DC position servo system," *Proceedings, The 15th Annual IEEE Newfoundland Electrical and Computer Engineering Conference*, St. Johns, Canada, Oct. 2005.

Journal Articles under review

1. E. Harinath and G. K. I. Mann, "Design and Tuning of Decoupled PID Controllers for Multivariable Processes," submitted to *IEEE Proceedings Control Theory and Applications*
2. Eranda Harinath and G.K. Mann, "Design of Standard Additive Model Based Fuzzy PID Controllers for MIMO Systems" submitted to *Fuzzy Sets and Systems*

Bibliography

- [1] K. L. Levien and M. Morari, "Internal model control of coupled distillation columns," *AIChE*, vol. 33, no. 1, pp. pp. 83–98, January 1987.
- [2] C. E. Garcia and M. Morari, "Internal model control 1: Unifying review and some new results." *Ind Eng Chem Process Des Dev*, vol. 21, no. 2, pp. 308–323, 1982.
- [3] B. W. Bequette, *Process Control Modeling, Design and Simulation*. Prentice-Hall of India, 2003.
- [4] D. Rivera, S. M. Morari, and S. Skogestad, "Internal model control 4. pid controller design," *Ind. Eng. Chem. Proc. Des. Dev.*, vol. 25, no. 1, pp. 252–265, January 1986.
- [5] A. Niederlinski, "A heuristic approach to the design of linear multivariable interacting control systems," *Automatica*, vol. 7, pp. 691–701, 1971.
- [6] B. R. Holt and M. Morari, "Design of resilient processing plants - vi. the effect of right-half-plane zeros on dynamic resilience," *Chemical Engineering Science*, vol. 40, no. 1, pp. 59–74, 1985.
- [7] ———, "Design of resilient processing plants - v. the effect of deadtime on dynamic resilience," *Chemical Engineering Science*, vol. 40, no. 7, pp. 1229–1237, 1985.

- [8] J. Lieslehto, J. T. Tantt, and H. N. Koivo, "An expert system for multivariable controller design," *Automatica*, vol. 29, no. 4, pp. 953–968, 1993.
- [9] J. Dong and C. B. Brosilow, "Design of robust multivariable pid controllers via imc," *Proceedings of the American Control Conference*, vol. 5, pp. 3380–3384, June 4-6 1997.
- [10] Q.-G. Wang, Y. Zhang, and M.-S. Chiu, "Decoupling internal model control for multivariable systems with multiple time delays," *American Control Conference*, vol. 6, pp. 3672 – 3676, 1998.
- [11] Q.-G. Wang, C. C. Hang, and X.-P. Yang, "Imc-based controller design for mimo systems," *Journal of Chemical Engineering of Japan*, vol. 35, no. 12, pp. 1231–1243, 2002.
- [12] C. E. Garcia, D. M. Prett, and M. Morari, "Model predictive control: Theory and practice - a survey," *Automatica*, vol. 25, no. 3, pp. 335–348, 1989.
- [13] T. A. Joe Qin, S. and Badgwell, "An overview of industrial model predictive control technology," *AIChE Symposium Series*, no. 316, p. 232, 1997.
- [14] S. J. Qin and B. T. A., "A survey of industrial model predictive control technology," *Control Engineering Practice*, vol. 11, no. 7, pp. 733–764, 2003.
- [15] E. F. Camacho and C. Bordons, *Model Predictive Control*. London: Springer, 1999.
- [16] M. C. Sousa and U. Kaymak, "Fuzzy decision making in modeling and control," *World Scientific Series in Robotics and Intelligent System*, vol. 27, pp. 137–314, 2002.

- [17] F. Yocum and J. Zimmerman, "Real time control of inverse response using dynamic matrix control," *Proceedings of the 1988 American Control Conference*, vol. 88, pp. 266–267, Jun 1988.
- [18] H. R. Karimi and M. R. J. Motlagh, "Robust feedback linearization control for a non linearizable mimo nonlinear system in the presence of model uncertainties," *Service Operations and Logistics, and Informatics, 2006 IEEE International Conference on*, pp. 965–970, 2006.
- [19] B. A. and L. Cong, "Adaptive fuzzy sliding mode controller for underwater vehicles," *Control and Automation, 2003. ICCA 2003. The Fourth International Conference on*, pp. 917–921, June 2003.
- [20] M. Garcia-Sanz, I. Egana, and M. Barreras, "Design of quantitative feedback theory non-diagonal controllers for use in uncertain multiple-input multiple-output systems," *Control Theory and Applications, IEE Proceedings*, vol. 152, no. 2, pp. 177–187, March 2005.
- [21] C. R. Cutler and B. Ramaker, "Dynamic matrix control-a computer control algorithm," San Francisco, CA, June 1980.
- [22] D. W. Clarke, C. Mohtadi, and P. S. Tuffs, "Generalized predictive control-part i. the basic algorithm," *Automatica*, vol. 23, no. 2, pp. 137–148, Mar 1987.
- [23] H.-T. Su and T. McAvoy, "Neural model predictive control of nonlinear chemical processes," *Intelligent Control, 1993., Proceedings of the 1993 IEEE International Symposium on*, pp. 25–27, Aug 1993.

- [24] M. A. Goodrich, W. Stirling, and R. Frost, "Model predictive satisficing fuzzy logic control," *Fuzzy Systems, IEEE Transactions on*, vol. 7, no. 3, pp. 319–332, June 1999.
- [25] Y. Huang, H. Lou, J. Gong, and T. Edgar, "Fuzzy model predictive control," *Fuzzy Systems, IEEE Transactions on*, vol. 8, no. 6, pp. 665–678, Dec 2000.
- [26] S. Piche, B. Sayyar-Rodsari, D. Johnson, and M. Gerules, "Nonlinear model predictive control using neural networks," *IEEE Control Systems Magazine*, vol. 20, no. 3, pp. 53–62, Jun 2000.
- [27] S. Molloy, T. van den Boom, F. Cuesta, A. Ollero, and R. Babuska, "Robust stability constraints for fuzzy model predictive control," *Fuzzy Systems, IEEE Transactions on*, vol. 10, no. 1, pp. 50–64, Feb 2002.
- [28] J. Chen, Y. Yea, and C.-W. Wang, "Neural network model predictive control for nonlinear mimo processes with unmeasured disturbances," *Journal of Chemical Engineering of Japan*, vol. 35, no. 2, pp. 150–159, Feb 2002.
- [29] S. J. Qin and T. A. Badgwell, "A survey of industrial model predictive control technology," *Control Engineering Practice*, vol. 11, no. 7, pp. 733–764, July 2003.
- [30] S. Yamamoto and I. Hashimoto, "Present status and future needs: The view of from japanese industry," *Proceedings of the 4th International Conference on Chemical Process Control*, i. Arkun and I. Ray, Eds. New York:AIChE, 1991.
- [31] L. A. Zadeh, "Outline of a new approach to the analysis of complex systems and decision processes," *IEEE Trans. Syst., Man, Cybern.*, vol. v SMC-3, no. 1, pp. 28–44, Jan. 1973.

- [32] E. H. Mamdani, "Application of fuzzy algorithms for control of simple dynamic plant," *Proceedings of the Institution of Electrical Engineers*, vol. 121, no. 12, pp. 1585–1588, 1974.
- [33] F. Lewis and K. Liu, "Towards a paradigm for fuzzy logic control," *Automatica*, vol. 32, no. 2, pp. 167–181, February 1996.
- [34] H. X. Li and S. Tong, "A hybrid adaptive fuzzy control for a class of nonlinear mimo systems," *Fuzzy Systems, IEEE Transactions on*, vol. 11, no. 1, pp. 24–34, Feb. 2003.
- [35] T. J. Ross, *Fuzzy Logic with Engineering Applications*, 2nd ed. The Atrium, Southern Gate, Chichester, West Sussex PO19 8SQ, England: John Wiley and Sons Ltd, 2004.
- [36] B. Kosko, *Fuzzy Engineering*. Simon and Schuster/A Viacom Company Upper Saddle River, New Jersey: Prentice-Hall, Inc, 1997.
- [37] H. A. Malki and D. Misir, "Determination of the control gains of a fuzzy pid controller using neural networks," *Fuzzy Systems, Proceedings of the Fifth IEEE International Conference on*, vol. 2, pp. 1303–1307, Sept. 1996.
- [38] Y. Yongquan, H. Ying, W. Minghui, Z. Bi, and Z. Guokun, "Fuzzy neural pid controller and tuning its weight factors using genetic algorithm based on different location crossover," *Systems, Man and Cybernetics, 2004 IEEE International Conference on*, vol. 4, pp. 3709–3713, 10-13 Oct. 2004.
- [39] K. J. Astrom, K. H. Johansson, and Q.-G. Wang, "Design of decoupled pid controllers for mimo systems," vol. 3, pp. 2015–2020, June 2001.

- [40] R. Sehab, M. Remy, and C. Renotte, "An approach to design fuzzy pi supervisor for a nonlinear system," *IFSA World Congress and 20th NAFIPS International Conference, 2001. Joint 9th*, vol. 2, pp. 894–899, 25-28 July 2001.
- [41] A. S. Ghafari and A. Alasty, "Design and real-time experimental implementation of gain scheduling pid fuzzy controller for hybrid stepper motor in micro-step operation," *Proceedings of the IEEE International Conference on Mechatronics ICM '04.*, pp. 421–426, June 2004.
- [42] R. A, R. F, and R. M, "A hybrid fuzzy logic and pid controller for control of nonlinear hvac systems," *IEEE Transactions on Systems, Man and Cybernetics*, vol. 3, pp. 2249–2254, October 2003.
- [43] D. Dubois and H. Prade, *Fuzzy Sets and Systems: Theory and Applications*. Academic Press, 1980.
- [44] M. Sugeno, *Industrial Application of Fuzzy Control*, Amsterdam, The Netherlands: North-Holland, 1985.
- [45] B. M. Mohan and A. V. Patel, "Analytical structures and analysis of the simplest fuzzy pd controllers," *IEEE Trans. Syst., Man, Cybern. B*, vol. 32, no. 2, pp. 239–248, Apr. 2002.
- [46] H. A. Malki, H. Li, and G. Chen, "New design and stability analysis of fuzzy proportional-derivative control systems," *IEEE Trans. Fuzzy Syst.*, vol. 2, pp. 345–354, Apr. 1994.
- [47] H. Ying, "Practical design of nonlinear fuzzy controllers with stability analysis for regulating processes with unknown mathematical models," *Automatica*, vol. 30, no. 7, pp. 1185–1195, 1994.

- [48] E. G. I and H. M. R, “Fuzzy multivariable control of a class of a biotechnology process,” *Proceedings of the IEEE International Symposium on Industrial Electronics*, vol. 1, pp. 419–424, July 1999.
- [49] P. Roy, G. Mann, and B. Hawlader, “Fuzzy rule-adaptive model predictive control for a multi-variable heating system,” *IEEE Conference on Control Applications*, pp. 260–265, August 2005.
- [50] K. J. Astrom and T. Hagglund, *PID Controllers: Theory, Design and Tuning*. Instrument Society of America, Research Triangle Park, NC, 1995.
- [51] J. G. Ziegler and N. Nichols, “Optimum settings for automatic controllers,” *Trans. ASME*, no. 64, pp. pp. 759–768, 1942.
- [52] W. L. Luyben, “Simple method for tuning siso controllers in multivariable systems,” *Ind. Eng. Chem. Process Des. Dev*, vol. 25, no. 3, pp. 654–660, Jul 1986.
- [53] G. K. I. Mann, B.-G. Hu, and R. G. Gosine, “Two-level tuning of fuzzy pid controllers,” *IEEE Transactions on Systems, Man and Cybernetics, Part B*, vol. 31, no. 2, pp. 263–269, April 2001.
- [54] J. X. Xu, C. Liu, and C. C. Hang, “Tuning of fuzzy pi controllers based on gain/phase margin specifications and itae index,” *ISA Transactions*, vol. 35, no. 1, pp. 79–91, May 1996.
- [55] ———, “Designing a stable fuzzy pi control system using extended circle criterion,” *Int. J. of Intelligent Control and Systems*, vol. 1, pp. 355–366, 1996.
- [56] S. Hayashi, “Auto-tuning fuzzy pi controller,” *Proceedings of the Intn'l Fuzzy Systems Association Conference*, pp. 41–44, 1991.

- [57] H. X. Li and H. B. Gatland, "A new methodology for designing a fuzzy logic controller," *IEEE Transactions on Systems, Man and Cybernetics*, vol. 25, no. 3, pp. 505–512, Mar 1995.
- [58] B. Hu, G. K. I. Mann, and R. G. Gosine, "New methodology for analytical and optimal design of fuzzy pid controllers," *IEEE Transactions on Fuzzy Systems*, vol. 7, no. 5, pp. 521–539, October 1999.
- [59] G. K. I. Mann, B.-G. Hu, and R. G. Gosine, "Analysis of direct action fuzzy pid controller structures," *IEEE Transactions on Systems, Man and Cybernetics, Part B*, vol. 29, no. 3, pp. 371–388, June 1999.
- [60] Y. Huang and S. Yasunobu, "A general practical design method for fuzzy pid control from conventional pid control," *Fuzzy Systems, 2000. FUZZ IEEE 2000. The Ninth IEEE International Conference on*, vol. 2, pp. 969–972, May 2000.
- [61] M. F. Witcher and T. J. McAvoy, "Interacting control systems: Steady state and dynamic measurement of interaction," *ISA Transactions*, vol. 16, no. 3, pp. 35–41, 1977.
- [62] K. H. Weng, H. L. Tong, and O. P. Gan, "Tuning of multiloop proportional-integral-derivative controllers based on gain and phase margin specifications," *Ind. Eng. Chem. Res.*, vol. 36, pp. 2231–2238, 1997.
- [63] A. Niederlinski, "A heuristic approach to the design of linear multivariable interacting control systems," *Automatica*, vol. 7, pp. 691–701, 1971.
- [64] D. chen and D. Seborg, "Multiloop pi/pid controller design based on gershgorin bands," vol. 5, pp. 4122–4127, Jun 25-27 2001.

- [65] H. H. Rosenbrock, "Design of multivariable control systems using the inverse nyquist array," *Instn Elec Engrs-Proc*, pp. 1929–36, Nov 1969.
- [66] E. H. Bristol, "On a new measure of interaction for multivariable process control," *IEEE Transactions on Automatic Control*, vol. 11, no. 1, pp. 133–134, Jan 1966.
- [67] M. Witcher and T. J. McAvoy, "Interacting control systems: Steady state and dynamic measurement of interaction," *ISA Transactions*, vol. 16, no. 3, pp. 35–41, 1977.
- [68] J. Lee and T. F. Edgar, "Interaction measure for decentralized control of multivariable processes," vol. 1, pp. 454–458, May 2002.
- [69] M. Moradi, M. Katebi, and M. Johnson, "The mimo predictive pid controller design," *Asian Journal of Control*, vol. 4, no. 4, pp. 452–463, December 2002.
- [70] K. Asrom and T. Hagglund, *PID Controllers: Theory, Design, and Tuning*, 2nd ed. Research Triangle Park, NC: Instrument Society of America, 1995.
- [71] H. H. Rosenbrock, *State -Space and Multivariable Theory*. London, U.K.: Nelson, 1970.
- [72] J. Maciejowski, *Multivariable Feedback Design*. Addison-Wesley, 1989.
- [73] W. K. Ho, T. H. Lee, W. Xu, J. R. Zhou, and E. B. Tay, "Direct nyquist array design of pid controllers," *IEEE Transactions on Industrial Electronics*, vol. 47, no. 1, pp. 175–185, Feb 2000.
- [74] E. Camacho and C. Bordons, *Model Predictive Control*. Springer-Verlag, London, 1999.

- [75] C.-L. Chen and P.-C. Chen, "Application of fuzzy logic controllers in single-loop tuning of multivariable system design," *Computers in Industry*, vol. 17, no. 1, pp. 33–41, 1991.
- [76] S. Li, H. Liu, W.-J. Cai, Y.-C. Soh, and L.-H. Xie, "A new coordinated control strategy for boiler-turbine system of coal-fired power plant," *IEEE Transactions on Control Systems Technology*, vol. 13, no. 6, pp. 943–954, November 2005.
- [77] H. B. Kazemian, "The sof-pid controller for the control of a mimo robot arm," *IEEE Transactions on Fuzzy Systems*, vol. 10, no. 4, pp. 523–532, August 2002.
- [78] C. W. Reynolds, "Flocks, herds, and shcools: A distributed behavioral model," *Computer Graphics*, vol. 21, no. 4, pp. 25–34, July 1987.
- [79] J. P. Martino, *Technological Forecasting for Decisionmaking*, 1st ed. Elsevier, 1972, vol. 8.
- [80] B.-G. Hu, G. Mann, and R. Gosine, "A systematic study of fuzzy pid controllers-function-based evaluation approach," *Fuzzy Systems, IEEE Transactions on*, vol. 9, no. 5, pp. 699–712, Oct. 2001.
- [81] B.-G. Hu and R. Mann, G.K.I.and Gosine, "Control curve design for nonlinear (or fuzzy) proportional actions using spline-based functions," *Automatica*, vol. 34, no. 9, pp. 1125–1133, Sep 1998.
- [82] B. Hu, G. Mann, and R. Gosine, "New methodology for analytical and optimal design of fuzzy pid controllers," *Fuzzy Systems, IEEE Transactions on*, vol. 7, no. 5, pp. 521–539, 1999.
- [83] G. B. Giannakis and E. Serpedin, "A bibliography on nonlinear system identification," *Signal Process.*, vol. 83, no. 3, pp. 533–580, 2001.

- [84] L. Ljung, *System Identification: Theory for the User*. Upper Saddle River, NJ: Prentice-Hall, 1999.
- [85] K. Narendra and K. Parthasarathy, "Identification and control of dynamical systems using neural networks," *Neural Networks, IEEE Transactions on*, vol. 1, no. 1, pp. 4–27, March 1990.
- [86] D. Owens and A. Chotai, "Robust control of unknown discrete multivariable systems," *Automatic Control, IEEE Transactions on*, vol. 27, no. 1, pp. 188–190, Feb 1982.
- [87] D. H. O. adn A. Chotai and A. A. Abiri, "Parameterization and approximation methods in feedback control with applications in high gain, fast sampling and cheap optimal control," *IMA. Intl. J. Math. Confr. Inform.*, vol. 1, pp. 147–171, 1984.
- [88] P. B. Deshpande and R. H. Ash, *Elements of Computer Process Control*. ISA, 1981.
- [89] K. Bousson, "Sequential parameter identification method for nonlinear systems," *Intelligent Control, 2002. Proceedings of the 2002 IEEE International Symposium on*, pp. 874–878, 2002.
- [90] S. Fiori and G. Maiolini, "Weighted least-squares blind deconvolution of non-minimum phase systems," *Vision, Image and Signal Processing, IEE Proceedings*, vol. 147, no. 6, pp. 557–563, Dec 2000.

Appendix A

Design Sketches for Realtime Implementation

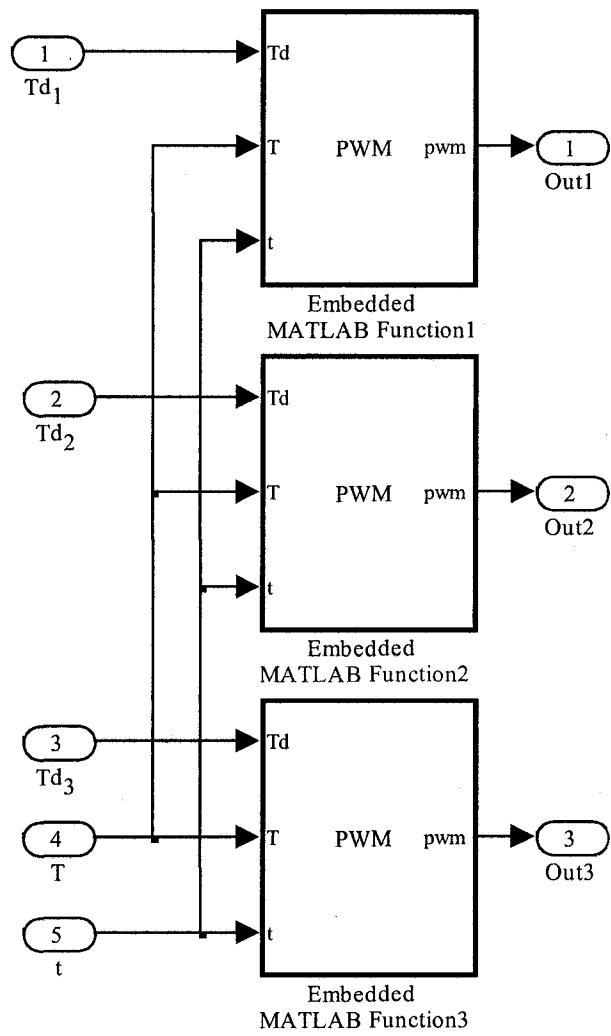


Figure A.1: SIMULINK implementation of Pulse Width Modulator (PWM) of power suppliers for real-time experimentations

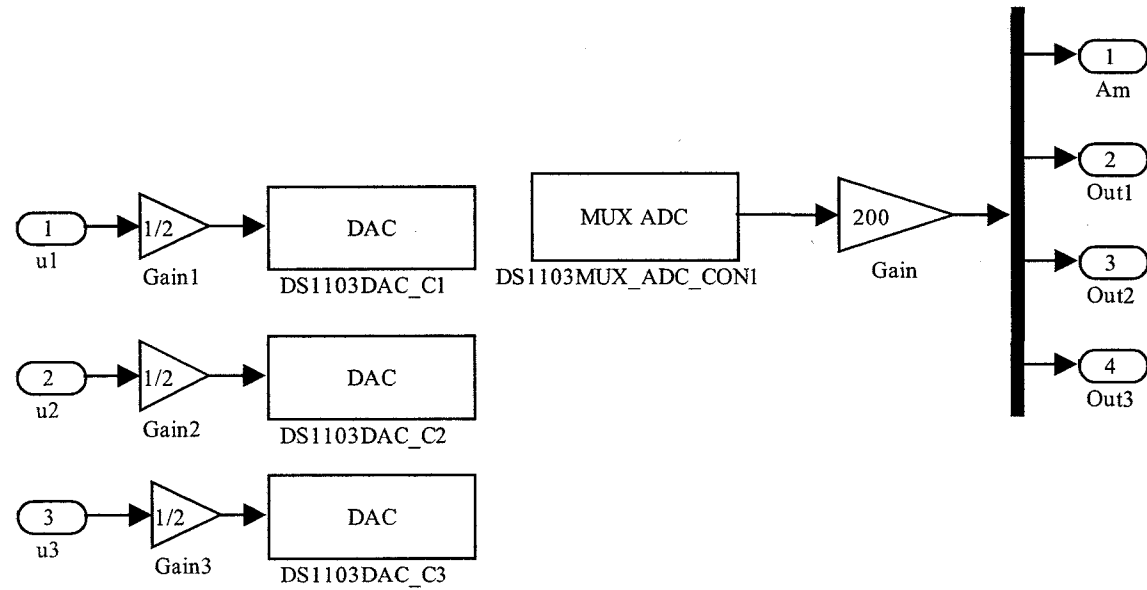


Figure A.2: SIMULINK implementation of I/O interface for real-time experimentations



